Title
Catalan and Crystal Combinatorics

Author
Pappe, Joseph

Publication Date
2023

Peer reviewed|Thesis/dissertation

Catalan and Crystal Combinatorics

By

Joseph H. Pappe

DISSERTATION

Submitted in partial satisfaction of the requirements for the degree of

DOCTOR OF PHILOSOPHY

in

MATHEMATICS

in the

OFFICE OF GRADUATE STUDIES

of the

UNIVERSITY OF CALIFORNIA

DAVIS

Approved:

Professor Anne Schilling, Chair

Professor Eugene Gorsky

Professor Monica Vazirani

Committee in Charge

2023

Contents

Catalan and Crystal Combinatorics

Abstract

The Catalan numbers are a ubiquitous sequence of natural numbers appearing in a diverse array of mathematical fields. However, even though these numbers have been well-studied, several conjectures and properties surrounding the Catalan numbers remain open. In this dissertation we first study the joint distribution of various statistics defined on Dyck paths. The first joint distribution involves the area and diagonal inversion statistic in the form of the q, t-Catalan polynomial. This polynomial arises from the study of the space of diagonal harmonics, and its symmetry has evaded a combinatorial proof. We introduce two new q, t-Catalan polynomials using two new statistics on Dyck paths. We are able to give a combinatorial proof of their symmetry and recover the usual q, t-Catalan polynomial in terms of our new statistics. Next, we explore the joint distribution of NE and NNE-factors within Dyck paths. We answer an open question by Bóna and Labelle regarding the symmetry of these numbers at certain values. Additionally, we prove various enumerative results of these numbers, including their real-rootedness and their connection to the number of cyclic compositions.

Kashiwara's crystal bases are combinatorial structures introduced in his study of the representations of quantum groups under a certain limit. Using Kashiwara's crystals, we explore the Burge correspondence sending labelled graphs to tableau. We give a Schensted-like result characterizing when a labelled graph is sent to a hook-shaped tableau and give a type A crystal structure on such graphs. Lastly, we merge these two topics by looking at the space of invariant tensors of the spin and vector representations in Type B. Using the promotion operator on Kashiwara's crystals, we construct a diagrammatic basis for these spaces in terms of chord diagrams such that rotation of the chord diagrams intertwines with the cyclic action on tensor factors. As a consequence of this, we are able to give a cyclic sieving phenomenon for fans of Dyck paths and vacillating tableaux respectively.

Acknowledgments

Without the following people's support, this dissertation would not have been possible.

First, I would like to thank my advisor, Anne Schilling, for introducing me to the world of Algebraic Combinatorics and being a wonderful mentor. Her patience, optimism, and insight has been instrumental in my completion of this thesis, and I am grateful for her guidance.

Next, I would like to acknowledge the teachers and instructors who had a deep impact on me during my formative years: Ms. Gerber, whose encouragement and guidance fostered my interest in Mathematics and started me down this journey; Mrs. Spoons, who allowed me to explore my mathematical interests freely; Ms. Dwyer and Mr. Jacotin, who both pushed me to be better academically; and Michael Lindstrom, who introduced me to mathematical research.

I am thankful to my academic siblings Jianping Pan, Wencin Poh, and Mary Claire Simone for being supportive and spending countless hours discussing and tackling problems with me. I would also like to thank my collaborators Miklós, Bóna, Stoyan Dimitrov, Yifei Li, Digjoy Paul, Stephan Pfannerer, Andrés R. Vindas-Meléndez, and Yan Zhuang, who were all a pleasure to collaborate with and whose knowledge and wealth of experience has been truly inspirational.

I am grateful for the Algebra and Combinatorics group, Ashleigh Adams, Alex Black, Milo Bechtloff-Weising, Erik Carlsson, Raymond Chou, Jonathan Erickson, Sean Griffin, James Hughes, David Kenepp, Yuze Luan, Tonie Scroggin, Chengyang Wang, Haihan Wu, Zhenyang Zhang, and Regina Zhou, for engaging conversations about research and other topics. I especially want to thank Eugene Gorsky and Monica Vazirani, for always being available to discuss problems and for serving on my dissertation and qualifying committee, and Fu Liu, for introducing me to Enumerative Combinatorics and for serving on my qualifying committee.

I would like to thank my friends and my cohort who supported me during various stages of this program: Albie, Alex, Anthony, Austin, Black, Carson, Chris, Dong Min, Hannah, Haolin, Haotian, Jake, Jessie, Josh, Justine, Kartik, Kate, Leonard, Lili, Mason, Matthew, Nate, Norman, Parth, Rommel, Rui, Shaofeng, Vishnu, Weidi, Yiran, ...

I would like to thank the National Science Foundation, for partially supporting this dissertation with grants DMS–1760329 and DMS–2053350.

Lastly, I am forever grateful to my family, Dad, Mom, and Danielle, for always being there.

CHAPTER 1

Introduction

1.1. Overview

The Catalan numbers given by $\frac{1}{n+1}\binom{2n}{n}$ enumerate a plethora of seemingly unrelated families of combinatorial objects. These families of Catalan objects include familiar objects such as Dyck paths, plane trees, and standard Young tableaux of two-rowed rectangles. In recent years refinements of the Catalan numbers via statistics on certain families of Catalan objects have been shown to be connected to other fields including representation theory and geometry. In the first half of this thesis, we investigate several refinements of the Catalan numbers by the joint distribution of various statistics on Dyck paths.

The first refinement we will explore is the q,t-Catalan polynomial. The q,t-Catalan functions were first introduced in connection with Macdonald polynomials and Garsia–Haiman's theory of diagonal harmonics [**36**] as certain rational functions in q and t. They can be obtained as the bigraded Hilbert series of the alternating component of a certain module of diagonal harmonics, where the dimension of this alternating component is equal to the Catalan number. In terms of symmetric functions, they can be expressed using the nabla operator and the elementary symmetric functions e_n as $\mathrm{Cat}_n(q,t) = \langle \nabla e_n, e_n \rangle$. The combinatorics of the q,t-Catalan polynomials was developed in various papers [**35**, **38**, **39**]. In particular, Haglund [**38**] gave a combinatorial formula as a sum over all Dyck paths graded by the area and bounce statistics (see (2.1.5)). Shortly thereafter, Haiman announced a different combinatorial formula using the area and dinv statistics (see (2.1.3)). The zeta map [**2**, **39**] relates these two combinatorial formulas. One of the main open problems related to the q,t-Catalan polynomials $\mathrm{Cat}_n(q,t)$ is a combinatorial proof of its symmetry in q and t.

In Chapter 2, we introduce two different q,t-analogues of the Catalan numbers. The first polynomial $F_n(q,t)$ (see (2.1.8)) is the sum over all Dyck paths graded by area and a new statistic called depth. The intuition for the depth statistic is that in the context of plane trees it is the sum over the depths of the various vertices in the plane tree. The second polynomial $G_n(q,t)$ (see (2.1.9)) is defined in terms of the dinv and dinv of depth statistic denoted ddinv. The dinv statistic can be formulated using the area sequence, so using the depth sequence instead yields the dinv of depth statistic. Unlike the usual q,t-Catalan polynomial, we are able to give a combinatorial proof that these new polynomials $F_n(q,t)$ and $G_n(q,t)$ are symmetric in q and t. This combinatorial proof involves defining a duality on plane trees, which switches the area and depth sequence. This duality turns out to be a composition of the maps in Definitions 1.2.1 and 2.1.1. We prove that on Dyck paths, the corresponding involution is equal to a recursively defined involution introduced by Deutsch [**25**]. In particular, this gives an alternative proof of the symmetry of the Tutte polynomial for the Catalan matroid [**3**].

The next refinement of the Catalan numbers that we investigate involves counting Dyck paths by certain subfactors. A classical example is given by the problem of counting the number of Dyck paths of semilength n containing k NE-factors (or peaks) which is known to be solved by the Narayana numbers $N_{n,k}$. These numbers are well-studied and satisfy the symmetry $N_{n,k} = N_{n,n+1-k}$ which has been shown combinatorially on Dyck paths by various involutions [**25**, **55**, **56**, **58**]. More generally, there is interest in enumerating Dyck paths by the joint distribution of occurrences of multiple kinds of factors. Two early works in this direction are [**24**, **83**]. In [**96**], Wang discusses a general technique that is useful for obtaining the relevant generating functions in many such cases; see also [**99**].

In this thesis, we will be concerned with the joint distribution of NE-factors and NNE-factors in Dyck paths. More specifically, we study the numbers $w_{n,k,m}$ which count the number of Dyck paths of semilength n, k NE-factors, and m NNE-factors. Using generating function techniques, a closed formula for $w_{n,k,m}$ was given by Bóna and Labelle [**11**] and can be obtained via results in Wang [**96**] and Lemus-Vidales [**59**]. From this formula, the numbers $w_{n,k,m}$ were observed by Bóna and Labelle to satisfy the symmetry $w_{2k+1,k,m} = w_{2k+1,k,k+1-m}$ resembling that of the Narayana numbers; however, it remained an open problem to find a combinatorial proof of this symmetry.

In Chapter 3 we answer this open question by giving an involution on Dyck paths with semilength $2k+1$ and k NE-factors that exhibits this symmetry. To construct this involution, we give a combinatorial proof of formula relating $w_{2k+1,k,m}$ to the Narayana number $N_{k,m}$ via a map involving cyclic compositions and plane trees. Composing this map with any involution demonstrating the well-established symmetry of the Narayana numbers gives the desired involution. This proof will be extended to give a combinatorial proof for the closed formula or $w_{n,k,m}$ and more generally for $w_{n,k_1,k_2,\dots,k_r}$ where $w_{n,k_1,k_2,\dots,k_r}$ denotes the number of Dyck paths with semilength n, k_1 NE-factors, k_2 NNE-factors, $\dots$, and k_r N^rE-factors. We conclude with some investigation of the polynomials $W_{n,k}(t) = \sum_{m=0}^{k} w_{n,k,m}t^m$, including real-rootedness and γ-positivity results, as well as a symmetric decomposition.

The latter half of this thesis will deal with Kashiwara's crystals. Crystals are combinatorial structures introduced by Kashiwara [**49**] in his study of the representations of $U_q(\mathfrak{g})$ at $q = 0$, where $U_q(\mathfrak{g})$ is the quantum group associated to the Lie algebra $\mathfrak{g}$. A more rigorous treatment is given in Section 1.2.2 and can be found for example in [**16**,**42**]. In this thesis, we will utilize crystals in two different contexts.

Our first application of Kashiwara's crystals will be to a generalization of the Robinson-Schensted-Knuth (RSK) correspondence [**52**,**79**,**84**] given by Burge [**17**]. The celebrated Robinson–Schensted (RS) correspondence [**79**,**84**] gives a bijection between words w in the alphabet $\{1, 2, \dots, n\}$ of length k and a pair of tableaux of the same shape λ, a partition of k with at most n parts, where the first tableau is a semistandard Young tableau in the same alphabet and the second tableau is a standard tableau. Schensted [**84**] proved that λ_1 (the biggest part of the partition λ) is the length of the longest increasing subword of w. Knuth's generalization of the RS correspondence [**52**], known as the RSK correspondence, provides a bijective proof of the Cauchy identity in symmetric function theory

$$\sum_{\lambda} s_\lambda(x)s_\lambda(y) = \prod_{i,j\geqslant 1} \frac{1}{1 - x_iy_j},$$

where the sum is over all partitions λ and $s_\lambda(x)$ is the Schur function in the variables $x_1, x_2, \dots$ indexed by the partition λ.

In [**17**, Section 4] Burge gives a variant of the RSK correspondence which acts as a bijection between simple labelled graphs (graphs without loops or multiple edges) and semistandard Young tableaux of threshold shape. A partition $\lambda = (\lambda_1, \lambda_2, \dots, \lambda_n)$ is called threshold if $\lambda^t_i = \lambda_i + 1$ for all $1 \leqslant i \leqslant d(\lambda)$, where λ^t_i is the length of i-th column of the Young diagram of λ and $d(\lambda)$ is the maximal d such that $(d, d) \in \lambda$. This bijection, called the Burge correspondence, gives a bijective proof of the Littlewood identity [**63**, Exer. I.5.9(a) and I.8.6(c)]

$$1 + \sum_{\lambda} s_\lambda(x_1, x_2, \ldots) = \prod_{i<j} (1 + x_i x_j)\,, \tag{1.1.1}$$

where the sum runs over all threshold partitions. A natural question is to find an analogue of Schensted's result for the RSK correspondence for the Burge correspondence.

In Chapter 4, we fully characterize the graphs whose shapes under the Burge correspondence are hook-shapes in terms of peak and valley conditions. This is the first step towards an analogue for the Burge correspondence of Schensted's result for the RSK correspondence, namely that increasing sequences under the RSK correspondence give tableaux of single row shape. Moreover, as the crystal on semistandard Young tableaux preserves the shape of the tableaux, we attempt to find a crystal structure on simple graphs that preserves the shape of the tableaux obtained under the Burge correspondence. We impose a type A crystal structure on simple graphs of hook shape and characterize the extremal vectors in this crystal.

The second application of crystals will be to a problem arising from invariant theory in which a connection to Catalan objects will be obtained. Since the work of Rumer, Teller, and Weyl [**82**], it has been desirable to give a diagrammatic basis for invariant spaces. Of particular interest is the invariant subspace $(V^{\otimes n})^G$ of the tensor product $V^{\otimes n}$ under the diagonal action of G for G a semisimple Lie group and V an irreducible representation of G. As the natural action of the symmetric group $\mathfrak{S}_n$ on $V^{\otimes n}$ commutes with this diagonal action, it is desirable to find a basis that respects the action of $\mathfrak{S}_n$. Thus, a preliminary question is to find a basis of the invariant subspace of $V^{\otimes n}$ under the action of the long cycle $(1, 2, \ldots, n)$.

Westbury [**97**] showed that the dimension of $(V^{\otimes n})^G$ is equal to the number of highest weight elements of weight zero in $\mathcal{B}^{\otimes n}$ where $\mathcal{B}$ is the crystal basis associated to V. Moreover, he showed that the action of the long cycle on $(V^{\otimes n})^G$ corresponds to applying promotion [**31**, **41**, **97**, **98**] on highest weight words of weight zero in $\mathcal{B}^{\otimes n}$ where promotion is defined is defined using Henriques' and Kamnitzer's commutor [**41**]. Thus it suffices to find a correspondence between highest weight elements of weight zero in $\mathcal{B}^{\otimes n}$ and diagram bases, such as chord diagrams, which intertwine promotion and rotation. For the vector representation of $SL(2)$ and $SL(3)$, this is given by Kuperberg's webs [**57**] as shown by Petersen, Pylyavskyy, and Rhoades [**73**] and Patrias [**72**]. For the vector representation of the symplectic group and the adjoint representation of the general linear group, such a correspondence was given in [**75**].

In Chapter 5, we construct an an injection from the set of r-fans of Dyck paths (resp. vacillating tableaux) of length n into the set of chord diagrams on $[n]$ that intertwines promotion and rotation. There is a natural correspondence between r-fans of Dyck paths (resp. vacillating tableaux) and highest weight elements in the tensor product of the spin crystal (resp. vector representation) of type B_r. We present this injection via fillings of promotion matrices and in terms of fillings of Fomin growth diagrams where the first description shows the map intertwines promotion and rotation while the second description shows injectivity. To show these descriptions are equivalent, we use virtualization of crystals (see for example [**16**]) and results of [**75**] for oscillating tableaux of weight zero (or equivalently highest weight words of weight zero for the vector representation type C_r).

In addition, Fontaine and Kamnitzer [**31**] as well as Westbury [**97**] tied the promotion action on highest weight elements of weight zero to the cyclic sieving phenomenon introduced by Reiner, Stanton and White [**77**]. We make this cyclic sieving phenomenon more concrete by providing the polynomial in terms of the energy function. For r-fans of Dyck paths, we conjecture another polynomial, which is the q-deformation of the number of r-fans of Dyck paths, to give a cyclic sieving phenomenon. For vacillating tableaux, we give a polynomial inspired by work of Jagenteufel [**48**] for a cyclic sieving phenomenon.

1.2. Preliminaries

1.2.1. Dyck Path and Plane Trees. A *Dyck path* of semilength n is a lattice path in $\mathbb{Z}^2_{\geq 0}$ going from $(0,0)$ to (n,n) consisting solely of North steps $(0,1)$ and East steps $(1,0)$ and never passing below the line $y = x$. Let D_n denote the set of all Dyck paths with semilength n. It is well-known that D_n is enumerated by the nth *Catalan number* $\mathrm{Cat}_n = \frac{1}{n+1}\binom{2n}{n}$.

Given a Dyck path $\pi \in D_n$ it will often be convenient to think of it as a word $\pi_1\pi_2\dots\pi_{2n}$ of length $2n$ in the alphabet $\{N, E\}$ where $\pi_i = N$ if the ith step of π consists of a North step and E if the ith step of π consists of an East step. We refer to this as the *Dyck word* of π, and we will

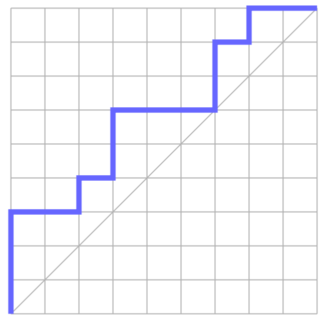

FIGURE 1.1. Example of a Dyck path $\pi \in D_9$.

often switch between the two interpretations of a Dyck path. Note that the condition that a Dyck path never dips below the line $y = x$ is equivalent to the condition that the number of N's in any prefix of a Dyck word is weakly greater than the number of E's. See Figure 1.1 for an example of a Dyck path corresponding to the Dyck word $NNNEENENNNEEENNENEE$.

Another family of combinatorial objects counted by the Catalan numbers are plane trees. Given a rooted tree T, the *principal subtrees* of T are the rooted trees obtained by deleting the root of T and considering the children of the root as the new roots of their respective tree. A *plane tree* is then defined recursively as a rooted tree consisting solely of a root r or a root r connected to its sequence of principal subtrees $(T_1, \ldots, T_k)$ which themselves are plane trees. Note that the principal subtrees are linearly ordered. For convenience, all plane trees will be thought of with the root drawn at the top and its principal subtrees drawn below from left to right. Let $\mathcal{T}_n$ denote the set of plane trees on n non-root vertices. As stated before, $\mathcal{T}_n$ is known to also be enumerated by Cat_n which can be shown via several bijections between D_n and $\mathcal{T}_n$. One such bijection, found for example in [**89**, Page 10], is defined below with two other bijections defined later in Section 2.1.3.

DEFINITION 1.2.1. *Let the* Stanley map $\sigma \colon D_n \to \mathcal{T}_n$ *be defined as follows:*

(1) Consider the Dyck word $\pi_1\pi_2\ldots\pi_{2n}$ *of* π*.*

(2) Start at the root node. Label this as vertex v*.*

(3) For $1 \leqslant i \leqslant 2n$*, if* $\pi_i = N$ *then add a child to the right of all preexisting children of* v*. Label this new child as* v*. If* $\pi_i = E$*, set* v *to be the parent of* v*.*

EXAMPLE 1.2.1. *See Figure 1.2 for the plane tree corresponding to the Dyck path in Figure 1.1 under* σ*.*

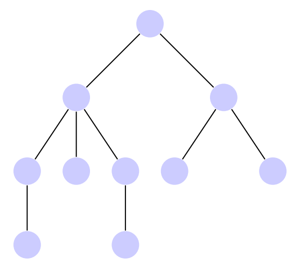

FIGURE 1.2. Plane tree $T \in \mathcal{T}_9$ corresponding to the Dyck path π in Figure 1.1.

1.2.2. Crystals. Let $\mathfrak{g}$ be a complex semisimple Lie algebra with weight lattice Λ and root system Φ. Let its simple roots and simple coroots be given by α_i and $\alpha_i^\vee$ respectively for $i \in I$ where I is the index set of the corresponding Dynkin diagram.

DEFINITION 1.2.2. *An abstract $U_q(\mathfrak{g})$-Kashiwara crystal of type Φ consists of a nonempty set $\mathcal{B}$ and maps*

$$
\begin{aligned}
& e_i, f_i \colon \mathcal{B} \to \mathcal{B} \sqcup \{\emptyset\} \\
& \varepsilon_i, \varphi_i \colon \mathcal{B} \to \mathbb{Z} \sqcup \{-\infty\} \qquad (1.2.1) \\
& \mathsf{wt} \colon \mathcal{B} \to \Lambda
\end{aligned}
$$

for $i \in I$, $\emptyset \notin \mathcal{B}$ which satisfy the following conditions

A1. *If $x, y \in \mathcal{B}$ then $e_i(x) = y$ if and only if $f_i(y) = x$. Moreover, in this case*

$$\mathsf{wt}(y) = \mathsf{wt}(x) + \alpha_i, \quad \varepsilon_i(y) = \varepsilon_i(x) - 1, \quad \varphi_i(y) = \varphi_i(x) + 1.$$

A2. *For all $x \in B$ and $i \in I$, we have*

$$\varphi_i(x) = \langle \mathsf{wt}(x), \alpha_i^\vee \rangle + \varepsilon_i(x)$$

where $-\infty + k = -\infty$ for all $k \in \mathbb{Z}$ and if $\varphi_i(x) = -\infty$, then $e_i(x) = f_i(x) = \emptyset$.

The operators e_i and f_i are called *raising* and *lowering operators*. The map wt is the *weight map*. If ε_i and φ_i satisfy

$$\varepsilon_i(b) = \max\{k \geqslant 0 \mid e_i^k(b) \neq \emptyset\} \quad \text{and} \quad \varphi_i(b) = \max\{k \geqslant 0 \mid f_i^k(b) \neq \emptyset\}.$$

for all $i \in I$ and $b \in \mathcal{B}$, then $\mathcal{B}$ is called a *seminormal crystal*. In this case, the maps ε_i and φ_i measure how often e_i and f_i respectively can be applied to a given crystal element b and will be called the *string lengths* of b. All crystals considered in this paper will be seminormal.

A crystal can be viewed graphically as a labelled directed graph where the vertex set is given by the underlying set $\mathcal{B}$ and if $f_i(u) = v$ for $u, v \in \mathcal{B}$ then a directed edge labelled i points from u to v in the graph.

EXAMPLE 1.2.2. *The type A_r seminormal crystal corresponding to the vector representation of $\mathfrak{gl}_{r+1}$ is given by*

$$\boxed{1} \xrightarrow{\quad 1 \quad} \boxed{2} \xrightarrow{\quad 2 \quad} \cdots \xrightarrow{\quad r \quad} \boxed{r+1}$$

where $\mathsf{wt}(i) = \mathbf{e}_i$, the ith standard basis vector.

An element $b \in \mathcal{B}$ is called *highest weight* if $e_i(b) = \emptyset$ for all $i \in I$. Thus, graphically, an element $b \in \mathcal{B}$ is a highest weight element if and only if it is a source vertex in the corresponding graph.

DEFINITION 1.2.3. *Let $\mathcal{B}$ and $\mathcal{C}$ be two abstract $U_q(\mathfrak{g})$-crystals. A* crystal morphism *is a map $\psi \colon \mathcal{B} \to \mathcal{C} \sqcup \{\emptyset\}$ satisfying:*

(1) If $b \in \mathcal{B}$ and $\psi(b) \in \mathcal{C}$, then

   (a) $\mathsf{wt}(\psi(b)) = \mathsf{wt}(b)$,

   (b) $\varepsilon_i(\psi(b)) = \varepsilon_i(b)$ for all $i \in I$, and

   (c) $\varphi_i(\psi(b)) = \varphi_i(b)$ for all $i \in I$.

(2) If $b, e_i(b) \in \mathcal{B}$ such that $\psi(b), \psi(e_i(b)) \in \mathcal{C}$, then $\psi(e_i(b)) = e_i(\psi(b))$.

(3) If $b, f_i(b) \in \mathcal{B}$ such that $\psi(b), \psi(f_i(b)) \in \mathcal{C}$, then $\psi(f_i(b)) = f_i(\psi(b))$.

The map ψ is said a *crystal isomorphism* if the induced map $\psi : \mathcal{B} \sqcup \{\emptyset\} \to \mathcal{C} \sqcup \{\emptyset\}$ with $\psi(\emptyset) = \emptyset$ is a bijection.

A remarkable property of crystals is that they respect *tensor products*. Given two $U_q(\mathfrak{g})$-crystals $\mathcal{B}$ and $\mathcal{C}$, their tensor product $\mathcal{B} \otimes \mathcal{C}$ will be a $U_q(\mathfrak{g})$-crystal with underlying set the Cartesian product $\mathcal{B} \times \mathcal{C}$. For $b \otimes c \in \mathcal{B} \otimes \mathcal{C}$, the weight map is given by $\mathsf{wt}(b \otimes c) = \mathsf{wt}(b) + \mathsf{wt}(c)$, the crystal operators given by

$$f_i(b \otimes c) = \begin{cases} f_i(b) \otimes c & \text{if } \varphi_i(c) \leqslant \varepsilon_i(b), \\ b \otimes f_i(c) & \text{if } \varphi_i(c) > \varepsilon_i(b), \end{cases}$$

and

$$e_i(b \otimes c) = \begin{cases} e_i(b) \otimes c & \text{if } \varphi_i(c) < \varepsilon_i(b), \\ b \otimes e_i(c) & \text{if } \varphi_i(c) \geqslant \varepsilon_i(b), \end{cases}$$

and the string lengths given by

$$\varphi_i(b \otimes c) = \mathsf{max}(\varphi_i(b), \varphi(c) + \langle \mathsf{wt}(b), \alpha_i^\vee \rangle)$$

and

$$\varepsilon_i(b \otimes c) = \mathsf{max}(\varepsilon_i(c), \varepsilon(b) - \langle \mathsf{wt}(c), \alpha_i^\vee \rangle).$$

If $\mathcal{B}$ and $\mathcal{C}$ are seminormal crystals, then so is $\mathcal{B} \otimes \mathcal{C}$.

While an abstract $U_q(\mathfrak{g})$-crystal may not correspond to a $U_q(\mathfrak{g})$ Stembridge [**90**] for simply-laced types characterized those crystals which are associated with quantum group representations in terms of local rules on the crystal graph. We define a *Stembridge crystal* to be any crystal satisfying these local rules. Crystals for non-simply-laced root systems that correspond to representations can be constructed using *virtual crystals*, see for example [**16**, Chapter 5]. A further discussion of virtual crystals will occur in Section 5.1.2.

CHAPTER 2

An area-depth symmetric q,t-Catalan polynomial

This chapter is based on work in collaboration with Digjoy Paul and Anne Schilling published in [**69**].

2.1. Background and Definitions

In Section 2.1.1, we define the q,t-Catalan polynomial. In Section 2.1.2, we define new statistics on Dyck paths and related polynomials. We conclude in Section 2.1.3 with further background on plane trees and their various connections to Dyck paths.

2.1.1. q,t-Catalan polynomial. Given a Dyck path $\pi \in D_n$, let the *area sequence* of π be the vector $(a_1(\pi), a_2(\pi), \ldots, a_n(\pi))$, where $a_i(\pi)$ is the number of full unit squares in the i-th row completely between π and the diagonal $y = x$. Let

$$\mathsf{area}(\pi) = \sum_{i=1}^{n} a_i(\pi), \tag{2.1.1}$$

that is, the total number of squares between the path π and the diagonal. Note that a Dyck path is uniquely determined by its area sequence. Additionally, a vector $(a_1, a_2, \ldots, a_n) \in \mathbb{Z}^n_{\geqslant 0}$ is an area sequence of some Dyck path in D_n if and only if $a_1 = 0$ and $0 \leqslant a_i \leqslant a_{i-1} + 1$ for $2 \leqslant i \leqslant n$.

Using the area sequence of a Dyck path π, we can define another statistic on Dyck paths as follows

$$\mathsf{dinv}(\pi) = |\{(i,j) \mid i<j,\, a_i(\pi) = a_j(\pi)\} \cup \{(i,j) \mid i<j,\, a_i(\pi) = a_j(\pi)+1\}|. \tag{2.1.2}$$

The *q,t-Catalan polynomial* is defined as

$$\mathrm{Cat}_n(q,t) = \sum_{\pi \in D_n} q^{\mathsf{area}(\pi)} t^{\mathsf{dinv}(\pi)}. \tag{2.1.3}$$

The polynomial $\mathrm{Cat}_n(q,t)$ is symmetric in q and t, that is, $\mathrm{Cat}_n(q,t) = \mathrm{Cat}_n(t,q)$ (see for example [**39**]). It is an open question to find a combinatorial proof of its symmetry.

To define the bounce statistic of $\pi \in D_n$, we first must construct the bounce path $\mathcal{B}(\pi)$ by the following algorithm:

(1) Start at the point (0,0).
(2) Continue North until the start of an East step of π is met.
(3) Continue East until the diagonal $y = x$ is met.
(4) If the bounce path has reached the point (n,n), then stop. Otherwise go back to step (2).

Let $(0,0) = (b_0,b_0),(b_1,b_1),\ldots,(b_k,b_k) = (n,n)$ be the points on the diagonal that $\mathcal{B}(\pi)$ touches. Then *bounce* is defined as

$$\mathsf{bounce}(\pi) = \sum_{i=1}^{k-1} n - b_i. \tag{2.1.4}$$

Proposition 2.1.1. *[**39**] We have*

$$\mathrm{Cat}_n(q,t) = \sum_{\pi \in D_n} q^{\mathsf{area}(\pi)} t^{\mathsf{bounce}(\pi)}. \tag{2.1.5}$$

There exists a bijection $\zeta \colon D_n \to D_n$ on Dyck paths, called the *zeta map*, which has the property that for $\pi \in D_n$

$$\mathsf{area}(\pi) = \mathsf{bounce}(\zeta(\pi)),$$

$$\mathsf{dinv}(\pi) = \mathsf{area}(\zeta(\pi)).$$

This proves that (2.1.3) and (2.1.5) are equal. The inverse of the zeta map first appeared in connection with nilpotent ideals in certain Borel subalgebras of $\mathfrak{sl}(n)$ [**2**]. For its connections with the combinatorics of q,t-Catalan polynomials, see [**39**]. The zeta map was further studied and generalized in [**4, 19, 20, 93**]. For the definition of the zeta map, see [**39**, Theorem 3.15]. In Proposition 2.1.2 below, we state another formulation of the zeta map in terms of plane trees (which can also serve as the definition).

2.1.2. Depth polynomials. Let $\pi \in D_n$. We produce a labelling for π column-by-column using the following algorithm:

(1) In the leftmost column, label all cells directly to the right of a North step with a 0.

(2) In the i-th column from the left, locate the bottommost cell c in the column that is directly right of a North step; note that such a cell may not exist. From c travel Southwest diagonally until a cell c' that is already labelled is reached. Let ℓ be the labelling of c'. Label all cells directly to the right of a North step in the i-th column with an $\ell + 1$.

Define this to be the *depth labelling* of π. The *depth sequence* $(d_1(\pi), d_2(\pi), \ldots, d_n(\pi))$ of π can be obtained by reading the entries of the depth labelling of π in the following manner:

(1) Let v be the empty vector. Let c be the cell directly right of the first North step of π.

(2) Append the label of c to the end of v. If the length of v is n, then stop and let

$$(d_1(\pi), d_2(\pi), \ldots, d_n(\pi)) = v.$$

(3) Otherwise, travel Northeast diagonally from c until a cell that is labelled is reached. If this cell exists and has not been seen before, then redefine c to be this cell. If no such cell exists or the cell was already visited before by the algorithm, then consider the set of all cells that have been visited already but have a labelled cell directly above them that has not been visited. Out of this set choose the rightmost one and let c be the cell directly above this cell. Go back to step (2).

Remark 2.1.1. *Note that in the above definition, the rightmost cell of all visited cells with a labelled cell directly above is also the cell in this set with the largest label. Namely, look at the lowest cell in the same column as c, which is labelled. All cells that were already visited but have a labelled cell directly above them are to the left of this cell on the same diagonal or lower. By the construction of the labels, these cells all have strictly smaller labels.*

Define the *depth* statistic as follows

$$\mathsf{depth}(\pi) = \sum_{i=1}^{n} d_i(\pi). \tag{2.1.6}$$

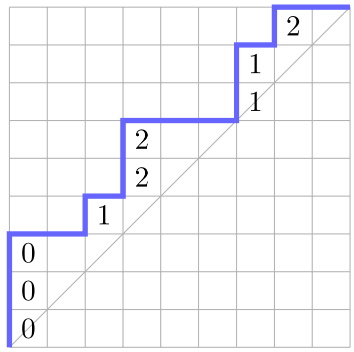

FIGURE 2.1. Example of a Dyck path $\pi \in D_9$ with its depth labelling.

Similar to how dinv was defined in terms of the area sequence in (2.1.2), we can associate a "dinv" type statistic called ddinv to the depth sequence of a Dyck path. Formally,

$$\mathsf{ddinv}(\pi) = |\{(i,j) \mid i < j,\ d_i(\pi) = d_j(\pi)\} \cup \{(i,j) \mid i < j,\ d_i(\pi) = d_j(\pi) + 1\}|. \tag{2.1.7}$$

EXAMPLE 2.1.1. *In Figure 2.1, a Dyck path $\pi \in D_9$ with its depth labelling is shown. The depth sequence is* $(0, 1, 1, 2, 0, 1, 2, 2, 0)$. *Hence the depth is* $\mathsf{depth}(\pi) = 9$. *Finally*

$$\{(1,5), (1,9), (5,9), (2,3), (2,6), (3,6), (4,7), (4,8), (7,8), (2,5), (2,9), (3,5), (3,9), (6,9), (4,6)\}$$

are pairs contributing to the ddinv *statistic in* (2.1.7), *hence* $\mathsf{ddinv}(\pi) = 15$.

Next we define two q,t-Catalan polynomials using the just introduced statistics:

$$F_n(q,t) = \sum_{\pi \in D_n} q^{\mathsf{area}(\pi)} t^{\mathsf{depth}(\pi)} \tag{2.1.8}$$

and

$$G_n(q,t) = \sum_{\pi \in D_n} q^{\mathsf{dinv}(\pi)} t^{\mathsf{ddinv}(\pi)}. \tag{2.1.9}$$

We will prove various properties of these polynomials in Section 2.2, including that they are symmetric in q and t.

Example 2.1.2. *We give the polynomials for when* $n = 4$*:*

$$\mathrm{Cat}_4(q,t) = q^6 + q^5t + q^4t^2 + q^3t^3 + q^2t^4 + qt^5 + t^6 + q^4t + q^3t^2 + q^2t^3 + qt^4 + q^3t + q^2t^2 + qt^3,$$

$$F_4(q,t) = q^6 + q^5t + q^4t^2 + 2q^3t^3 + q^2t^4 + qt^5 + t^6 + q^4t + qt^4 + q^3t + 2q^2t^2 + qt^3,$$

$$G_4(q,t) = q^6 + q^4t^2 + q^2t^4 + t^6 + q^5t^2 + q^4t^3 + q^3t^4 + q^2t^5 + 2q^3t + 2qt^3 + q^2t + qt^2$$

Remark 2.1.2. *Note that* $\mathrm{Cat}_n(1,1) = F_n(1,1) = G_n(1,1) = \mathrm{Cat}_n$ *are all equal to the* n*-th Catalan number. The difference* $F_n(q,t) - \mathrm{Cat}_n(q,t)$ *can be written as* $(1-t)(1-q)M_n(q,t)$*. Evaluating* $M_n(1,1)$ *yields the sequence* $0, 0, 0, 1, 14, 124, 888, 5615, 32714, \ldots$*, which curiously is the 5-th number after each 1 in the Riordan array, see [**46**]. Both* $(G_n - \mathrm{Cat}_n)/((q-1)(t-1))$ *and* $(G_n - F_n)/((q-1)(t-1))$ *are also conjectured to have positive coefficients. At* $q = t = 1$*, the corresponding sequences are* $0, 0, 0, 1, 11, 83, 530, 3071, 16997, 86778, 436084, \ldots$ *and* $0, 0, 0, 1, 10, 69, 406, 2183, 11082, 54064, 256204, \ldots$*, which do not seem to appear in [**46**].*

2.1.3. Plane Trees. Here, we discuss two other bijections between Dyck paths and plane trees that will be useful. The first bijection is the restriction of a bijection between parking functions and labelled trees to Dyck paths and can be found, for example, in [**40**] and [**39**, Chapter 5].

Definition 2.1.1. *Let the Haglund–Loehr map* $\eta\colon D_n \to \mathcal{T}_n$ *be defined as follows:*

(1) For each cell in the first column that lies directly right of a North step attach a child to the root vertex. Associate the rightmost child to the topmost cell in the first column, the second rightmost child to the second topmost cell in the first column, and so on such that the leftmost child is associated with the bottommost cell in the first column.

(2) To determine the children of any other vertex v*, travel on the Northeast diagonal from its associated cell under* π *until it reaches a cell directly to the right of a North step. If this cell exists and is the bottommost cell in its column that is directly right of a North step, then attach* k *children to* v*, where* k *is the number of cells in this column that lie directly right of a North step. For each of these new vertices, associate them to the appropriate cell as laid out above.*

Example 2.1.3. *The Dyck path in Figure 2.1 is sent to the plane tree in Figure 2.2B under* η*.*

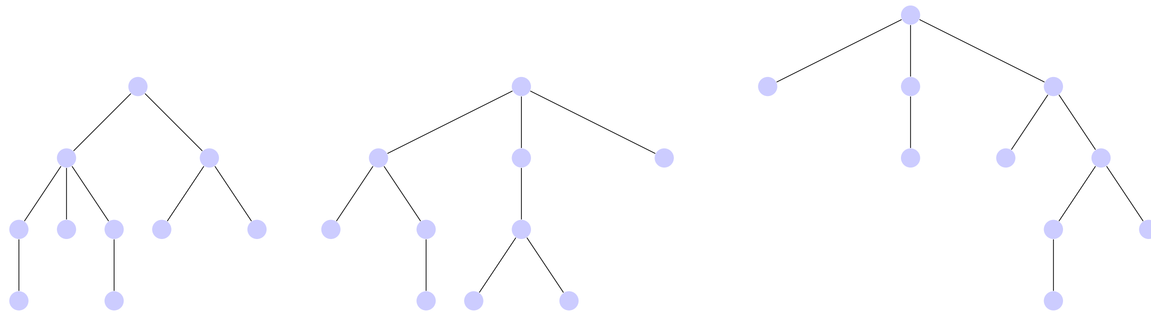

(A) $\sigma(\pi)$ (B) $\eta(\pi)$ (C) $\beta(\pi)$

FIGURE 2.2. Plane trees corresponding to the Dyck path π of Figure 2.1 under σ, η, and β, respectively.

The next map we mention can be found in [**9**].

DEFINITION 2.1.2. *Let the* Benchekroun–Moszkowski map $\beta\colon D_n \to \mathcal{T}_n$ *be defined as follows:*

(1) Consider the Dyck word $\pi_1\pi_2\dots\pi_{2n}$ of π in the alphabet $\{N, E\}$ corresponding to the North and East steps of π. Append $\pi_0 = E$ to the front of the string.

(2) For each vertex, we attach one of two states: "Checked" or "Not Checked". Start with just the root vertex in the "Not Checked" state.

(3) Recursively consider π_i for $i = 0, 1, \dots, 2n$. If $\pi_i = E$, then find the set of all closest vertices to the root in the "Not Checked" state. Out of these vertices choose the leftmost vertex and label this vertex as v. Let k be the number of consecutive North steps directly following π_i. Append k children to v all in "Not Checked" state. Change the state of vertex v to "Checked". If $\pi_i = N$, then perform no action on the graph.

EXAMPLE 2.1.4. *The Dyck path of Figure 2.1 is sent to the plane tree in Figure 2.2C under β.*

It turns out that σ and β can be used to obtain the zeta map.

PROPOSITION 2.1.2. *[**9**] Let $\pi \in D_n$. Then $\zeta(\pi) = \beta^{-1} \circ \sigma(\pi)$.*

2.2. Results

In Section 2.2.1, we prove a recursion for the polynomials $F_n(q,t)$. In Section 2.2.2, we introduce the notion of a dual plane tree using various reading words. We use this to prove in Section 2.2.3 that $F_n(q,t)$ and $G_n(q,t)$ are symmetric in q and t. This also gives an expression of the usual

Catalan polynomials in terms of the depth and dinv of depth statistics. In Section 2.2.4, we relate the involution that interchanges depth and area used to prove the symmetry in Section 2.2.3 to an involution by Deutsch [**25**]; this yields an easy proof of the symmetry of the Tutte polynomials of the Catalan matroid [**3**].

2.2.1. Recursion for $F_n(q,t)$. We begin by giving a recursion for $F_n(q,t)$ which implicitly proves its q,t-symmetry.

PROPOSITION 2.2.1. *We have $F_0(q,t) = 1$ and for any $n \geqslant 1$*

$$F_n(q,t) = \sum_{k=1}^{n} q^{k-1} t^{n-k} F_{k-1}(q,t) F_{n-k}(q,t).$$

PROOF. Let

$$D_n(k) = \{\pi \in D_n \mid \pi \text{ first touches the diagonal at } (k,k)\}.$$

Let $f\colon D_n(k) \to D_{k-1} \times D_{n-k}$ be the classical bijection sending

$$\pi = \pi_1\pi_2 \ldots \pi_{2n} \quad \mapsto \quad (\pi_2 \ldots \pi_{2k-1}, \pi_{2k+1} \ldots \pi_{2n}).$$

Let $f_1(\pi)$ and $f_2(\pi)$ be the first and second component of $f(\pi)$, respectively. Note that appending a North step to the beginning and an East step at the end of a Dyck path of semilength m increases the area by m. As π is obtained by concatenating N, $f_1(\pi)$, E, and $f_2(\pi)$, we have $q^{\mathsf{area}(\pi)} = q^{k-1} q^{\mathsf{area}(f_1(\pi))} q^{\mathsf{area}(f_2(\pi))}$. Now consider the depth labelling of π. Observe that the labellings of all North steps after π_{2k+1} can be uniquely determined by the labelling to the right of π_{2k+1}. Since the labelling to the right of the first North step is 0 and (k,k) is the first time π touches the diagonal, we have that the labelling to the right π_{2k+1} is 1. However, looking at the corresponding depth labelling in $f_2(\pi)$, this value is a zero. Thus, to get from the depth labelling of $f_2(\pi)$ to the that of $\pi_{2k+1} \ldots \pi_{2n}$ in π, we must add 1 to each of the $n-k$ labels. Additionally, from the definition of the depth labelling, we see that the portion of π from $(0,1)$ to $(k-1,k)$ corresponding to $f_1(\pi)$ has the same depth labelling as $f_1(\pi)$. This gives us that

$t^{\mathsf{depth}(\pi)} = t^{n-k} t^{\mathsf{depth}(f_1(\pi))} t^{\mathsf{depth}(f_2(\pi))}$. Therefore,

$$\sum_{\pi \in D_n(k)} q^{\mathsf{area}(\pi)} t^{\mathsf{depth}(\pi)} = q^{k-1} t^{n-k} F_{k-1}(q,t) F_{n-k}(q,t). \tag{2.2.1}$$

Summing over k from 1 to n gives the desired result. $\square$

The recursion in Proposition 2.2.1 relates the polynomials $F_n(q,t)$ to the q,t-Catalan polynomials in [**47**, Section 5] in terms of increasing/decreasing factorizations and to Hurwitz graphs [**1**] since they satisfy the same recurrence. Note that in [**1**] the authors defined a statistics bmaj on Dyck paths, which corresponds to our depth statistics. However, depth and bmaj are defined in different ways. In particular, the depth sequence is a refinement of depth, which will be used in subsequent sections to define a duality.

2.2.2. Dual plane trees. We define two labellings of plane trees and an associated reading word to each labelling.

Definition 2.2.1. *The labelling A of a plane tree T, denoted by T_A, is defined recursively by the following algorithm:*

(1) Label the root as 0.
(2) For any other vertex v, let m be the labelling of its parent w. Label v as $m+k-1$, where v is the k-th leftmost child of w.

Definition 2.2.2. *Let T be a plane tree with n non-root vertices. The reading word of T_A, denoted by $\mathsf{read}_A(T)$, is given by the following algorithm:*

(1) Start by setting $\mathsf{read}_A(T)$ to be an empty vector. Append the labels of the children of the root in increasing order.
(2) If the length of $\mathsf{read}_A(T)$ equals n, then output $\mathsf{read}_A(T)$. Otherwise, consider the set of vertices whose labels have already been added to $\mathsf{read}_A(T)$ but whose children's labels have not been added. Find the vertex in this set with the largest label and at least one child. Call this vertex v. Append the labels of all the children of v in increasing order.

Note that the definition of the reading word in Definition 2.2.2 is well-defined. To show this, it suffices to explain why no two vertices with the same label will be considered by the definition at

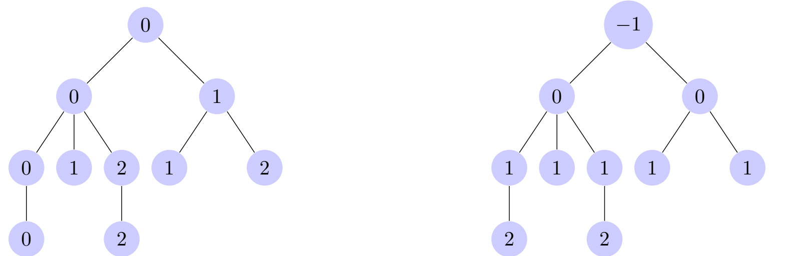

(A) T_A (B) T_D

FIGURE 2.3. Plane tree labellings T_A and T_D of the plane tree in Figure 2.2A.

the same step. Let v and w be any two vertices that have the same label. If one is an ancestor of the other, then they would not be considered at the same point anywhere in the algorithm. Otherwise, consider the closest common ancestor of v and w and label it x. Let v' (resp. w') be the child of x on the path from v (resp. w) to x. As the label of w' is strictly larger than that of v', w will be considered before v' and thus before v in the algorithm.

EXAMPLE 2.2.1. *The labelling T_A of the tree T in Figure 2.2A is given in Figure 2.3A. The corresponding reading word is* $\mathsf{read}_A(T) = (0, 1, 1, 2, 0, 1, 2, 2, 0)$.

DEFINITION 2.2.3. *The labelling D of a plane tree T, denoted by T_D, is defined by labelling a vertex v by the number of edges in the path from v to the root minus one.*

DEFINITION 2.2.4. *Let T be a plane tree with n non-root vertices. The reading word of T_D, denoted by $\mathsf{read}_D(T)$, is defined by the following algorithm:*

(1) Start by setting $\mathsf{read}_D(T)$ to be an empty vector. Append the label of the root.
(2) If the length of $\mathsf{read}_D(T)$ equals $n+1$, then remove the label corresponding to the root from $\mathsf{read}_D(T)$ and output $\mathsf{read}_D(T)$. Otherwise consider the set of all vertices whose vertices have already been added to $\mathsf{read}_D(T)$ but have at least one child whose label has not been added. Find the vertex in this set with the largest label and call the vertex v. Attach to $\mathsf{read}_D(T)$ the label of the leftmost child of v that has not already been added.

This definition is also well-defined as vertices with the same labels will never be considered at the same time.

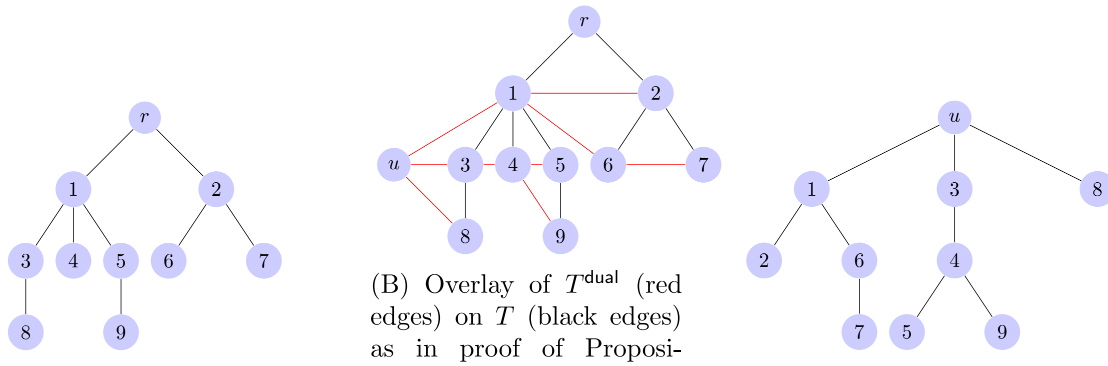

(A) T with labels.

(B) Overlay of T^{dual} (red edges) on T (black edges) as in proof of Proposition 2.2.2.

(C) T^{dual} with labels.

FIGURE 2.4. Construction of the dual plane tree T^{dual} of the plane T in Figure 2.2A.

EXAMPLE 2.2.2. *The labelling T_D of the tree T in Figure 2.2A is given in Figure 2.3B. The corresponding reading word is* $\mathsf{read}_D(T) = (0, 1, 2, 1, 1, 2, 0, 1, 1)$.

DEFINITION 2.2.5. *Let T be a plane tree. Let the k-th child of a vertex v be the k-th leftmost child of v. We define the* dual plane tree *of T, denoted by T^{dual}, by the following algorithm:*

(1) ***Initialization:*** *Set T^{dual} to be a single vertex u which we label as the root of T^{dual}. If the root of T has a child, then add a child to u of T^{dual}. Set this to be the 1-st child of u and associate this child with the 1-st child of the root in T.*

(2) ***Determining if a non-root vertex v in T^{dual} has a child:*** *Look at the associated vertex v' of v in the original plane tree T. If v' has a sibling to its right, then attach a child to v which will be the 1-st child of v. Associate the child of v in T^{dual} with the sibling directly right of v' in T. If v' has no sibling to its right, then v has no children.*

(3) ***Determining if a vertex v (including the root) in T^{dual} has a k-th child for $k > 1$:*** *Let w be the $(k-1)$-th child of v. Look at the associated vertex w' of w in T. If w' has a child, then attach a k-th child to v. Associate the k-th child of v to the 1-st child of w'. If w' has no children, then v has no k-th child.*

EXAMPLE 2.2.3. *The dual plane tree T^{dual} of the plane tree T in Figure 2.2A is given in Figure 2.4C. Observe, by comparing with Figure 2.2, that in this example $T^{\mathsf{dual}} = \eta \circ \sigma^{-1}(T)$. This will be proved in general in Corollary 2.2.2.*

It is easy to see that $T^{\mathsf{dual}} \in \mathcal{T}_n$ by observing that every non-root node of T is paired with a non-root node of T^{dual}, there are no loops in T^{dual}, and the children of every vertex are given a proper ordering. To show that the term dual plane tree is not a misnomer, we also prove that this operation is an involution.

PROPOSITION 2.2.2. *Let T be a plane tree. Then $(T^{\mathsf{dual}})^{\mathsf{dual}} = T$.*

PROOF. Draw the plane tree T in the canonical way with every vertex sitting above all of its descendants and the order of its children increasing from left to right. Next place the root of T^{dual} to the left of all vertices in T and draw the plane tree T^{dual} on top of T such that any vertex in T^{dual} is drawn on top of its corresponding vertex in T. Under this configuration all vertices in T^{dual} sit to the left of their descendants, and the order of their children increase from top to bottom. Since a vertex v and its corresponding vertex v' lie on top of each other in the specified configuration, we will abuse notation and refer to both as vertex v. Interchanging the position of the two trees (i.e. flipping the plane along the perpendicular bisector of the two root nodes), we clearly see that for a vertex v in T its first child corresponds to the sibling on the right of v in T^{dual} and its k-th child corresponds to the first sibling of the $(k-1)$-th child of v for $k > 1$. Thus, $(T^{\mathsf{dual}})^{\mathsf{dual}} = T$. $\square$

The two reading words are related under the dual map on plane trees.

PROPOSITION 2.2.3. *Let T be a plane tree. Then*

$$\mathsf{read}_D(T^{\mathsf{dual}}) = \mathsf{read}_A(T) \quad \textit{and} \quad \mathsf{read}_A(T^{\mathsf{dual}}) = \mathsf{read}_D(T).$$

PROOF. It suffices to prove that $\mathsf{read}_D(T) = \mathsf{read}_A(T^{\mathsf{dual}})$ since this implies that $\mathsf{read}_D(T^{\mathsf{dual}}) = \mathsf{read}_A((T^{\mathsf{dual}})^{\mathsf{dual}})$ which equals $\mathsf{read}_A(T)$ by Proposition 2.2.2.

Let $\mathsf{read}_D(T) = (r_1, r_2, \dots, r_n)$ and $\mathsf{read}_A(T^{\mathsf{dual}}) = (s'_1, s'_2, \dots, s'_n)$. Let v_i be the vertex in T that has label r_i. Similarly, let w_i be the vertex in T^{dual} that has label s'_i. We will prove by induction that $(r_1, r_2, \dots, r_k) = (s'_1, s'_2, \dots, s'_k)$ and that w_k corresponds to v_k under dual for $1 \leqslant k \leqslant n$. We have that both w_1 and v_1 are the leftmost child of their respective root nodes and the labelling of each is equal to zero. By the definition of T^{dual}, we have w_1 corresponds to v_1. Assume that $(r_1, r_2, \dots, r_k) = (s'_1, s'_2, \dots, s'_k)$ and that w_k corresponds to v_k. If v_{k+1} is a child of v_k, then $r_{k+1} = r_k + 1$. Note that by definition of T^{dual}, w_k must have a sibling to its right.

This implies that w_{k+1} is the sibling directly right of w_k and w_{k+1} corresponds to v_{k+1}. We have $r_{k+1} = r_k + 1 = s'_k + 1 = s'_{k+1}$. If v_{k+1} is not a child of v_k, then v_{k+1} is the leftmost unvisited child of y, where $y = v_i$ for some $1 \leqslant i < k$ and y has the largest label out of all parents with unvisited children. Note as v_k does not have any children, w_k has no siblings to its right. Thus, to find w_{k+1} we look for the leftmost child of the vertex x, where $x = w_\ell$ for some $1 \leqslant \ell \leqslant k$ and x has the largest label out of all parents with unvisited children. The condition that x has unvisited children in T^{dual} implies that the parent of its corresponding vertex $x' = v_\ell$ in T has an unvisited child. Thus the parent of x' either is y or has label smaller than y. If it has a label smaller than y then by the definition of T^{dual} and our inductive hypothesis, there exists v_j with $1 \leqslant 1 \leqslant k$ that has unvisited children and label strictly greater than x which is a contradiction. Therefore x' is the rightmost visited child of y and the leftmost child of x corresponds to the sibling to the right of x'. This implies that w_{k+1} corresponds with v_{k+1} and $w_{k+1} = w_\ell = v_\ell = v_{k+1}$. $\square$

2.2.3. Symmetry of $F_n(q,t)$ and $G_n(q,t)$. In this section, we prove the symmetry of the polynomials $F_n(q,t)$ and $G_n(q,t)$. We do so by defining an involution on Dyck paths using the Stanley and Haglund–Loehr maps σ and η, which switches the area and depth statistics. We begin by relating the area and depth sequences under the Stanley and Haglund–Loehr maps using the two reading words above. Recall that $a_i(\pi)$ and $d_i(\pi)$ are defined in Sections 2.1.1 and 2.1.2.

Proposition 2.2.4. *Let $\pi \in D_n$. Then*

$$\mathsf{read}_D(\sigma(\pi)) = (a_1(\pi), a_2(\pi), \ldots, a_n(\pi)),$$

$$\mathsf{read}_A(\sigma(\pi)) = (d_1(\pi), d_2(\pi), \ldots, d_n(\pi)).$$

Proof. Let $(r_1, r_2, \ldots, r_n) = \mathsf{read}_D(\sigma(\pi))$. We use induction on $1 \leqslant k \leqslant n$ to prove that

$$(r_1, r_2, \ldots, r_k) = (a_1(\pi), a_2(\pi), \ldots, a_k(\pi))$$

and the k-th vertex (excluding the root) added in the creation of $\sigma(\pi)$ corresponds to the vertex with label r_k. Observe that r_1 corresponds to the label of the leftmost child of the root node. Note that this is the first node added in $\sigma(\pi)$. Thus, $r_1 = 0 = a_1(\pi)$. Assume that $(r_1, r_2, \ldots, r_k) = (a_1(\pi), a_2(\pi), \ldots, a_k(\pi))$ and r_k is the label of the k-th vertex v_k added in the creation of $\sigma(\pi)$

excluding the root. If the $(k+1)$-th vertex v_{k+1} added to $\sigma(\pi)$ is a child of v_k, then in the Dyck path $a_{k+1}(\pi) = a_k(\pi) + 1$. Since the label of v_k was added last to $(r_1, \ldots, r_k)$, we know that in the previous step the parent of v_k had the largest label out of all parents containing a child whose label was not already appended to the reading word. As v_k has a larger label than its parent and contains a child v_{k+1}, r_{k+1} is the label of the leftmost available child of v_k which would coincide with v_{k+1}. We have the label of v_{k+1} is one more than v_k giving us $r_{k+1} = r_k + 1 = a_k(\pi) + 1 = a_{k+1}(\pi)$. Now assume that v_{k+1} is not a child of v_k. In the Dyck path, this corresponds to a block of East steps after the k-th North step. Let ℓ denote the size of this block of East steps. We see that $a_{k+1}(\pi) = a_k(\pi) + \ell - 1$. In the tree, this corresponds to going ℓ vertices towards the root along the path from v_k to the root and attaching a new vertex v_{k+1} to this vertex w. Note that this implies that v_k and all vertices strictly between v_k and w do not have any additional children that have not already been added. This implies that w has the largest label of all vertices that contain a child whose label has not been appended to the reading word. Thus, r_{k+1} corresponds to the label of v_{k+1} which is one more than the label of w. Thus, $r_{k+1} = r_k - \ell + 1 = a_k(\pi) - \ell + 1 = a_{k+1}(\pi)$. By induction, we obtain $\mathsf{read}_D(\sigma(\pi)) = (a_1(\pi), a_2(\pi), \ldots, a_n(\pi))$.

Let $(s_1, s_2, \ldots, s_n) = \mathsf{read}_A(\sigma(\pi))$. Similar to the previous paragraph, we use induction on $1 \leqslant k \leqslant n$ to prove that

$$(s_1, s_2, \ldots, s_k) = (d_1(\pi), d_2(\pi), \ldots, d_k(\pi))$$

and the North step corresponding to $d_k(\pi)$ created the vertex v corresponding to the label s_k in $\sigma(\pi)$. We have that $d_1(\pi) = 0$ corresponds to the first North step which created the leftmost child of the root node. Note that $s_1 = 0$ and also corresponds to the leftmost vertex of the root node. Assume that $(s_1, s_2, \ldots, s_k) = (d_1(\pi), d_2(\pi), \ldots, d_k(\pi))$ and the North step corresponding to $d_k(\pi)$ in the Dyck path created the vertex v_k corresponding to the label s_k in $\sigma(\pi)$. If the vertex v_{k+1} corresponding to s_{k+1} is a sibling of v_k then $s_{k+1} = s_k + 1$. By the previous paragraph, siblings correspond to North steps on the same diagonal. Note that no other North step can lie between the diagonal connecting the North step N_k of v_k and the North step N_{k+1} of v_{k+1} (keep in mind that N_k does not mean the k-th North step of π). Also, N_{k+1} needs to be the bottommost North step in its column, otherwise v_k and v_{k+1} would not be siblings in $\sigma(\pi)$. Since the depth label $d_k(\pi)$ corresponds to N_k, we have that $d_{k+1}(\pi)$ is the labelling of N_{k+1}. Thus,

$d_{k+1}(\pi) = d_k(\pi) + 1 = s_k + 1 = s_{k+1}$. Assume that the vertex v_{k+1} corresponding to s_{k+1} is not a sibling of v_k. This implies that v_{k+1} is the leftmost child of the vertex w with the largest labelling in $(s_1, s_2, \ldots, s_k)$ whose children's labels have not been added yet. Looking at the North step N_k corresponding to d_k, we have that the first North step reached by traveling northeast from N_k is not in the bottom of its column. Thus to find the North step corresponding to $d_{k+1}(\pi)$, we must find the largest labeled cell visited by $(d_1(\pi), d_2(\pi), \ldots, d_k(\pi))$ that has a labelled cell directly above which has not been visited. Note that having a labeled cell directly above corresponds to having a child. Thus the North step corresponding to $d_{k+1}(\pi)$ is the same as the North step corresponding to v_{k+1} and is one cell directly above the North step corresponding to w. Note that the labelling of w is s_i and the labelling of its corresponding North step is $d_i(\pi)$ for some $1 \leqslant i \leqslant n$. As v_{k+1} is the leftmost child of w, we have $s_{k+1} = s_i$. Similarly, as $d_{k+1}(\pi)$ lies in the same column as $d_i(\pi)$, we have $d_{k+1}(\pi) = d_i(\pi)$. By induction $d_i(\pi) = s_i$, implying $d_{k+1}(\pi) = s_{k+1}$. By induction we obtain $\mathsf{read}_A(\sigma(\pi)) = (d_1(\pi), d_2(\pi), \ldots, d_n(\pi))$. □

PROPOSITION 2.2.5. *Let $\pi \in D_n$. Then*

$$\mathsf{read}_A(\eta(\pi)) = (a_1(\pi), a_2(\pi), \ldots, a_n(\pi)),$$

$$\mathsf{read}_D(\eta(\pi)) = (d_1(\pi), d_2(\pi), \ldots, d_n(\pi)).$$

PROOF. The first equality can be easily seen from the results in [**40**].

We prove the second equality by induction. Let $(r_1, r_2, \ldots, r_n) = \mathsf{read}_D(\eta(\pi))$. We prove that $(r_1, r_2, \ldots, r_k) = (d_1(\pi), d_2(\pi), \ldots, d_k(\pi))$ for $1 \leqslant k \leqslant n$ and the North step corresponding to $d_k(\pi)$ created the vertex v corresponding to the label r_k in $\eta(\pi)$. We have that $d_1(\pi) = 0$ and it lies to the right of the first North step. The first North step under the map η creates the leftmost child of the root which is precisely the vertex whose label is $r_1 = 0$. Assume that $(r_1, r_2, \ldots, r_k) = (d_1(\pi), d_2(\pi), \ldots, d_k(\pi))$ and the North step corresponding to $d_k(\pi)$ created the vertex v_k whose label is r_k. Let v_{k+1} be the vertex whose label is r_{k+1}. Also define N_k and N_{k+1} to be the North steps that created v_k and v_{k+1}, respectively. Assume that the vertex v_{k+1} is a child of v_k. As v_{k+1} is a child of v_k, we obtain $r_{k+1} = r_k + 1$. By the definition of read_D, we have that v_{k+1} is the leftmost child of v_k. This implies that their A label is the same. Since $\mathsf{read}_A(\eta(\pi)) = (a_1(\pi), a_2(\pi), \ldots, a_n(\pi))$, we have the North steps that created v_k and v_{k+1} under η

lie on the same diagonal. By the definition of η, we have that N_{k+1} must be at the bottom of its column and no other North step lies between the N_k and N_{k+1}. Thus $d_{k+1}(\pi)$ is the depth labelling of N_{k+1} which satisfies $d_{k+1}(\pi) = d_k(\pi) + 1 = r_k + 1$. Assume now that v_{k+1} is not a child of v_k which implies by the definition of read_D that v_k does not have any children. Consider the subset S' of $S = \{v_1, v_2, \ldots, v_k\}$ containing all vertices with a child that is not also in S. Let w be the vertex in S' with the largest label. We have that v_{k+1} is the leftmost child of w that is not in S. As v_k does not have a child, the first North step attained by traveling Northeast from N_k is not at the bottom of its column or does not exist. Thus to find N_{k+1}, we must find the largest labeled cell visited by $(d_1(\pi), d_2(\pi), \ldots, d_k(\pi))$ that has a labelled cell directly above which has not been visited. Note that having two North steps consecutively corresponds to them being siblings under η. Additionally, observe that the vertex in S with the largest label out of vertices in S containing a sibling not in S is a child of w. Thus v_{k+1} and the node created by N_{k+1} are the same. All the children of w have the same D labelling, and depth labelings in the same column of π are equal. Paired with the inductive hypothesis, this implies $r_{k+1} = d_{k+1}$. □

We are now ready to show that combining the Stanley and Haglund–Loehr maps gives an involution that interchanges area and depth.

Proposition 2.2.6. *Let $\omega = \sigma^{-1} \circ \eta \colon D_n \to D_n$. Then ω is an involution which interchanges the depth and area sequence.*

Proof. By Propositions 2.2.4 and 2.2.5 we have that

$$(d_1(\omega(\pi)), d_2(\omega(\pi)), \ldots, d_n(\omega(\pi))) = (a_1(\pi), a_2(\pi), \ldots, a_n(\pi)),$$

$$(a_1(\omega(\pi)), a_2(\omega(\pi)), \ldots, a_n(\omega(\pi))) = (d_1(\pi), d_2(\pi), \ldots, d_n(\pi)).$$

Additionally, we have $(a_1(\omega^2(\pi)), a_2(\omega^2(\pi)), \ldots, a_n(\omega^2(\pi))) = (d_1(\omega(\pi)), d_2(\omega(\pi)), \ldots, d_n(\omega(\pi)))$ implying $(a_1(\omega^2(\pi)), a_2(\omega^2(\pi)), \ldots, a_n(\omega^2(\pi))) = (a_1(\pi), a_2(\pi), \ldots, a_n(\pi))$. Since the area sequence uniquely determines a Dyck path, we have that ω is an involution. □

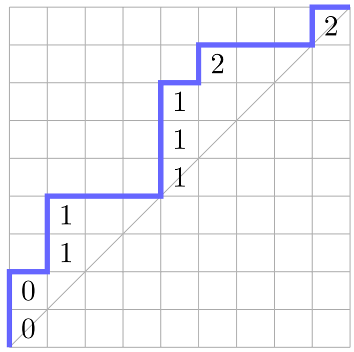

FIGURE 2.5. $w(\pi)$ with π as in Figure 2.1 with depth labelling.

EXAMPLE 2.2.4. *Consider the Dyck path π in Figure 2.1 with area and depth sequences (see also Example 2.1.1)*

$$a(\pi) = (0,1,2,1,1,2,0,1,1) \quad \textit{and} \quad d(\pi) = (0,1,1,2,0,1,2,2,0).$$

Then $\omega(\pi)$ is given in Figure 2.5 and it is easy to check that $a(\omega(\pi)) = d(\pi)$ and $d(\omega(\pi)) = a(\pi)$.

COROLLARY 2.2.1. *Let $\pi \in D_n$. Then $\omega(\pi) = \sigma^{-1}((\sigma(\pi))^{\mathsf{dual}}) = \eta^{-1}((\eta(\pi))^{\mathsf{dual}})$.*

PROOF. By Proposition 2.2.6, it suffices to prove that the area sequences of $\sigma^{-1}((\sigma(\pi))^{\mathsf{dual}})$ and $\eta^{-1}((\eta(\pi))^{\mathsf{dual}})$ are equal to the depth sequence of π. Using Propositions 2.2.3, 2.2.4, and 2.2.5, we observe that this is indeed the case. $\square$

COROLLARY 2.2.2. *Let $T \in \mathcal{T}_n$. Then $T^{\mathsf{dual}} = \eta \circ \sigma^{-1}(T)$.*

PROOF. This follows directly from Proposition 2.2.6 and Corollary 2.2.1. $\square$

Finally, we are ready to prove the symmetry of $F_n(q,t)$ and $G_n(q,t)$.

THEOREM 2.2.1. *We have*

$$F_n(q,t) = F_n(t,q) \qquad \textit{and} \qquad G_n(q,t) = G_n(t,q).$$

PROOF. By Proposition 2.2.6, ω is a bijection on D_n that interchanges the area and depth sequence of a Dyck path. As area and depth are defined as the sum of their respective sequences, we have that ω interchanges area and depth, thereby proving symmetry of $F_n(q,t)$.

By (2.1.2) and (2.1.7), the definitions of dinv and ddinv are identical except with the area and depth sequence interchanged. Since by Proposition 2.2.6 the involution ω interchanges the area and depth sequences, ω also interchanges dinv and ddinv. Thus, $G_n(q,t)$ is symmetric in q and t. □

From a similar argument, we obtain the following corollary.

Corollary 2.2.3. *We have*

$$\mathrm{Cat}_n(q,t) = \sum_{\pi \in D_n} q^{\mathsf{depth}(\pi)} t^{\mathsf{ddinv}(\pi)}.$$

2.2.4. The Deutsch involution and ω. We now define an involution $(\cdot)'$ on Dyck paths first introduced by Deutsch in [**25**].

Definition 2.2.6. *We define $(\cdot)' \colon D_n \to D_n$ recursively as follows:*

(1) $\varepsilon' = \varepsilon$, where ε is the empty Dyck word.

(2) For $\pi \in D_n$ and $n \geqslant 1$, write $\pi = N\alpha E\beta$, where α and β are Dyck words. Note that α, β are allowed to be empty. Then define $\pi' = N\beta' E\alpha'$.

The map $\omega = \sigma^{-1} \circ \eta$ gives an explicit description of Deutsch's recursive operator as we first observed using FindStat [**81**].

Proposition 2.2.7. *Let $\pi \in D_n$. Then $\omega(\pi) = \pi'$.*

Proof. By Proposition 2.2.6, it suffices to prove that

$$(d_1(\pi), d_2(\pi), \ldots, d_n(\pi)) = (a_1(\pi'), a_2(\pi'), \ldots, a_n(\pi')).$$

We proceed by induction on n. We have that both the area and depth sequence of ε are $\emptyset$. Assume that $(d_1(\pi), d_2(\pi), \ldots, d_j(\pi)) = (a_1(\pi'), a_2(\pi'), \ldots, a_j(\pi'))$ for all $\pi \in D_j$, where $0 \leqslant j \leqslant n$. Let $\pi \in D_{n+1}$ and let α and β be Dyck words such that $\pi = N\alpha E\beta$. Let $k-1$ be the semilength of α. We have that (k,k) is the first time the path π touches the diagonal after $(0,0)$. From the definition of the depth labelling and the argument in the proof of Proposition 2.2.1, we have $(d_1(\pi), d_2(\pi), \ldots, d_{n+1}(\pi)) = (0, d_1(\beta)+1, d_2(\beta), \ldots, d_{n+1-k}(\beta), d_1(\alpha), d_2(\alpha), \ldots, d_{k-1}(\alpha))$. From the definition of the area sequence and $(\cdot)'$, we have that $(a_1(\pi'), a_2(\pi'), \ldots, a_{n+1}(\pi')) = (0, a_1(\beta')+$

$1, a_2(\beta') + 1, \ldots, a_{n+1-k}(\beta') + 1, a_1(\alpha'), a_2(\alpha'), \ldots, a_{k-1}(\alpha'))$. Note that α and β have semilength strictly less than $n+1$. Hence by induction $(d_1(\beta), \ldots, d_{n+1-k}(\beta)) = (a_1(\beta'), \ldots, a_{n+1-k}(\beta'))$ and $(d_1(\alpha), d_2(\alpha), \ldots, d_{k-1}(\alpha)) = (a_1(\alpha'), a_2(\alpha'), \ldots, a_{k-1}(\alpha'))$. Thus, $(d_1(\pi), d_2(\pi), \ldots, d_{n+1}(\pi)) = (a_1(\pi'), a_2(\pi'), \ldots, a_{n+1}(\pi'))$. $\square$

Using Corollary 2.2.1 and Proposition 2.2.7, we find a relation between the $(\cdot)^{\mathsf{dual}}$ operator defined on plane trees and the one defined on Dyck paths.

Corollary 2.2.4. *The following diagram commutes:*

$$\begin{tikzcd}
D_n \arrow[r, leftrightarrow, "(\cdot)'"] \arrow[d, "\sigma\ or\ \eta"'] & D_n \arrow[d, "\sigma\ or\ \eta"] \\
\mathcal{T}_n \arrow[r, leftrightarrow, "(\cdot)^{\mathsf{dual}}"] & \mathcal{T}_n.
\end{tikzcd}$$

Deutsch proved [**25**] that the operator $(\cdot)'$ interchanges the initial rise (IR) of a Dyck path (the number of North steps before the first East step) with its number of returns (RET) (the number of times the Dyck path touches the diagonal excluding the point $(0,0)$). We see that the initial rise and the number of returns of a Dyck path correspond to the length of the leftmost path from the root to a leaf and the number of children of the root, respectively, under σ (and vice versa under η). This gives an alternate explanation of the symmetry of the *Tutte polynomial*

$$T_{\mathsf{Cat}_n}(q,t) = \sum_{\pi \in D_n} q^{\mathsf{IR}(\pi)} t^{\mathsf{RET}(\pi)}$$

associated with the Catalan matroid Cat_n defined in [**3**].

Stump [**91**] proved that the coefficient of $q^a t^b$ of $T_{\mathsf{Cat}_n}(q,t)$ only depends on the sum $a+b$ using a map given by Speyer [**86**]. This map τ fixes Dyck paths π, where $\mathsf{RET}(\pi) = 1$ and sends Dyck words $\pi = N\alpha_1 E N\alpha_2 E N\alpha_3 E \ldots N\alpha_k E$ to $NN\alpha_1 E\alpha_2 E N\alpha_3 E \ldots N\alpha_k E$, where $\mathsf{RET}(\pi) = k > 1$ and α_i is a Dyck word that is possibly empty. Speyer's map has a nice relation with ω as follows.

Proposition 2.2.8. *Let $\pi \in D_n$. Then $\tau^{-1} \circ \omega(\pi) = \omega \circ \tau(\pi)$.*

Proof. If $\mathsf{RET}(\pi) = 1$, then $\tau(\pi) = \pi$ and $\omega \circ \tau(\pi) = \omega(\pi)$. As ω interchanges initial rises and the number of returns, we have $\mathsf{IR}(\omega(\pi)) = 1$. This implies that $\tau^{-1} \circ \omega(\pi) = \omega(\pi)$. Thus, we have $\tau^{-1} \circ \omega(\pi) = \omega \circ \tau(\pi)$.

If $\mathsf{RET}(\pi) = k > 1$, let $\pi = N\alpha_1 EN\alpha_2 EN\alpha_3 E \ldots N\alpha_k E$, where α_i is a possibly empty Dyck word. We show $\omega(\pi) = \tau \circ \omega \circ \tau(\pi)$. From Definition 2.2.6 and Proposition 2.2.7

$$\omega(\pi) = N(N\alpha_2 EN\alpha_3 E \ldots N\alpha_k E)' E\alpha_1'.$$

On the other hand,

$$\begin{aligned}
\tau(\pi) &= NN\alpha_1 E\alpha_2 EN\alpha_3 E \ldots N\alpha_k E, \\
\omega \circ \tau(\pi) &= N(N\alpha_3 E \ldots N\alpha_k E)' E(N\alpha_1 E\alpha_2)' \\
&= N(N\alpha_3 E \ldots N\alpha_k E)' EN\alpha_2' E\alpha_1', \\
\tau \circ \omega \circ \tau(\pi) &= NN(N\alpha_3 E \ldots N\alpha_k E)' E\alpha_2' E\alpha_1' \\
&= N(N\alpha_2 EN\alpha_3 E \ldots N\alpha_k E)' E\alpha_1'.
\end{aligned}$$

Hence, $\omega(\pi) = \tau \circ \omega \circ \tau(\pi)$. $\square$

CHAPTER 3

Combinatorial proof of a symmetry on refined Narayana numbers

This chapter is based on work in collaboration with Miklós Bóna, Stoyan Dimitrov, Gilbert Labelle, Yifei Li, Andrés R. Vindas-Meléndez, and Yan Zhuang in [**11**].

3.1. Background and Definitions

In Section 3.1.1 we review the Narayana numbers and a refinement that we will be interested in. In Section 3.1.2 we define cyclic compositions and review the cycle lemma which will be needed for the proofs in subsequent sections.

3.1.1. Narayana numbers.

Given a word w in the alphabet $\{N, E\}$, we say that $\pi \in D_n$ has a *w-factor* if its associated Dyck word contains w as a substring. The *Narayna numbers* $N_{n,k} = \frac{1}{n}\binom{n}{k}\binom{n}{k-1}$ are known to count the number of Dyck paths of semilength n that contain exactly k NE-factors (or *peaks*). Moreover, the Narayna numbers are known to exhibit the symmetry $N_{n,k} = N_{n,n+1-k}$, which can be proved combinatorially via several involutions; see, for example, [**55, 56, 58**]. In fact the Deutsch involution defined in Definition 2.2.6 was shown in [**25**] to also exhibit this symmetry.

In an effort to explore the joint distribution of occurrences of overlapping factors, Bóna and Labelle [**11**] defined a refinement of the Narayana numbers given by $w_{n,k,m}$ which count the number of Dyck paths of semilength n with k NE-factors and m NNE-factors. As these factors overlap, each NNE-factor will contain a NE-factor implying $w_{n,k,m} = 0$ whenever $m > k$. Using generating function techniques, Bóna and Labelle derived the following theorem giving a closed formula for the numbers $w_{n,k,m}$.

Theorem 3.1.1. *[**11, 59, 96**] We have*

$$w_{n,k,m} = \begin{cases} \frac{1}{k}\binom{n}{k-1}\binom{n-k-1}{m-1}\binom{k}{m}, & \text{if } m > 0,\ m \leq k, \text{ and } k+m \leq n, \\ 1, & \text{if } m = 0 \text{ and } n = k, \\ 0, & \text{otherwise.} \end{cases}$$

Remark 3.1.1. *The closed formula for $w_{n,k,m}$ can also be obtained via results from Wang [**96**] and Lemus-Vidales [**59**].*

Furthermore, Bóna and Labelle observed that when $n = 2k+1$, the numbers $w_{n,k,m}$ satisfy a symmetry similar to that of the Narayana numbers.

Theorem 3.1.2. *[**11**] For all $1 \leq m \leq k$, we have $w_{2k+1,k,m} = w_{2k+1,k,k+1-m}$.*

While Theorem 3.1.2 can readily be seen from Theorem 3.1.1, it remained open to give a combinatorial proof of this symmetry and of the closed formula. Such proofs will be given in Section 3.2.1 and Section 3.3.1 respectively.

As in Chapter 2, it will be useful to reinterpret these statistics on Dyck paths in terms statistics on plane trees. Given a non-root vertex v of a plane tree T, we say that v is a *leaf* of T if it has no children. In particular, the root is not considered to be a leaf even if T is the plane tree consisting solely of the root. We say that a leaf v is a *good leaf* if v is the leftmost child of a non-root vertex. See Figure 3.1 for an example of a plane tree with its good leaves circled. We have the following interpretation of the numbers $w_{n,k,m}$ in terms of plane trees which can readily be seen by using the Stanley map σ given in Definition 1.2.1 between Dyck paths and plane trees.

Proposition 3.1.1. *The number $w_{n,k,m}$ counts the number of plane trees with n non-root vertices, k leaves, and m good leaves.*

3.1.2. Cyclic compositions and the cycle lemma. Given a sequence $p = p_1p_2\cdots p_n$, we say that a sequence p' is a *cyclic shift* (or *cyclic rotation*) of p if p' is of the form

$$p' = p_ip_{i+1}\cdots p_np_1p_2\cdots p_{i-1}$$

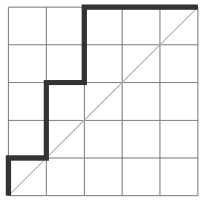

(A) Dyck path of semilength 5 with 3 NE-factors and 2 NNE-factors.

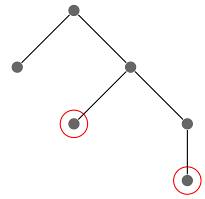

(B) Plane tree on 5 non-root vertices with 3 leaves and 2 good leaves (circled in red).

FIGURE 3.1. Dyck path and its corresponding plane tree under the map σ defined in Definition 1.2.1.

for some $1 \le i \le n$. Let us write $p \sim p'$ whenever p and p' are cyclic shifts of each other.

Let $\mathsf{Comp}_{n,k}$ denote the set of all compositions of n into k parts, i.e., a sequence of k positive integers whose sum is n. We define a *cyclic composition* $[\mu]$ to be the equivalence class of a composition μ under cyclic shift. Let $\mathsf{CComp}_{n,k}$ be the set of cyclic compositions consisting of compositions of n into k parts, which is well-defined because the number of parts of a composition and the sum of its parts are clearly invariant under cyclic shift. Let us say that an element of $\mathsf{CComp}_{n,k}$ is a cyclic composition of n into k parts.

We define the *order* of a cyclic composition $[\mu]$, denoted by $\mathsf{ord}[\mu]$, to be the number of representatives of $[\mu]$—that is, the number of distinct compositions that can be obtained from cyclically shifting μ. Note that applying $\mathsf{ord}[\mu]$ number of cyclic shifts to μ will return back μ. If $[\mu] \in \mathsf{CComp}_{n,k}$ has order k, then we say that $[\mu]$ is *primitive*.

For any $[\mu] \in \mathsf{CComp}_{n,k}$, there exists a positive integer d dividing both n and k such that $[\mu]$ is a *concatenation* of d copies of a primitive cyclic composition $[\nu] \in \mathsf{CComp}_{n/d,k/d}$, which means that there exists $\bar{\nu} \in [\nu]$ for which μ is a concatenation of d copies of $\bar{\nu}$. In this case, $\mathsf{ord}[\mu] = k/d = \mathsf{ord}[\nu]$. (If $d = 1$, then $[\mu]$ itself is primitive and is a concatenation of itself.) For example, the cyclic composition $[1, 2, 1, 1, 2, 1]$ is a concatenation of two copies of the primitive cyclic composition $[1, 2, 1]$, and both of these cyclic compositions have order 3. It is easy to see that this decomposition of cyclic compositions into primitive cyclic compositions is unique.

LEMMA 3.1.1. *If n and k are relatively prime, then $[\mu] \in \mathsf{CComp}_{n,k}$ is primitive.*

Proof. Let $[\mu] \in \mathsf{CComp}_{n,k}$. Then $[\mu]$ can be uniquely decomposed as a concatenation of d copies of a primitive cyclic composition, where d is a common divisor of n and k. Since n and k are relatively prime, it follows that $d = 1$, whence it follows that $[\mu]$ itself is primitive. $\square$

The cycle lemma will play an important role in our proofs. Given a positive integer k and a sequence $p = p_1 p_2 \cdots p_l$ consisting only of Ns and Es, we say that p is *k-dominating* if every prefix of p—that is, every sequence $p_1 p_2 \cdots p_i$ where $1 \leq i \leq l$—has more copies of N than k times the number of copies of E.

Lemma 3.1.2 (Cycle lemma [**28**]). *Let k be a positive integer. For any sequence $p = p_1 p_2 \cdots p_{m+n}$ consisting of m copies of N and n copies of E, there are exactly $m - kn$ cyclic shifts of p that are k-dominating.*

We refer to [**23**] for a proof of the cycle lemma as well as some applications. We note that Raney [**76**] showed that the cycle lemma is equivalent to the Lagrange inversion formula; Raney's proof was later generalized to the multivariate case by Bacher and Schaeffer [**7**].

Corollary 3.1.1 (of the cycle lemma). *Any sequence of k copies of $\bigcirc$ and $k+1$ copies of $\square$ has exactly one cyclic shift with no proper prefix having more $\square$s than $\bigcirc$s.*

Proof. Given any sequence λ of k copies of $\bigcirc$ and $k+1$ copies of $\square$, let $\tilde{\lambda}$ be the reverse sequence of λ—that is, the sequence consisting of the entries of λ but in reverse order. The cycle lemma guarantees that there is exactly one cyclic shift of $\tilde{\lambda}$ that is 1-dominating. The reverse sequence of this 1-dominating cyclic shift is the cyclic shift of λ that has no proper prefix having more $\square$s than $\bigcirc$s. $\square$

3.2. Combinatorial proofs of symmetry

In Section 3.2.1, we relate the numbers $w_{n,k,m}$ to the Narayana numbers $N_{k,m}$ when $n = 2k+1$. This will in turn give a combinatorial proof of the desired symmetry in Theorem 3.1.2. In Section 3.2.1, we prove the numbers $w_{n,k,m}$ satisfy a related symmetry when $n = 2k-1$.

3.2.1. Combinatorial proof of Theorem 3.1.2. We focus our attention on finding a combinatorial proof of Theorem 3.1.2. See Figure 3.2 for an example—using the plane tree interpretation of the numbers $w_{n,k,m}$—of the symmetry in Theorem 3.1.2 that we wish to prove. In order to give such a proof, we will give a combinatorial proof of the following theorem which will induce the desired proof for Theorem 3.1.2.

THEOREM 3.2.1. *For all $k \geq 1$ and $m \geq 0$, we have*

$$w_{2k+1,k,m} = \binom{2k+1}{k-1} N_{k,m}. \tag{3.2.1}$$

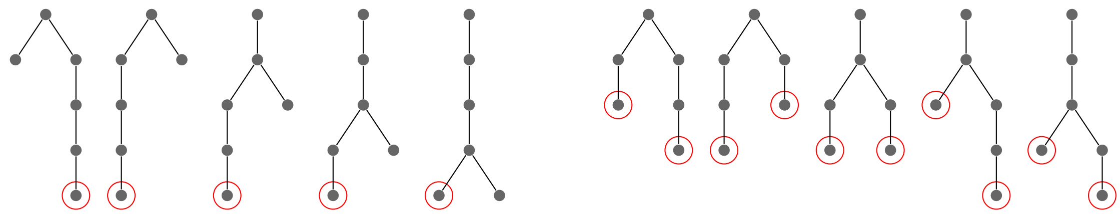

(A) $w_{5,2,1} = 5$ (B) $w_{5,2,2} = 5$.

FIGURE 3.2. Plane trees on 5 non-root vertices with 2 leaves with the good leaves circled.

Our proof will mostly rely on two important lemmas. The first lemma gives a combinatorial interpretation for Narayana numbers in terms of cyclic compositions.

LEMMA 3.2.1. *Let $k \geq 1$ and $m \geq 0$. Then the Narayana number $N_{k,m}$ is the number of cyclic compositions of $2k+1$ into k parts such that exactly m parts are at least 2.*

PROOF. We will give a bijective map that takes a cyclic composition of $2k+1$ into k parts, exactly m of which are at least 2, to a Dyck path of semilength k with m NE-factors, which are counted by the Narayana numbers $N_{k,m}$.

Given a cyclic composition $[\mu_1, \mu_2, \dots, \mu_k]$ of $2k+1$ with exactly m parts that are at least 2, consider the word $N^{\mu_1 - 1} E N^{\mu_2 - 1} E \cdots N^{\mu_k - 1} E$, which has $k+1$ copies of N and k copies of E. By the cycle lemma, there is exactly one cyclic shift of this word that is 1-dominating—that is, with more Ns than Es in every prefix. Then the first two entries of this 1-dominating sequence are necessarily Ns. Removing the first N, we obtain a Dyck path of semilength k with exactly m NE-factors.

It is easily verified that the inverse procedure is given by the following: from a semilength k Dyck path with m NE-factors, we get a sequence $(a_1, a_2, \dots a_k)$ where a_i is the number of Ns that immediately precede the ith E. For example, from $NENNEENE$ we get the sequence $(1, 2, 0, 1)$. Then we add 2 to a_1 and 1 to each other a_i, forming a composition μ of $2k+1$ into k parts, exactly m of which are at least 2. Taking the cyclic composition $[\mu]$ completes the inverse. $\square$

We note that the map used in the proof of Lemma 3.2.1 is related to the standard bijection between Łukasiewicz paths and Dyck paths. A *Łukasiewicz path* of length n is a path in $\mathbb{Z}^2$ with step set $\{(1,-1),(1,0),(1,1),(1,2),\ldots\}$, starting from $(0,0)$ and ending at $(n,0)$, that never traverses below the x-axis; these paths were introduced in relation to the preorder degree sequence of a plane tree, which determines the tree unambiguously [**29**, Chapter 1.5].

The statement and proof of our second lemma are more involved, and will require the notion of "extended leaves" and the decomposition of a plane tree into extended leaves.

Definition 3.2.1. *An* extended leaf *is an unlabeled path graph with exactly one end-vertex designated as the* leaf.[1] *The length of an extended leaf E, denoted by $\ell(E)$, is the number of edges in E.*

Let v_i be the ith leaf, as read from left to right, of a plane tree T with k leaves. Let us now describe the *extended leaf decomposition* of T, which is obtained as follows. For each leaf v_i, we trace the path from v_i to the closer of the two:

(1) the root, or
(2) the closest ancestor of v_i that has two or more children, and v_i is not the leftmost of those children nor a descendant of the leftmost child.

This path is the extended leaf E_i. In other words, to find E_i, we start at the leaf v_i and then trace the path from v_i toward the root until we reach a vertex a that has another child to the left of the path; if no such a exists, we take a to be the root. The path from v_i to a is the extended leaf E_i. The sequence $E_1E_2\cdots E_k$ is the extended leaf decomposition of T; it is not difficult to see that this decomposition is unique.

[1]A path graph has two end-vertices, both of which are typically considered leaves, but in an extended leaf, we only think of one of them as being a leaf.

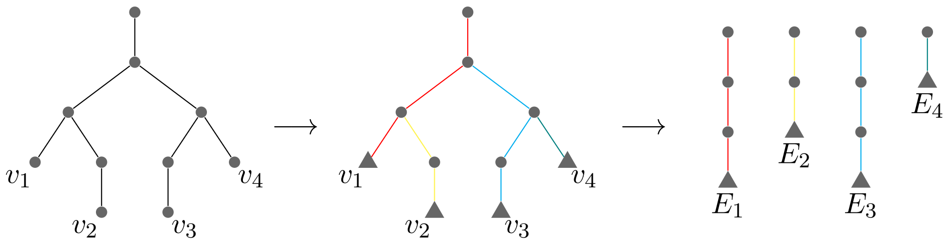

FIGURE 3.3. Decomposition of a plane tree into its extended leaves.

EXAMPLE 3.2.1. *Figure 3.3 shows a decomposition of a plane tree into* 4 *extended leaves,* E_1 *(red),* E_2 *(orange),* E_3 *(blue), and* E_4 *(green), ordered from left to right with* $\ell(E_1) = 3$*,* $\ell(E_2) = 2$*,* $\ell(E_3) = 3$*, and* $\ell(E_4) = 1$*. The triangular nodes represent the leaves of the extended leaves.*

We define a *necklace of extended leaves* (or simply a *necklace*) to be the equivalence class of a sequence of extended leaves under cyclic shift. Often it is more convenient for us to view a necklace as simply a collection of extended leaves with a given cyclic order; it will be clear from context when we do so. Let $\mathsf{Neck}_{n,k}$ denote the set of all necklaces with k extended leaves and a total of n non-leaf vertices. Note that the total number of edges in each of those necklaces is also n.

Let ψ be the map taking a composition $(\mu_1, \mu_2, \ldots, \mu_k)$ of n to the sequence $E_1 E_2 \cdots E_k$ of extended leaves where $\ell(E_i) = \mu_i$ for each i. It is easy to see that ψ is a bijection between compositions of n with k parts and sequences of k extended leaves with a total of n edges; moreover, ψ induces a bijection—which we also denote ψ by a slight abuse of notation—from $\mathsf{CComp}_{n,k}$ to $\mathsf{Neck}_{n,k}$. To be precise, the necklace $\psi[\mu]$ is the equivalence class of $\psi(\bar{\mu})$ for any $\bar{\mu} \in [\mu]$, which clearly does not depend on the choice of representative.

We define a *marking* of a necklace of extended leaves $[E_1, \ldots, E_k]$ to be the necklace $[E_1, \ldots, E_k]$ with $k-1$ non-leaf vertices marked. If $[\mu]$ is primitive—that is, if $\mathsf{ord}[\mu] = k$—then it is easy to see that the necklace $\psi[\mu]$ has $\binom{n}{k-1}$ distinct markings.[2]

LEMMA 3.2.2. *Let* $k \geq 1$*. Given a cyclic composition* $[\mu] \in \mathsf{CComp}_{2k+1,k}$*, there are exactly* $\binom{2k+1}{k-1}$ *plane trees whose extended leaf decomposition belongs to the necklace* $\psi[\mu] \in \mathsf{Neck}_{2k+1,k}$*.*

[2]The skeptical reader may wish to visit Lemma 3.3.1 proven later, which is a more general result from which this claim follows as a special case.

Proof. Let $[\mu] = [\mu_1, \mu_2, \ldots, \mu_k] \in \mathsf{CComp}_{2k+1,k}$ so that $\psi[\mu] = [E_1, E_2, \ldots, E_k]$ is a necklace of k extended leaves with $\ell(E_i) = \mu_i$ for each i and with a total of $2k+1$ non-leaf vertices. Since $2k+1$ and k are relatively prime, Lemma 3.1.1 implies that $[\mu]$ is primitive, so $\psi[\mu]$ has $\binom{2k+1}{k-1}$ distinct markings. We will show that each marking of $\psi[\mu]$ determines a unique plane tree whose extended leaf decomposition belongs to the necklace $\psi[\mu]$. Consequently, we will have $\binom{2k+1}{k-1}$ plane trees that correspond to $\psi[\mu]$. Given a marking of $\psi[\mu]$, we record the $k-1$ marked vertices and k extended leaves using a sequence of $\bigcirc$s and $\square$s as follows. We start with any extended leaf in the necklace $\psi[\mu]$. First record a $\bigcirc$ for each marked vertex on this extended leaf, and then record a $\square$ for this extended leaf. We do the same for the next extended leaf in the cyclic order of $\psi[\mu]$, and this process is repeated until we have traversed through all the marked vertices and extended leaves in $\psi[\mu]$.

We now have a sequence of $k-1$ copies of $\bigcirc$ and k copies of $\square$. It then follows from Corollary 3.1.1 that there is exactly one cyclic shift $\sigma = \sigma_1\sigma_2\cdots\sigma_{2k-1}$ of this sequence whose every proper prefix has at least as many $\bigcirc$s as the number of $\square$s. Note that $\sigma_1 = \bigcirc$ and $\sigma_{2k-2}\sigma_{2k-1} = \square\square$. Then we obtain from σ a sequence $E_1E_2\cdots E_k$ of extended leaves by taking E_1 to be the extended leaf containing the marked vertex corresponding to σ_1, and proceeding in accordance with the cyclic order of $\psi[\mu]$.

We will build a plane tree using the sequence $E_1E_2\cdots E_k$ in the following manner. Henceforth, we make use of the term "*top vertex*" to refer to the vertex on an extended leaf furthest from its leaf, i.e., the other end-vertex of that extended leaf.

(1) Take the root of our tree to be the top vertex of E_1.
(2) Take the marked vertex on E_1 that is furthest from the root—call it v_1—and attach the next extended leaf E_2 to E_1 by identifying the top vertex of E_2 with v_1.
(3) Remove the mark of v_1. The partially-built tree currently has two extended leaves E_1 and E_2.
(4) Attach the next extended leaf E_i to the tree by identifying the top vertex of E_i with the unused marked vertex that is furthest from the root on the current partially-built tree.
(5) Remove the mark of that vertex after attaching E_i.
(6) Repeat (4) and (5) until we have attached all k extended leaves.

There will always be at least one unused marked vertex on a partially-built tree to indicate where the next extended leaf should be attached, because the number of marked vertices (the $\bigcirc$s) will always be at least the number of extended leaves (the $\square$s) that need attaching. Also, note that since we always use the marked vertex that is furthest from the root, there can only be marked vertices on the shortest path connecting the root and the rightmost leaf on a partially-built tree at any stage; thus, there must be a unique marked vertex that is furthest from the root. The $k-1$ marked vertices determine how the extended leaves $E_1, E_2, \ldots, E_k$ are put together, forming a plane tree T having the extended leaf decomposition $E_1 E_2 \cdots E_k$, which belongs to the necklace $\psi[\mu]$.

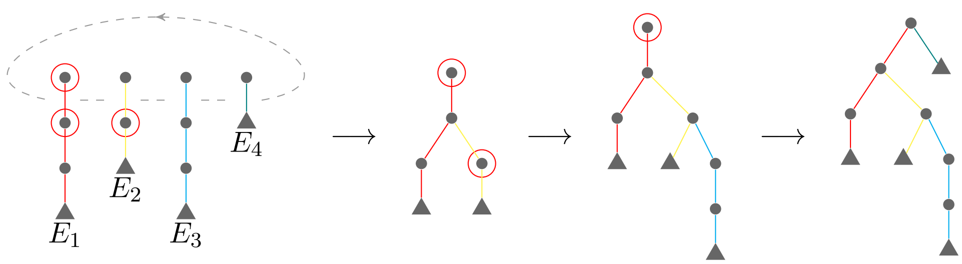

FIGURE 3.4. Building a plane tree using a marked necklace of extendend leaves.

Figure 3.4 illustrates the process of building a tree from a marking of a necklace with four extended leaves. On the left is a marked necklace. The marked vertices are circled and the leaf of each E_i is denoted by a triangular node. The top vertex of E_1 will be the root of this tree. Then E_2 is attached to the marked vertex on E_1 that is furthest from the root, and we remove the mark after attaching E_2 (see the second step in Figure 3.4). Now on the partially-built tree consisting of E_1 and E_2, the furthest unused marked vertex from the root is the one on E_2. In the third step, E_3 is attached to that marked vertex, leaving only one unused marked vertex, which is where we attach E_4 in the last step. Because the choice of E_1 is unique, we can only build one plane tree from our marked necklace.

Conversely, consider a plane tree whose extended leaf decomposition $E_1 E_2 \cdots E_k$ belongs to $\psi[\mu] \in \mathsf{Neck}_{2k+1,k}$. Following the detaching process that is described below, one can retrieve a unique marking of $\psi[\mu]$, which is the marked necklace that determines this tree via the procedure already described above. We detach extended leaves one-by-one from the last (rightmost) extended leaf to the first (leftmost) extended leaf. For each E_i, let j be the largest index less than i such that E_j and E_i share a common vertex. When E_i is detached, the vertex on E_j that is shared with E_i is marked on E_j. Note that this shared vertex is necessarily the top vertex of E_i. All marked vertices are kept on the extended leaf when detaching that extended leaf. We will mark one vertex when detaching each of the $k-1$ extended leaves $E_2, E_3, \ldots, E_k$, which yields a marking of the necklace $\psi[\mu]$.

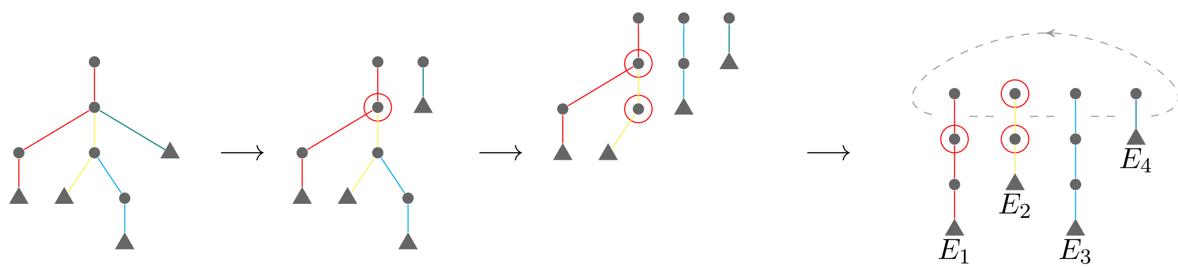

FIGURE 3.5. Retrieving marked vertices from a plane tree.

As shown in Figure 3.5, when E_4 is detached, we mark the vertex on E_2 that is common to E_2 and E_4. This vertex is marked on E_2 not E_1 because $2 > 1$. In other words, E_2 is the closest extended leaf to E_4 that is still on the left of E_4 and shares a common vertex with E_4. Then we detach E_3 and mark the vertex on E_2 that is shared with E_3. When E_2 is detached, the two marked vertices are kept on E_2, and a vertex on E_1 is marked.

It is straightforward to verify that the two procedures described above are inverse bijections between markings of a necklace $\psi[\mu] \in \mathsf{Neck}_{2k+1,k}$ and plane trees whose extended leaf decomposition belong to $\psi[\mu]$. Since there are exactly $\binom{2k+1}{k-1}$ such markings, the conclusion follows. $\square$

We are now ready to complete our combinatorial proof of Theorem 3.2.1.

PROOF OF THEOREM 3.2.1. Recall that $w_{2k+1,k,m}$ counts plane trees with $2k+1$ non-root vertices, k leaves, and m good leaves; these are precisely the plane trees with $2k+1$ non-root vertices whose extended leaf decomposition has k extended leaves, exactly m of which have length at least 2. These extended leaf decompositions belong to necklaces corresponding to cyclic compositions of $2k+1$ into k total parts and m parts at least 2, which are counted by $N_{k,m}$ as established in

Lemma 3.2.1. Furthermore, by Lemma 3.2.2, there are exactly $\binom{2k+1}{k-1}$ plane trees corresponding to each necklace. It follows that $w_{2k+1,k,m} = \binom{2k+1}{k-1} N_{k,m}$ as desired. $\square$

From the proofs of Lemmas 3.2.1 and 3.2.2 we implicitly obtain a bijection that demonstrates the symmetry $w_{2k+1,k,m} = w_{2k+1,k,k+1-m}$. For the sake of completeness, we explicitly write out the bijection that we obtain and give an example in Figure 3.6.

Definition 3.2.2. *Let T be a plane tree with $2k+1$ non-root vertices, k leaves, and m good leaves. Construct a plane tree T' on $2k+1$ non-root vertices, k leaves, and $k+1-m$ good leaves via the following algorithm:*

(1) Set M to be the marked necklace of extended leaves associated to T via Lemma 3.2.2.

(2) Decompose M into a pair consisting of its underlying unmarked necklace of extended leaves $\mathcal{N}$ and a $(k-1)$-subset S of $[2k+1] = \{1, 2, \ldots, 2k+1\}$ containing the positions of the non-leaf vertices marked in M.

(3) Set P to be the Dyck path of semilength k with m NE-factors that is associated to $\mathcal{N}$ via the bijective map in Lemma 3.2.1.

(4) Set P' to be a Dyck path of semilength k with $k+1-m$ NE-factors obtained via any bijection demonstrating the Narayana symmetry (e.g. the Deutsch involution).

(5) Set N' to be the necklace of extended leaves associated to P' via Lemma 3.2.1.

(6) Set M' to be the marked necklace of extended leaves obtained from the necklace $\mathcal{N}'$ and subset S.

(7) Set T' to be the plane tree with $2k+1$ non-root vertices, k leaves, and $k+1-m$ good leaves associated to M' via Lemma 3.2.2.

Remark 3.2.1. *In Steps (2) and (6), there is some choice of how to label the positions of the non-leaf vertices in a necklace $\mathcal{N} \in \mathsf{Neck}_{2k+1,k}$ such that one can pass from a marked necklace to a pair consisting of its underlying unmarked necklace and a $(k-1)$-subset of $[2k+1]$ and vice versa. We detail a choice of labelling that we deem to be canonical. By Lemma 3.2.1, there is a unique ordering $(E_1, E_2, \ldots, E_k)$ of the extended leaves in $\mathcal{N}$ such that $N^{\mu_1-1}EN^{\mu_2-1}E\cdots N^{\mu_k-1}E$ is 1-dominating where $\mu_i = \ell(E_i)$. Starting from the vertex furthest away from the leaf and moving* *inwards, label the non-leaf vertices in E_1 with the numbers $1, 2, \ldots, \mu_1$, label the non-leaf vertices in E_2 with the numbers $\mu_1 + 1, \ldots, \mu_1 + \mu_2$, and so on.*

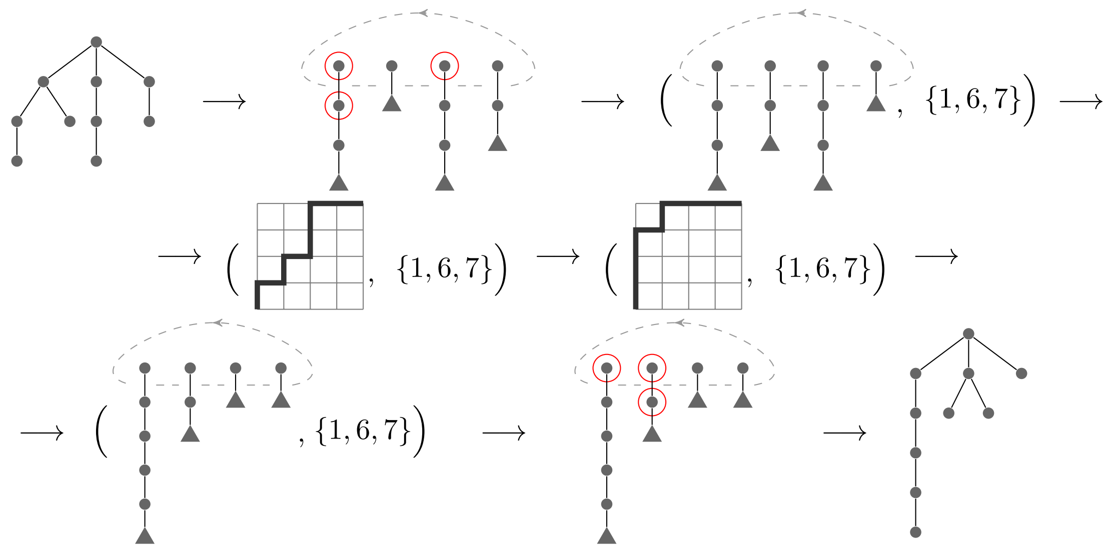

FIGURE 3.6. Example of the bijection given in Definition 3.2.2 for $k = 4$ where the Deutsch involution is used in Step (4).

3.2.2. Combinatorial proof of a related symmetry. In addition to the symmetry in Theorem 3.1.2, it can also be observed that $w_{2k-1,k,m} = w_{2k-1,k,k-m}$ for all $1 \leq m \leq k$, which is a consequence of the following variation of Theorem 3.2.1.

THEOREM 3.2.2. *For all $k \geq 1$ and $m \geq 0$, we have*

$$w_{2k-1,k,m} = \binom{2k-1}{k-1} N_{k-1,m}. \tag{3.2.2}$$

Theorem 3.2.2 can be proven in a way that is completely analogous to our combinatorial proof of Theorem 3.2.1, but relying on Lemmas 3.2.3 and 3.2.4 below.

LEMMA 3.2.3. *Let $k \geq 1$ and $m \geq 0$. Then the Narayana number $N_{k-1,m}$ is the number of cyclic compositions of $2k - 1$ into k parts such that exactly m parts are at least 2.*

PROOF. We follow the proof of Lemma 3.2.1 closely. Given a cyclic composition $[\mu_1, \mu_2, \ldots, \mu_k]$ of $2k - 1$ with exactly m parts that are at least 2, we build a sequence consisting of $k - 1$ copies of N and k copies of E in the same way as in the proof of Lemma 3.2.1. By Corollary 3.1.1, there is exactly one cyclic shift of this sequence such that any proper prefix of the sequence contains at least as many Ns as the number of Es. Then the last entry of this cyclic shift is a E; removing this last E, we obtain a Dyck path of semilength $k-1$ and exactly m NE-factors.

Conversely, consider a Dyck path of semilength $k-1$ with exactly m NE-factors. We append a E to the corresponding Dyck word, and form the sequence $a_1, a_2, \ldots, a_k$, where a_i is the number of Ns that immediately precede the ith E. We then add 1 to every number in this sequence and take the equivalence class of its cyclic shifts, yielding a cyclic composition of $2k-1$ into k parts, exactly m of which are at least 2. $\square$

Lemma 3.2.4. *Let $k \geq 1$. Given a cyclic composition $[\mu] \in \mathsf{CComp}_{2k-1,k}$, there are exactly $\binom{2k-1}{k-1}$ plane trees whose extended leaf decomposition belongs to the necklace $\psi[\mu] \in \mathsf{Neck}_{2k-1,k}$.*

Proof. The proof of Lemma 3.2.2 can be readily adapted to prove Lemma 3.2.4; we omit the details. $\square$

3.3. Combinatorial proofs of generalized formulas

In Section 3.3.1 we give a combinatorial proof for the closed formula of $w_{n,k,m}$ and relate these numbers to Callan's r-generalized Narayana numbers. In 3.3.2, we use our results to give enumerative formulas for the number of cyclic compositions and further generalizations of the numbers $w_{n,k,m}$.

3.3.1. Combinatorial proof of generalized formulas for $w_{n,k,m}$. We have demonstrated a combinatorial proof of Theorem 3.2.1, which expresses the numbers $w_{2k+1,k,m}$ in terms of the Narayana numbers. In fact, the numbers $w_{n,k,m}$, for any $n \neq 2k$, can be expressed in terms of a family of generalized Narayana numbers due to Callan [**18**], and the purpose of this section is to describe how our combinatorial proof for Theorem 3.2.1 can be adapted to prove this more general result. Along the way, we will give a combinatorial proof for our explicit formula for the numbers $w_{n,k,m}$ stated in Theorem 3.1.1.

Given $[\mu] \in \mathsf{CComp}_{n,k}$, let $\mathsf{MNeck}[\mu]$ be the set of all marked necklaces of extended leaves corresponding to the cyclic composition $[\mu]$. In the proof of Lemma 3.2.2, we used the fact that $|\mathsf{MNeck}[\mu]| = \binom{n}{k-1}$ when $[\mu]$ is primitive. More generally, we have the following:

Lemma 3.3.1. *Given $[\mu] \in \mathsf{CComp}_{n,k}$, we have*

$$|\mathsf{MNeck}[\mu]| = \frac{\mathsf{ord}[\mu]}{k}\binom{n}{k-1}.$$

Proof. Let $\mathcal{N}$ denote the necklace of extended leaves corresponding to $[\mu]$, and fix a sequence $E_1E_2\cdots E_k \in N$ of extended leaves. Then there are $\binom{n}{k-1}$ ways to choose the $k-1$ non-leaf vertices to be marked in $E_1E_2\cdots E_k$. Upon taking all k cyclic shifts of $E_1E_2\cdots E_k$, observe that each cyclic shift appears $k/\mathsf{ord}[\mu]$ times; accordingly, each of the markings counted by $\binom{n}{k-1}$ is $k/\mathsf{ord}[\mu]$ times the number of markings in $\mathsf{MNeck}[\mu]$. In other words, we have

$$\frac{k}{\mathsf{ord}[\mu]}|\mathsf{MNeck}[\mu]| = \binom{n}{k-1},$$

which is equivalent to our desired conclusion. □

A Dyck word $\pi = \pi_1\cdots\pi_{2n}$ with exactly k NE-factors can be expressed uniquely in the form $\pi = N^{a_1}E^{b_1}\cdots N^{a_k}E^{b_k}$, where $(a_1,\ldots,a_k)$ and $(b_1,\ldots,b_k)$ are both compositions of n. Let us call $(a_1,\ldots,a_k)$ the *rise composition* of π. Given a cyclic composition $[\mu]$, denote by $\mathsf{D}[\mu]$ the set of all Dyck words with rise composition contained in the equivalence class $[\mu]$.

Lemma 3.3.2. *Given $[\mu] \in \mathsf{CComp}_{n,k}$, we have*

$$|\mathsf{D}[\mu]| = \frac{\mathsf{ord}[\mu]}{k}\binom{n}{k-1}. \tag{3.3.1}$$

Proof. From Lemma 3.3.1, it suffices to find a bijection from $D[\mu]$ to $\mathsf{MNeck}[\mu]$. Once again, we appeal to the plane tree interpretation of Dyck paths from which the bijection to $\mathsf{MNeck}[\mu]$ follows similarly to that of Lemma 3.2.2. □

Let $\mathsf{Comp}_{n,k,m}$ denote the set of all compositions in $\mathsf{Comp}_{n,k}$ with exactly m parts at least 2 and let $\mathsf{CComp}_{n,k,m}$ be its cyclic counterpart. Using Lemma 3.3.2, we obtain a combinatorial proof for Theorem 3.1.1. The proof of the nontrivial case is given below.

Combinatorial proof of Theorem 3.1.1. First, we take the Dyck paths counted by $w_{n,k,m}$ and partition them by the cyclic equivalence classes of their rise compositions. Then we have

$$w_{n,k,m} = \sum_{[\mu]\in\mathsf{CComp}_{n,k,m}} |D[\mu]| = \sum_{[\mu]\in\mathsf{CComp}_{n,k,m}} \frac{\mathsf{ord}[\mu]}{k}\binom{n}{k-1} \tag{3.3.2}$$

upon applying Lemma 3.3.2. Next, recall that every cyclic composition $[\mu] \in \mathsf{CComp}_{n,k,m}$ contains $\mathsf{ord}[\mu]$ distinct compositions in $\mathsf{Comp}_{n,k,m}$, so we have

$$w_{n,k,m} = \sum_{\mu\in\mathsf{Comp}_{n,k,m}} \frac{1}{\mathsf{ord}[\mu]}\frac{\mathsf{ord}[\mu]}{k}\binom{n}{k-1} = \frac{1}{k}\binom{n}{k-1}|\mathsf{Comp}_{n,k,m}|. \tag{3.3.3}$$

Finally, we claim that

$$|\mathsf{Comp}_{n,k,m}| = \binom{n-k-1}{m-1}\binom{k}{m}; \tag{3.3.4}$$

indeed, we can uniquely generate all compositions of n into k parts with exactly m parts at least 2 using the following process:

(1) Take the composition (1^k) consisting of k copies of 1, and choose m positions $1 \le i_1 < i_2 < \cdots < i_m \le k$ within this composition; there are $\binom{k}{m}$ ways to do this.

(2) Choose a composition $\mu = (\mu_1, \mu_2, \ldots, \mu_m)$ of $n-k$ into m parts; there are $\binom{n-k-1}{m-1}$ ways to do this.

(3) For each $1 \le j \le m$, add μ_j to the i_jth entry of (1^k). The result is a composition of n into k parts with exactly m parts at least 2.

Substituting (3.3.4) into (3.3.3) completes the proof. $\square$

Given $0 \le r \le n$ and $0 \le k \le n-r$, define the *r-generalized Narayana number* $N^{(r)}_{n,k}$ by

$$N^{(r)}_{n,k} = \frac{r+1}{n+1}\binom{n+1}{k}\binom{n-r-1}{k-1}.$$

Observe that the usual Narayana numbers $N_{n,k}$ can be obtained by setting $r = 0$ in $N^{(r)}_{n,k}$. For $k < 0$, we use the convention that $\binom{n}{k} = 0$ except for the special case when $n = k = -1$, where we define $\binom{-1}{-1}$ to be 1.

The following is a generalization of Theorems 3.2.1 and 3.2.2.

Theorem 3.3.1. *For all $j, k \geq 1$ and $m \geq 0$, we have*

$$w_{2k+j,k,m} = \frac{1}{j}\binom{2k+j}{k-1} N^{(j-1)}_{k+j-1,m}$$

and for all $1 \leq j \leq k$ and $m \geq 0$, we have

$$w_{2k-j,k,m} = \frac{1}{j}\binom{2k-j}{k-1} N^{(j-1)}_{k-1,m}.$$

Before proving Theorem 3.3.1, we first introduce a generalization of Dyck paths and prove a useful lemma. Consider paths in $\mathbb{Z}^2$ from $(0,0)$ to $(n-r, n)$, consisting of n North steps $(0,1)$ and $n-r$ East steps $(1,0)$, that never pass below the line $y = x$. Denote by $D^{(r)}_{n,k}$ the set of words on the alphabet $\{N, E\}$ corresponding to such paths with exactly k NE-factors. As shown by Callan and Schulte [**18**], $N^{(r)}_{n,k}$ is the cardinality of $D^{(r)}_{n,k}$.

For $\omega, \nu \in D^{(r)}_{n,k}$, let us write $\omega \sim \nu$ if the words $N\omega$ and $N\nu$ are cyclic shifts of each other. The relation $\sim$ is an equivalence relation on $D^{(r)}_{n,k}$, and we denote the set of its equivalence classes by $\tilde{D}^{(r)}_{n,k}$. For $[\omega] \in \tilde{D}^{(r)}_{n,k}$, let $\mathsf{ord}[\omega]$ be the number of distinct elements of $D^{(r)}_{n,k}$ contained within the equivalence class $[\omega]$.

Definition 3.3.1. *For $j, k \geq 1$, let $\phi_{j,k}$ be the map from $\mathsf{CComp}_{2k+j,k,m}$ to $\tilde{D}^{(j-1)}_{k+j-1,m}$ where $\phi_{j,k}[\mu]$ is obtained via the following algorithm:*

(1) For $[\mu] = [\mu_1, \dots, \mu_k] \in \mathsf{CComp}_{2k+j,k,m}$, set $\omega = N^{\mu_1 - 1}EN^{\mu_2-1}E\cdots N^{\mu_k-1}E$.

(2) Let $\nu = \nu_1\nu_2\cdots\nu_{2k+j}$ be any cyclic shift of ω that is 1-dominating.

(3) Set $\phi_{j,k}[\mu]$ to be the equivalence class of the subword $\nu_2\cdots\nu_{2k+j}$.

It is not immediately clear from the above definition whether the map $\phi_{j,k}$ is well-defined, but this will be established in the proof of the following lemma.

Lemma 3.3.3. *For all $j, k \geq 1$, the map $\phi_{j,k}$ is a bijection. Moreover, for all $[\mu] \in \mathsf{CComp}_{2k+j,k,m}$, we have*

$$\frac{\mathsf{ord}(\phi_{j,k}[\mu])}{\mathsf{ord}[\mu]} = \frac{j}{k}.$$

Proof. We first prove that $\phi_{j,k}$ is well-defined. Since ω contains $k+j$ copies of N and k copies of E, the cycle lemma guarantees that at least one cyclic shift of ω is 1-dominating. By construction of ω, the word ν must contain exactly m NE-factors. The fact that ν is 1-dominating and contains m NE-factors implies that its subword $\nu_2 \cdots \nu_{2k+j}$ is an element of $D^{(j-1)}_{k+j-1,m}$. From the definition of $\sim$ on $D^{(j-1)}_{k+j-1,m}$, any 1-dominating cyclic shift of ω will be sent to the same equivalence class in $\tilde{D}^{(j-1)}_{k+j-1,m}$. This same argument also implies that $\phi_{j,k}[\mu]$ does not depend on the representative of $[\mu]$ that is chosen.

Injectivity and surjectivity are straightforward to check from the definition of $\phi_{j,k}$. By the cycle lemma, there are exactly j cyclic shifts of ω that are 1-dominating; among these j words, there are $j \cdot \mathsf{ord}[\mu]/k$ *distinct* cyclic shifts as each of them appears $k/\mathsf{ord}[\mu]$ times. These 1-dominating sequences are in bijection with paths in the equivalence class of $\phi_{j,k}[\mu]$ by removing the first N from the sequence. Thus, $\mathsf{ord}(\phi_{j,k}[\mu]) = j \cdot \mathsf{ord}[\mu]/k$. □

We are now ready to prove Theorem 3.3.1.

Proof of Theorem 3.3.1. From Lemma 3.3.3, we have

$$|\mathsf{Comp}_{2k+j,k,m}| = \frac{k}{j}|D^{(j-1)}_{k+j-1,m}| = \frac{k}{j}N^{(j-1)}_{k+j-1,m}.$$

Plugging this into (3.3.3) gives the desired result

$$w_{2k+j,k,m} = \frac{1}{j}\binom{2k+j}{k-1}N^{(j-1)}_{k+j-1,m}.$$

The proof for $w_{2k-j,k,m}$ follows similarly by defining an analogous map $\varphi_{j,k}$ from $\mathsf{CComp}_{2k-j,k,m}$ to $\tilde{D}^{(j-1)}_{k-1,m}$ and reproving Lemma 3.3.3 for $\varphi_{j,k}$. □

3.3.2. Further generalizations and applications. We now detail several interesting generalizations and applications that can be obtained from our results in Section 3.3.1.

First, we obtain a formula for the Catalan numbers Cat_n in terms of primitive cyclic compositions via Lemma 3.3.2.

Corollary 3.3.1. *For all $n \geq 1$, we have*

$$\mathrm{Cat}_n = \frac{1}{n+1}\binom{2n}{n} = \sum_{d|n} \sum_{\substack{[\mu]\in\mathsf{CComp}_{n/d} \\ \text{primitive}}} \frac{1}{d}\binom{n}{\mathsf{ord}[\mu]\cdot d - 1},$$

where CComp_n is the set of all cyclic compositions of n.

PROOF. Grouping Dyck paths by their cyclic rise composition, we have

$$\mathrm{Cat}_n = \sum_{[\mu]\in\mathsf{CComp}_n} D[\mu].$$

Recall that every cyclic composition of n can be uniquely expressed as the concatenation of d copies of a primitive cyclic composition of n/d for some divisor d of n. Similarly, for every divisor d of n, each primitive cyclic composition of n/d can be made into a cyclic composition of n by concatenating d copies. This gives us

$$\mathrm{Cat}_n = \sum_{[\mu]\in\mathsf{CComp}_n} D[\mu] = \sum_{d|n} \sum_{\substack{[\mu]\in\mathsf{CComp}_{n/d}\\ \text{primitive}}} D([\mu]^d)$$

where $[\mu]^d$ is the concatenation of d copies of $[\mu]$. From Lemma 3.3.2, this gives us precisely

$$\mathrm{Cat}_n = \sum_{d|n} \sum_{\substack{[\mu]\in\mathsf{CComp}_{n/d}\\ \text{primitive}}} D([\mu]^d) = \sum_{d|n} \sum_{\substack{[\mu]\in\mathsf{CComp}_{n/d}\\ \text{primitive}}} \frac{1}{d}\binom{n}{\mathsf{ord}[\mu]\cdot d-1}. \qquad \square$$

Next, Lemma 3.3.3 naturally leads to the following generalization of Lemmas 3.2.1 and 3.2.3, which expresses the number of cyclic compositions in $\mathsf{CComp}_{2k\pm j,k,m}$ in terms of r-generalized Narayana numbers. Below, φ denotes Euler's totient function.

PROPOSITION 3.3.1. *Let $k \geq 1$ and $m, j \geq 0$, and let $d = \mathsf{gcd}(k, m, j)$.*[3]

(a) If $j \geq 1$, we have $|\mathsf{CComp}_{2k+j,k,m}| = \dfrac{1}{j}\displaystyle\sum_{s|d} \varphi(s) N^{(j/s-1)}_{(k+j)/s-1,\, m/s}$.

(b) If $j = 0$, we have $|\mathsf{CComp}_{2k,k,m}| = \dfrac{1}{k}\displaystyle\sum_{s|d} \varphi(s)\binom{\frac{k}{s}-1}{\frac{m}{s}-1}\binom{\frac{k}{s}}{\frac{m}{s}}$.

(c) If $1 \leq j \leq k$, we have $|\mathsf{CComp}_{2k-j,k,m}| = \dfrac{1}{j}\displaystyle\sum_{s|d} \varphi(s) N^{(j/s-1)}_{k/s-1,\, m/s}$.

PROOF. Let us call an (ordinary) composition μ *primitive* if $[\mu]$ is primitive, and let $\mathsf{PComp}_{n,k,m}$ denote the set of primitive compositions of n with k parts with exactly m parts at least two. Let

[3] If $m = 0$ or $j = 0$, then $\mathsf{gcd}(k, m, j)$ is defined to be the greatest common divisor of the nonzero numbers among k, m, and j.

$1 \leq k \leq m$ and $j \geq 0$, and let $d = \mathsf{gcd}(k, m, j)$. Given $\ell \mid d$, define

$$f(\ell) = |\mathsf{Comp}_{(2k+j)\ell/d,\, k\ell/d,\, m\ell/d}| \quad \text{and} \quad g(\ell) = |\mathsf{PComp}_{(2k+j)\ell/d,\, k\ell/d,\, m\ell/d}|.$$

Every composition can be uniquely decomposed as a concatenation of one or more copies of a primitive composition, which leads to the formula $f(\ell) = \sum_{s|\ell} g(s)$. By Möbius inversion, we then have $g(\ell) = \sum_{s|\ell} \mathsf{Möb}(s) f(\ell/s)$ where $\mathsf{Möb}$ is the Möbius function. Observe that

$$|\mathsf{CComp}_{2k+j,k,m}| = \sum_{\ell|d} \frac{\ell}{k} |\mathsf{PComp}_{(2k+j)/\ell,\, k/\ell,\, m/\ell}|;$$

after all, every cyclic composition in $\mathsf{CComp}_{2k+j,k,m}$ is a concatenation of ℓ copies of a primitive cyclic composition with k/ℓ parts for some ℓ dividing d, and this primitive cyclic composition is the cyclic equivalence class of k/ℓ elements of $\mathsf{PComp}_{(2k+j)/\ell,\, k/\ell,\, m/\ell}$. We then have

$$\begin{aligned}
|\mathsf{CComp}_{2k+j,k,m}| &= \sum_{\ell|d} \frac{\ell}{k} |\mathsf{PComp}_{(2k+j)/\ell,\, k/\ell,\, m/\ell}| \\
&= \sum_{\ell|d} \frac{\ell}{k} g\Big(\frac{d}{\ell}\Big) \\
&= \frac{1}{k} \sum_{\ell|d} \sum_{q|(d/\ell)} \mathsf{Möb}(q) \ell f\Big(\frac{d}{\ell q}\Big) \\
&= \frac{1}{k} \sum_{s|d} \sum_{\ell q = s} \mathsf{Möb}(q) \frac{s}{q} f\Big(\frac{d}{s}\Big). \\
&= \frac{1}{k} \sum_{s|d} \varphi(s) f\Big(\frac{d}{s}\Big),
\end{aligned}$$

where the last step uses the well-known identity $\varphi(s) = \sum_{q|s} \mathsf{Möb}(q) s/q$. If $j \geq 1$, then we have

$$f\Big(\frac{d}{s}\Big) = |\mathsf{Comp}_{2(k/s)+j/s,\, k/s,\, m/s}| = \frac{k}{j} N^{(j/s-1)}_{(k+j)/s-1,\, m/s}$$

by Lemma 3.3.3, and if $j = 0$, then we instead have

$$f\Big(\frac{d}{s}\Big) = |\mathsf{Comp}_{2(k/s),\, k/s,\, m/s}| = \binom{\frac{k}{s} - 1}{\frac{m}{s} - 1} \binom{\frac{k}{s}}{\frac{m}{s}}$$

by (3.3.4); substituting appropriately completes the proof of parts (a) and (b). We omit the proof of (c) as it is similar to that of (a). $\square$

Remark 3.3.1. *Proposition 3.3.1 has an interesting interpretation related to permutation enumeration, as* $|\mathsf{CComp}_{n,k,m}|$ *is the number of distinct cyclic descent sets among cyclic permutations of length* n *with* k *cyclic descents and* m *cyclic peaks* $($*for all* $1 \leq k < n)$*; see [**26, 27, 61, 62**] for definitions. In particular, when* $j \neq 0$ *and* $\mathsf{gcd}(k, j, m) = 1$*, the number of cyclic descent classes among such cyclic permutations of length* $2k + j$ *is equal to a generalized Narayana number divided by* j*. The case* $j = \pm 1$ $($*Lemmas 3.2.1 and 3.2.3*$)$ *yields a new interpretation of the* $($*ordinary*$)$ *Narayana numbers* $N_{k,m}$ *in terms of cyclic descent classes.*

Finally, many of our results can be generalized to the numbers $w_{n,k_1,k_2,\ldots,k_r}$ which count Dyck paths of semilength n with k_1 NE-factors, k_2 NNE-factors, $\ldots$, and k_r N^rE-factors. Let $\mathsf{Comp}_{n,k_1,k_2,\ldots,k_r}$ denote the set of compositions of n with k_1 parts, exactly k_2 parts larger than 1, $\ldots$, and exactly k_r parts larger than $r-1$, and let $\mathsf{CComp}_{n,k_1,k_2,\ldots,k_r}$ be the set of corresponding cyclic compositions. Using Lemma 3.3.2 and the proofs of Lemmas 3.2.1 and 3.2.3, we obtain the following symmetries for $w_{n,k_1,k_2,\ldots,k_r}$.

Corollary 3.3.2. *For all* $r \geq 1$ *and* $1 \leq m \leq k$*, taking* $k_1 = k_2 = \cdots = k_{r-1} = k$*, we have*

$$w_{rk+1,k_1,k_2,\ldots,k_{r-1},m} = w_{rk+1,k_1,k_2,\ldots,k_{r-1},k+1-m}$$

and

$$w_{rk-1,k_1,k_2,\ldots,k_{r-1},m} = w_{rk-1,k_1,k_2,\ldots,k_{r-1},k-m}$$

Proof. Let $\mu \in \mathsf{CComp}_{rk+1,k,k,\ldots,k,m}$. From Lemma 3.3.2, we have $D[\mu] = \binom{rk+1}{k-1}$ as $[\mu]$ must be primitive. Note that $|\mathsf{CComp}_{rk+1,k,k,\ldots,k,m}| = N_{k,m}$ which can be shown via an argument analogous to that in the proof of Lemma 3.2.1. Thus, we have $w_{rk+1,k,k,\ldots,k,m} = \binom{n}{k-1}N_{k,m}$, which gives the desired symmetry in light of the Narayana symmetry. The symmetry for the numbers $w_{rk-1,k,k,\ldots,k,m}$ can be proven similarly. $\square$

Note that the $r = 1$ case of Corollary 3.3.2 is the Narayana symmetry $N_{n,k} = N_{n,n+1-k}$, whereas setting $r = 2$ recovers our symmetries for the numbers $w_{2k\pm1,k,m}$.

In addition, as a direct consequence of our combinatorial proof for Theorem 3.1.1, we have the following formula for $w_{n,k_1,k_2,\ldots,k_r}$.

Corollary 3.3.3. *Let $r \geq 1$, $k_1 \geq k_2 \geq \cdots \geq k_r \geq 0$, and $n \geq k_1 + k_2 + \cdots + k_r$. For convenience, write $\hat{k} = k_1 + k_2 + \cdots + k_{r-1}$. Then*

$$w_{n,k_1,k_2,\ldots,k_r} = \begin{cases} \frac{1}{k_1}\binom{n}{k_1-1}\binom{n-\hat{k}-1}{k_r-1}\binom{k_1}{k_1-k_2, k_2-k_3, \ldots, k_{r-1}-k_r, k_r}, & \text{if } k_r > 0, \\ \frac{1}{k_1}\binom{n}{k_1-1}\binom{k_1}{k_1-k_2, k_2-k_3, \ldots, k_{r-1}-k_r, k_r}, & \text{if } k_r = 0 \text{ and } n = \hat{k}, \\ 0, & \text{otherwise.} \end{cases}$$

Corollary 3.3.3 specializes to the formula for Narayana numbers upon setting $r = 1$, and to Theorem 3.1.1 for $r = 2$.

3.4. Polynomials

In Section 3.4.1 we show the polynomial associated to the sequence $w_{n,k,m}$ is real-rooted and give several interlacing conjectures. In Section 3.4.2 we look into the gamma-positivity and symmetry of these polynomials.

3.4.1. Real-rootedness. A natural question is whether or not the sequence $\{w_{n,k,m}\}_{0\leq m\leq k}$, for a fixed n and k, is unimodal. In other words, for fixed n and k, does there always exist $0 \leq j \leq k$ such that

$$w_{n,k,0} \leq w_{n,k,1} \leq \cdots \leq w_{n,k,j} \geq w_{n,k,j+1} \geq \cdots \geq w_{n,k,k}?$$

One powerful way to prove unimodality results in combinatorics is through real-rootedness. A polynomial with coefficients in $\mathbb{R}$ is said to be *real-rooted* if all of its roots are in $\mathbb{R}$. (We use the convention that constant polynomials are also real-rooted.) It is well known that if a polynomial with non-negative coefficients is real-rooted, then the sequence of its coefficients are unimodal (see [**14**], for example).

Let $W_{n,k}(t)$ be the polynomial defined by

$$W_{n,k}(t) = \sum_{m=0}^{k} w_{n,k,m} t^m.$$

In what follows, we prove that the polynomials $W_{n,k}(t)$ are real-rooted, thus implying the unimodality of the sequences $\{w_{n,k,m}\}_{0\le m\le k}$.

We begin with a simple result involving the roots of $W_{n,k}(t)$.

Proposition 3.4.1. *For all $1 \le k \le n-1$, the polynomials $W_{n,k}(t)$ and $W_{n,n-k}(t)$ have the same roots.*

Proof. This follows from the fact that $w_{n,k,m} = \frac{k(k+1)}{(n-k)(n-k+1)} w_{n,n-k,m}$, which is readily verified from Theorem 3.1.1. $\square$

To prove the real-rootedness of the $W_{n,k}(t)$, we make use of Malo's result regarding the roots of the Hadamard product of two real-rooted polynomials.

Theorem 3.4.1 ([**65**]). *Let $f(t) = \sum_{i=0}^{m} a_i t^i$ and $g(t) = \sum_{i=0}^{n} b_i t^i$ be real-rooted polynomials in $\mathbb{R}[t]$ such that all the roots of g have the same sign. Then their Hadamard product*

$$f * g = \sum_{i=0}^{\ell} a_i b_i t^i,$$

where $\ell = \min\{m,n\}$, is real-rooted.

Theorem 3.4.2. *For all $n, k \ge 0$, the polynomials $W_{n,k}(t)$ are real-rooted.*

Proof. From Theorem 3.1.1, we have

$$W_{n,k}(t) = \begin{cases} 0, & \text{if } n < k, \\ 1, & \text{if } n = k, \\ \frac{1}{k}\binom{n}{k-1} \sum_{m=1}^{\min\{k,n-k\}} \binom{n-k-1}{m-1}\binom{k}{m} t^m, & \text{if } n > k. \end{cases} \tag{3.4.1}$$

Thus it suffices to check that the polynomial $\sum_{m=1}^{\min\{k,n-k\}} \binom{n-k-1}{m-1}\binom{k}{m} t^m$ is real-rooted, which follows from applying Theorem 3.4.1 to $f(t) = t(t-1)^{n-k-1}$ and $g(t) = (t-1)^k$. $\square$

More generally, we conjecture the polynomials $W_{n,k}(t)$ satisfy stronger conditions which we presently define. For two real-rooted polynomials f and g, let $\{u_i\}$ be the roots of f and $\{v_i\}$ the roots of g, both in non-increasing order. We say that g *interlaces* f, denoted by $g \to f$, if either

$\deg(f) = \deg(g) + 1 = d$ and

$$u_d \leq v_{d-1} \leq u_{d-1} \leq \cdots \leq v_1 \leq u_1,$$

or if $\deg(f) = \deg(g) = d$ and

$$v_d \leq u_d \leq v_{d-1} \leq u_{d-1} \leq \cdots \leq v_1 \leq u_1.$$

(By convention, we assume that a constant polynomial interlaces with every real-rooted polynomial.) We say that a sequence of real-rooted polynomials $f_1, f_2, \ldots$ is a *Sturm sequence* if $f_1 \to f_2 \to \cdots$. Moreover, a finite sequence of real-rooted polynomials $f_1, f_2, \ldots, f_n$ is said to be *Sturm-unimodal* if there exists $1 \leq j \leq n$ such that

$$f_1 \to f_2 \to \cdots \to f_j \leftarrow f_{j+1} \leftarrow \cdots \leftarrow f_n.$$

CONJECTURE 3.4.1. *For any fixed $k \geq 1$, the polynomials $\{W_{n,k}(t)\}_{n \geq k}$ form a Sturm sequence.*

CONJECTURE 3.4.2. *For any fixed $n \geq 1$, the sequence $\{W_{n,k}(t)\}_{1 \leq k \leq n}$ is Sturm-unimodal.*

Our result expressing the numbers $w_{n,k,m}$ in terms of generalized Narayana numbers has a natural polynomial analogue. Let $\mathrm{Nar}_k^{(r)}(t)$ denote the kth *r-generalized Narayana polynomial* defined by

$$\mathrm{Nar}_k^{(r)}(t) = \sum_{m=0}^{k-r} N_{k,m}^{(r)} t^m = \frac{r+1}{k+1} \sum_{m=0}^{k-r} \binom{k+1}{m} \binom{k-r-1}{m-1} t^m.$$

Setting $r = 0$ recovers the usual *Narayana polynomials* $\mathrm{Nar}_k(t) = \sum_{m=0}^{k} N_{k,m} t^m$. From Theorem 3.3.1 and straightforward computations, we have the following expressions for $W_{n,k}(t)$.

PROPOSITION 3.4.2. *Let $k \geq 1$.*

(a) For all $j \geq 1$, we have $W_{2k+j,k}(t) = \frac{1}{j}\binom{2k+j}{k-1} \mathrm{Nar}_{k+j-1}^{(j-1)}(t)$.

(b) We have $W_{2k,k}(t) = C_k \sum_{m=1}^{k} \binom{k-1}{m-1}\binom{k}{m} t^m$ where C_k denotes the kth Catalan number.

(c) For all $1 \leq j \leq k$, we have $W_{2k-j,k}(t) = \frac{1}{j}\binom{2k-j}{k-1} \mathrm{Nar}_{k-1}^{(j-1)}(t)$.

The real-rootedness of the r-generalized Narayana polynomials was recently shown in [**21**] using a different approach; Proposition 3.4.2 shows that the real-rootedness of the $W_{n,k}(t)$ implies the real-rootedness of the $\mathrm{Nar}_k^{(r)}(t)$, thus giving an alternative proof of this result.

3.4.2. Symmetry, γ-positivity, and a symmetric decomposition. It is fitting that we end this chapter by returning full circle to the topic of symmetry. First, we note that our symmetries for the numbers $w_{2k+1,k,m}$ and $w_{2k-1,k,m}$ immediately imply the following:

PROPOSITION 3.4.3. *The polynomials $W_{2k+1,k}(t)$ and $W_{2k-1,k}(t)$ are symmetric.*

A symmetric polynomial of degree d can be written uniquely as a linear combination of the polynomials $\{t^j(1+t)^{d-2j}\}_{0\leq j\leq \lfloor d/2\rfloor}$, referred to as the *gamma basis*. A symmetric polynomial is called *γ-positive* if its coefficients in the gamma basis are nonnegative. Gamma-positivity has shown up in many combinatorial and geometric contexts; see [**5**] for a thorough survey. It is well known that the coefficients of a γ-positive polynomial form a unimodal sequence, and that γ-positivity is connected to real-rootedness in the following manner:

THEOREM 3.4.3 ([**12**]). *If f is a real-rooted, symmetric polynomial with nonnegative coefficients, then f is γ-positive.*

The γ-positivity of the polynomials $W_{2k+1,k}(t)$ and $W_{2k-1,k}(t)$ then follows directly from Theorem 3.4.2, Proposition 3.4.3, and Theorem 3.4.3. Furthermore, we can get explicit formulas for their gamma coefficients by exploiting their connection to the Narayana polynomials.

PROPOSITION 3.4.4. *The polynomials $W_{2k+1,k}(t)$ and $W_{2k-1,k}(t)$ are γ-positive for all $k\geq 1$. More precisely, we have the following gamma expansions:*

(a) $$W_{2k+1,k}(t)=\sum_{j=1}^{\lfloor\frac{k+1}{2}\rfloor}\binom{2k+1}{k-1}\frac{(k-1)!}{(k-2j+1)!\,(j-1)!\,j!}\,t^j(1+t)^{k+1-2j}\ \textit{for all } k\geq 1;$$

(b) $$W_{2k-1,k}(t)=\sum_{j=1}^{\lfloor\frac{k+1}{2}\rfloor}\binom{2k-1}{k-1}\frac{(k-2)!}{(k-2j)!\,(j-1)!\,j!}\,t^j(1+t)^{k+1-2j}\ \textit{for all } k\geq 2.$$

Proof. The Narayana polynomials are known to be γ-positive with gamma expansion

$$\mathrm{Nar}_k(t) = \sum_{j=1}^{\lfloor \frac{k+1}{2} \rfloor} \frac{(k-1)!}{(k-2j+1)!\,(j-1)!\,j!}\, t^j (1+t)^{k+1-2j}$$

for all $k \geq 1$ [**5**, Theorem 2.32], and this implies the desired result by the $j = 1$ case of Proposition 3.4.2 (a) and (c). $\square$

Remark 3.4.1. *The gamma coefficients of the Narayana polynomials have a nice combinatorial interpretation in terms of lattice paths:* $\frac{(k-1)!}{(k-2j+1)!\,(j-1)!\,j!}$ *is the number of Motzkin paths of length* $k-1$ *with* $j-1$ *North steps [**10**]. We can use this fact to give combinatorial interpretations of the gamma coefficients of* $W_{2k+1,k}(t)$ *and* $W_{2k-1,k}(t)$*. It would be interesting to find a combinatorial proof for Proposition 3.4.4 using Motzkin paths, perhaps in the vein of the "valley-hopping" proof for the* γ*-positivity of Narayana polynomials [**13**].*

While the polynomials $W_{n,k}(t)$ are not symmetric in general, it turns out that we can always express $W_{n,k}(t)$ as the sum of two symmetric polynomials.

Theorem 3.4.4. *Let* $1 \leq k \leq n$*, and let* $\widetilde{m} = \deg W_{n,k}(t)$*. Then there exist symmetric polynomials* $W^+_{n,k}(t)$ *and* $W^-_{n,k}(t)$*, both with nonnegative coefficients, such that:*

(a) if $n = \widetilde{m} + k$ *and* $\widetilde{m} \neq k$*, then* $W_{n,k}(t) = W^+_{n,k}(t) - tW^-_{n,k}(t)$*;*
(b) if $n = \widetilde{m} + k$ *and* $\widetilde{m} = k$*, then* $W_{n,k}(t) = W^+_{n,k}(t) + tW^-_{n,k}(t)$*;*
(c) and if $n > \widetilde{m} + k$*, then* $W_{n,k}(t) = -W^+_{n,k}(t) + tW^-_{n,k}(t)$*.*

Proof. Since n and k are fixed, let us simplify notation by writing w_m in place of $w_{n,k,m}$, so that $W_{n,k}(t) = \sum_{m=0}^{k} w_m t^m$. Let

$$w^+_{i+1} = \Big(\sum_{j=0}^{i+1} w_j\Big) - \Big(\sum_{j=0}^{i} w_{k-j}\Big) \quad \text{and} \quad w^-_i = -\Big(\sum_{j=0}^{i} w_j\Big) + \Big(\sum_{j=0}^{i} w_{k-j}\Big) \tag{3.4.2}$$

for all $1 \le i \le k$; also take $w_0^+ = 1$ when $k = n$ and $w_0^+ = 0$ otherwise. Observe that

$$w_i^+ + w_{i-1}^- = \Big(\sum_{j=0}^{i} w_j\Big) - \Big(\sum_{j=0}^{i-1} w_{k-j}\Big) - \Big(\sum_{j=0}^{i-1} w_j\Big) + \Big(\sum_{j=0}^{i-1} w_{k-j}\Big) = w_i, \tag{3.4.3}$$

$$w_i^+ - w_{k-i}^+ = \Big(\sum_{j=0}^{i} w_j\Big) - \Big(\sum_{j=0}^{i-1} w_{k-j}\Big) - \Big(\sum_{j=0}^{k-i} w_j\Big) + \Big(\sum_{j=0}^{k-i-1} w_{k-j}\Big) = 0, \quad \text{and} \tag{3.4.4}$$

$$w_{i-1}^- - w_{k-i}^- = -\Big(\sum_{j=0}^{i-1} w_j\Big) + \Big(\sum_{j=0}^{i-1} w_{k-j}\Big) + \Big(\sum_{j=0}^{k-i} w_j\Big) - \Big(\sum_{j=0}^{k-i} w_{k-j}\Big) = 0. \tag{3.4.5}$$

A standard induction argument utilizing the explicit formula in Theorem 3.1.1 yields the following:

- the w_i^+ are positive when $n = \widetilde{m} + k$,
- the w_i^+ are negative when $n > \widetilde{m} + k$,
- the w_i^- are positive when $n = \widetilde{m} + k$ for $\widetilde{m} = k$ and when $n > \widetilde{m} + k$, and
- the w_i^- are negative when $n = \widetilde{m} + k$ for $\widetilde{m} \neq k$.

Define the polynomials $W_{n,k}^+(t)$ and $W_{n,k}^-(t)$ by

$$W_{n,k}^+(t) = \sum_{i=0}^{\widetilde{m}} |w_i^+|\, t^i \quad \text{and} \quad W_{n,k}^-(t) = \sum_{i=0}^{k} |w_i^-|\, t^i,$$

respectively. These polynomials are symmetric by (3.4.4) and (3.4.5), and the decompositions given in (a)–(c) hold by construction in light of (3.4.3). $\square$

CHAPTER 4

The Burge correspondence and crystal graphs

This chapter is based on work in collaboration with Digjoy Paul and Anne Schilling published in [**70**].

4.1. The Burge correspondence

In this section, we define the Burge correspondence [**17**]. We review some preliminaries in Section 4.1.1. We remind the reader of Schensted's result on longest increasing subwords of words in Section 4.1.2 before introducing the Burge correspondence in Section 4.1.3. In Section 4.1.4, we show that the Burge correspondence intertwines with standardization.

4.1.1. Preliminaries. A *partition* λ of a nonnegative integer n, denoted by $\lambda \vdash n$, is a weakly decreasing sequence $\lambda = (\lambda_1, \lambda_2, \ldots, \lambda_\ell)$ of positive integers λ_i such that $\sum_{i=1}^{\ell} \lambda_i = n$. The *length* of λ is ℓ. The *Young diagram* $Y(\lambda)$ of λ is a left-justified array of boxes with λ_i boxes in row i from the top. (This is also known as the English convention for Young diagrams of partitions). A partition λ is a *hook* if $Y(\lambda)$ does not contain any 2×2 squares. A partition $\lambda = (\lambda_1, \lambda_2, \ldots, \lambda_n)$ is called *threshold* if $\lambda_i^t = \lambda_i + 1$ for all $1 \leqslant i \leqslant d(\lambda)$, where λ_i^t is the length of i-th column of the Young diagram of λ and $d(\lambda)$ is the maximal d such that $(d, d) \in \lambda$.

Definition 4.1.1. *Let λ be a partition. A* semistandard Young tableau *of shape λ in the alphabet $[n] := \{1, 2, \ldots, n\}$ is a filling of the Young diagram of λ with letters in $[n]$ such that the numbers weakly increase along rows and strictly increase along columns. We denote by* $\mathrm{Tab}_n(\lambda)$ *the set of all semistandard Young tableaux of shape λ in the alphabet $[n]$.*

Let T be a semistandard Young tableau. The *shape* of T is denoted $\mathsf{sh}(T)$. The *weight* of a semistandard Young tableau T, denoted $\mathsf{wt}(T)$, is the integer vector $(\mu_1, \ldots, \mu_n)$, where μ_i is the number of times the number i occurs. The subset of $\mathrm{Tab}_n(\lambda)$ consisting of all semistandard Young tableaux of weight μ is denoted by $\mathrm{Tab}(\lambda, \mu)$.

Given an integer vector $\mu = (\mu_1, \dots, \mu_n)$, let x^μ denote the monomial $x_1^{\mu_1} x_2^{\mu_2} \cdots x_n^{\mu_n}$ in the n variables $x_1, x_2, \dots, x_n$.

Definition 4.1.2. *For each integer partition λ, the* Schur polynomial *in n variables corresponding to λ is defined as*

$$s_\lambda(x_1, \dots, x_n) = \sum_{T \in \mathrm{Tab}_n(\lambda)} x^{\mathsf{wt}(T)}.$$

Given a simple graph $G = ([n], E)$ with vertex set $[n] = \{1, 2, \dots, n\}$ and edge set E, the degree d_i of a vertex i is the number of neighbors of i. The *degree sequence* of G is the tuple $d_G = (d_1, d_2, \dots, d_n)$, and the *degree partition* of G is the partition $\tilde{d}_G$ obtained by rearranging d_G in weakly decreasing manner. A graph G is called *threshold* if the associated degree partition is threshold. For alternative definitions and characterizations of threshold graphs, see [**64**, Chapter 3].

Example 4.1.1. *The simple graph in Figure 4.1 is threshold as its degree partition* $(3, 2, 2, 1)$ *is threshold.*

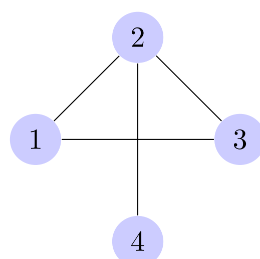

Figure 4.1. A threshold graph

4.1.2. Schensted algorithm and longest increasing subwords. The Burge correspondence (as well as the celebrated Robinson–Schensted–Knuth (RSK) correspondence [**52**, **79**, **84**]) uses the *Schensted row insertion* algorithm. Given a semistandard Young tableau T in the alphabet $[n]$, a letter $i \in [n]$ can be inserted into T in the following way: if i is larger than or equal to all the entries of the first row of T, a new box containing i is added at the end of first row and the process stops. Otherwise, i replaces the smallest leftmost number j of the first row such that $j > i$. Then j is inserted in the second row of T in the same way and so on. The procedure stops when a new box is added to T at the end of a row. The result is denoted $T \leftarrow i$. The shape of $T \leftarrow i$ contains one new box compared to the shape of T.

Given a tableau T and a letter x that lies at the end of some row of T, the *Schensted reverse bumping* algorithm generates a pair of a tableau T' and a letter y in the following way: Let t be the row index of x and x_1 be the rightmost entry of row $t-1$ such that $x_1 < x$. Replace x_1 by x in T and output x_1. Repeat the process for x_1 and continue until an element of the first row say y is obtained as output. The resulting tableau is T'. We shall denote the pair (T', y) by $T \rightarrow x$.

Given a word $w = w_1 w_2 \dots w_k$ in the alphabet $\{1, 2, \dots, n\}$, the *Schensted insertion tableau* is defined as $P(w) := \emptyset \leftarrow w_1 \leftarrow w_2 \leftarrow \cdots \leftarrow w_k$. The shape of the semistandard Young tableau $P(w)$, denoted $\lambda(w) = (\lambda_1, \lambda_2, \dots)$, is called the *shape of the word* w. Schensted [**84**] proved that λ_1 is the length of the longest increasing subword of w. In particular, the shape $\lambda(w)$ is a single row if w is weakly increasing. Greene [**37**] extended the result of Schensted by interpreting the rest of the shape of λ. For a poset theoretic viewpoint of the map $w \mapsto \lambda(w)$ and various applications including in the context of flag varieties, see Britz and Fomin [**15**] and references therein.

4.1.3. The Burge correspondence. We begin by recalling the definition of a Burge array from [**17**, Section 4].

Definition 4.1.3. *Given a simple graph $G = ([n], E)$ with $|E| = r$, define a two line array known as the* Burge array

$$\mathcal{A}_G = \begin{bmatrix} a_1 & a_2 & \dots & a_r \\ b_1 & b_2 & \dots & b_r \end{bmatrix}$$

satisfying:

(1) Each pair (a_k, b_k) is an edge of G and $a_k > b_k$ for each $1 \leqslant k \leqslant r$.

(2) The top line is weakly increasing, that is, $a_k \leqslant a_{k+1}$ for all $1 \leqslant k < r$.

(3) If $a_k = a_{k+1}$ for some $1 \leqslant k < r$, then $b_k > b_{k+1}$.

Notice that G is completely determined by the associated Burge array $\mathcal{A}_G$ assuming that $[n]$ is known. Note that singletons in the simple graph do not appear in the Burge array $\mathcal{A}_G$.

Given a threshold partition λ, by definition, the Young diagram $Y(\lambda)$ of λ is divided into two symmetric pieces. The bottom piece consists of all boxes that lie strictly below the diagonal and

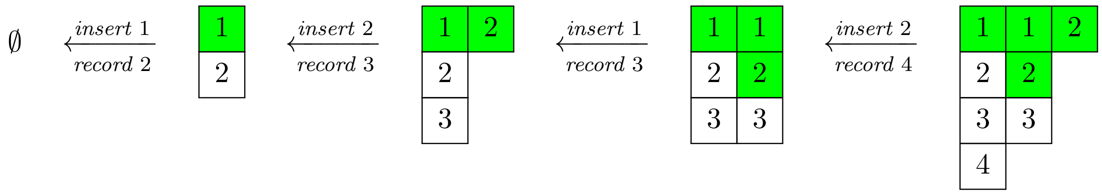

FIGURE 4.2. Burge insertion associated to Example 4.1.2.

the top piece consists of the rest. Each position in the top (bottom) piece of the Young diagram of $Y(\lambda)$ corresponds to a unique position, called the *opposite position*, in the bottom (top) piece of $Y(\lambda)$. The opposite position $\mathsf{op}(s,t)$ of (s,t) is defined to be $(t+1,s)$ if $s \leqslant t$ and $(t,s-1)$ otherwise.

Having defined all the necessary tools, we now state the main algorithm of the *Burge correspondence*. Starting with the empty tableau T_0, we shall insert all the edges of G, as ordered in $\mathcal{A}_G$, into T_0. Let T_k be the tableau obtained by inserting the edge (a_k, b_k) into T_{k-1} in the following way:

(1) First insert b_k into T_{k-1} using the Schensted insertion algorithm. This adds a new cell to the shape, say in position (s_k, t_k).
(2) Place the entry a_k in the cell $\mathsf{op}(s_k, t_k)$. Observe that each addition of an edge transforms a tableau of threshold shape to another tableau of threshold shape.

Finally, the tableau $T_G := T_r$ is the threshold tableau associated with the graph G under the Burge correspondence.

Burge [**17**] proved that this tableau is semistandard. Given such a tableau T, we recover the Burge array in the following way: Let a_r be the largest entry of T with largest column index. Remove a_r from T. Let z_r be the value at the opposite position of the cell containing a_r. Let $b_r = y_r$ where $T \to z_r = (T_{r-1}, y_r)$. Repeat the process for T_{r-1} and continue until the empty tableau is obtained in the output.

EXAMPLE 4.1.2. *The Burge array $\mathcal{A}_G$ for the graph in Figure 4.1 is* $\begin{bmatrix} 2 & 3 & 3 & 4 \\ 1 & 2 & 1 & 2 \end{bmatrix}$. *The associated tableau T_G of threshold shape $(3,2,2,1)$ is obtained by inserting the edges of G as ordered in $\mathcal{A}_G$ as depicted in Figure 4.2.*

In the same spirit as the shape of a word under the RSK correspondence, we can define the shape of a graph under the Burge correspondence.

Definition 4.1.4. *The shape of a simple graph G is the partition $\lambda_G := \mathsf{sh}(T_G)$, where T_G is the tableau associated with G by the Burge correspondence.*

A natural question analogous to those answered by Schensted and Greene [**37**,**84**] for the RSK correspondence is as follows.

Problem 4.1.1. *Given a simple graph G, what is its shape?*

It can be observed that the shape of a threshold graph G is its degree partition $\tilde{d}_G$. Namely, let G be a threshold graph with degree sequence d_G. If T is the semistandard Young tableau of threshold shape λ and weight d_G, then d_G is less than or equal to λ in dominance order. Since d_G is a threshold sequence by assumption, we know that the only partition that dominates a threshold sequence is the corresponding partition. Hence $\lambda = \tilde{d}_G$.

We call a simple graph G a *hook-graph* if the associated tableau T_G has hook shape. Given the nature of the Burge algorithm, determining when a T_G has hook shape is analogous to asking when a tableau under the RSK algorithm has single row shape. In Section 4.2, we characterize all hook-graphs.

4.1.4. Standardization. Both $\mathrm{Tab}_m(\lambda)$ and words over $[m]$ with length n have the notion of *standardization*. Standardization intertwines with RSK in the sense that they form a commuting diagram. We show that an analogous result holds true for the Burge correspondence.

First, we review the standardization map for semistandard Young tableaux. Let $\lambda \vdash n$ and let $C = \{c_1 < \cdots < c_n\}$ be a subset of $\mathbb{N}$. The standardization of $T \in \mathrm{Tab}(\lambda, \mu)$ with respect to the alphabet C, denoted by $\mathsf{stand}_C(T)$, is the map replacing all the 1's in T from left to right with the numbers c_1 through c_{μ_1}, replacing all the 2's from left to right with the numbers c_{μ_1+1} through $c_{\mu_1+\mu_2}$, etc.

The standardization map on words over the alphabet $[m]$ can be defined similarly. Let ω be a word using the alphabet $[m]$ with length n and let μ denote its content. In other words, let $\mu = (\mu_1, \mu_2, \ldots, \mu_m)$ be an integer vector, where μ_i denotes the number of i's in ω. The standardization of ω with respect to C, which we also denote by $\mathsf{stand}_C(\omega)$, is defined by replacing the 1's in ω from left to right with the numbers c_1 through c_{μ_1}, replacing the 2's in ω from left to right with the numbers c_{μ_1+1} through $c_{\mu_1+\mu_2}$, etc. The following result formalizes the relationship between standardization and RSK, see for example [**87**, Lemma 7.11.6].

PROPOSITION 4.1.1. *Let ω be a word in the alphabet $[m]$ with length n. Then $\mathsf{stand}_C(P(\omega)) = P(\mathsf{stand}_C(\omega))$.*

Analogously, we define the standardization of a Burge array $\mathcal{A}_G$. Given a Burge array $\mathcal{A}_G$ with r columns and a subset $C = \{c_1 < \cdots < c_{2r}\}$ of $\mathbb{N}$, define the standardization of $\mathcal{A}_G$ with respect to C, denoted by $\overline{\mathsf{stand}}_C(\mathcal{A}_G)$, to be the map that replaces the 1's in $\mathcal{A}_G$ from left to right with the numbers c_1 through c_{d_1}, replaces the 2's from left to right with the numbers c_{d_1+1} through $c_{d_1+d_2}$, etc. where $d_G = (d_1, d_2, \ldots, d_n)$ is the degree sequence of G.

For T a semistandard Young tableau, the *reading word* of T denoted by $R(T)$ is obtained by reading the entries within a row from left to right starting with the bottommost row.

PROPOSITION 4.1.2. *Let $\mathcal{A}_G$ be a Burge array and $\mathcal{B}_G = \overline{\mathsf{stand}}_C(\mathcal{A}_G)$. Let T_G (resp. S_G) be the tableau associated to $\mathcal{A}_G$ (resp. $\mathcal{B}_G$) under the Burge correspondence. Then $S_G = \mathsf{stand}_C(T_G)$.*

PROOF. We proceed by induction on the number of columns of $\mathcal{A}_G = \begin{bmatrix} a_1 & a_2 & \ldots & a_r \\ b_1 & b_2 & \ldots & b_r \end{bmatrix}$. Note that the base case of $r = 0$ is trivial. Let $\mathcal{A}_{r-1}$ (resp. $\mathcal{B}_{r-1}$) denote the Burge array formed by the first $r-1$ columns of $\mathcal{A}_G$ (resp. $\mathcal{B}_G$). We have $\mathcal{B}_{r-1} = \overline{\mathsf{stand}}_{C-\{c_{i_r}, c_{2r}\}}(\mathcal{A}_{r-1})$ where $[c_{2r}, c_{i_r}]^T$ is the last column of $\mathcal{B}_G$. From our inductive hypothesis, $S_{r-1} = \mathsf{stand}_{C-\{c_{i_r}, c_{2r}\}}(T_{r-1})$. As the reading word $R(S_{r-1})$ is the standardization of $R(T_{r-1})$, we have $(R(S_{r-1}), c_{i_r})$ is the standardization of $(R(T_{r-1}), b_r)$. By Proposition 4.1.1, $S_{r-1} \leftarrow c_{i_r} = \mathsf{stand}_{C-\{c_{2r}\}}(T \leftarrow b_r)$. Thus the a_r and c_{2r} must be placed in the same position of their respective tableau. From the inverse of the Burge correspondence, a_r is the largest value in T_G and lies in a column to the right of any equivalent letters. Therefore, a_r in T_G gets sent to c_{2r} by stand_C and does not affect the mapping of the other letters in the tableau. Hence, $S_G = \mathsf{stand}_C(T_G)$. $\square$

4.2. Characterization of the shape of graphs

While answering Problem 4.1.1 in full generality seems far-achieving, we determine necessary and sufficient conditions of a hook-graph in this section. In Section 4.2.1, we give a necessary necessary condition for a connected hook-graphs. In Section 4.2.2, we define peak and valley conditions on Burge arrays which fully characterize hook-graphs.

4.2.1. Trees. We begin by establishing a necessary condition for a connected graph to be of hook shape.

PROPOSITION 4.2.1. *Let G be a simple graph and let k be the number of connected components of G that contain at least one edge. If G contains k edges $e_1, \ldots, e_k$ such that $G - \{e_1, \ldots, e_k\}$ has the same number of connected components as G, then G is not a hook-graph.*

PROOF. Let $C_1, \ldots, C_k$ denote the k connected components of G that contain at least one edge. Denote by n_i the number of vertices in C_i and let $n = \sum_{i=1}^{k} n_i$. If each C_i was minimally connected, it would contain $n_i - 1$ edges. Thus, G contains at least $\sum_{i=1}^{k}(n_i - 1) = n - k$ edges. The condition that "G contains k edges $e_1, \ldots, e_k$ such that $G - \{e_1, \ldots, e_k\}$ has the same number of connected components as G" implies that G has at least $n - k + k = n$ edges. Observe that the length of d_G is precisely n. However, the length of the partition $(e, 1^e)$ is at least $n + 1$, where $e \geqslant n$ is the number of edges of G. This implies that the partition $(e, 1^e)$ is not weakly greater than $\tilde{d}_G$ in dominance order. Thus, there are no semistandard Young tableaux of shape $(e, 1^e)$ with weight d_G, and T_G is not hook-shaped. $\square$

Recall that an undirected graph is called a *tree* if it is connected and does not contain any cycle. Setting $k = 1$ into Proposition 4.2.1, we obtain the following necessary condition for connected (excluding singletons) hook-graphs.

COROLLARY 4.2.1. *The only connected hook-graphs are trees.*

REMARK 4.2.1. *A tree need not be a hook-graph always. For example, the tree whose Burge array is* $\begin{bmatrix} 2 & 4 & 4 \\ 1 & 3 & 2 \end{bmatrix}$ *has the shape* $(2, 2, 2)$*.*

4.2.2. Peak and valley condition. We now introduce peak and valley conditions which characterize when a graph has hook shape.

Definition 4.2.1 (Peak). *A simple graph G with $\mathcal{A}_G$ as in Definition 4.1.3 is said to have a* peak *if there exist* $1 \leqslant i < j < k \leqslant r$ *such that*

(1) $b_i \leqslant b_k$,

(2) j *is the minimum index with* $b_k < b_j$,

(3) $a_i \leqslant b_j$.

Definition 4.2.2 (Valley). *A simple graph G with $\mathcal{A}_G$ as in Definition 4.1.3 is said to have a* valley *if there exist* $1 \leqslant i < j < k \leqslant r$ *such that the following conditions hold:*

(1) $b_j \leqslant b_k < a_j$,

(2) $b_j < b_i$.

Example 4.2.1.

(1) The graph with Burge array $\begin{bmatrix} 2 & 4 & 4 \\ 1 & 3 & 2 \end{bmatrix}$ *of Remark 4.2.1 has a peak with* $i = 1, j = 2, k = 3$, *but no valley.*

(2) The graph G with $\mathcal{A}_G = \begin{bmatrix} 4 & 5 & 6 & 7 \\ 1 & 3 & 5 & 2 \end{bmatrix}$ *does not have a peak as* $b_1 < b_4 < b_2$ *but* $a_1 > b_2$. *Note that* $b_1 < b_4 < b_3$, *but* $j = 3$ *is not the minimal j satisfying this condition. Also,* $\mathcal{A}_G$ *does not have a valley.*

(3) The graph considered in Example 4.1.2 has both a peak and a valley.

We refer to a Burge array as being *PV-free* if the Burge array does not contain a peak or a valley.

Theorem 4.2.1. *Let G be a simple graph on $[n]$. The graph G is a hook-graph if and only if its corresponding Burge array is PV-free.*

Proof. We prove the equivalent statement that the shape of G is *non-hook* if and only if G has either a peak or a valley.

Proof of forward direction $\Rightarrow$:

Let T_G be the tableau of non-hook shape associated with the Burge array $\mathcal{A}_G = \begin{bmatrix} a_1 & a_2 & \dots & a_r \\ b_1 & b_2 & \dots & b_r \end{bmatrix}$. Let T_ℓ denote the tableau corresponding to the sub-array consisting of the first ℓ columns of $\mathcal{A}_G$. Choose k minimal such that the shape of T_k is non-hook, that is, let k be the column that creates the cells $(2,2)$ and $(3,2)$ when applying the Burge algorithm. We claim that there exist j_1, j_2 with $1 \leqslant j_1 < j_2 < k$ such that $\begin{bmatrix} a_{j_1} & a_{j_2} & a_k \\ b_{j_1} & b_{j_2} & b_k \end{bmatrix}$ is either a peak or a valley.

Let x be the first row entry of T_{k-1} that is bumped by b_k in k-th step of the Burge algorithm. Let y be the entry in position $(2,1)$ (first entry of 2nd row) of T_{k-1}, see Figure 4.3. Note that $x > b_k$ and $y \leqslant x$. There are two different cases depending on whether x is an inserted letter or a

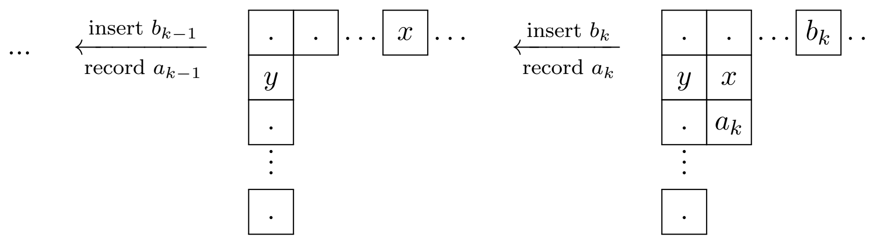

FIGURE 4.3. Tableau after $(k-1)$ insertions (left) and tableau after k insertions (right)

recorded letter.

Case 1: Let x be the inserted letter b_j for some $1 < j \leqslant k-1$.

Subcase A: If y is a recorded letter, then the only possibility is $y = a_1$. This implies that position $(1,1)$ of T_{k-1} is b_1 and the arm of T_{k-1} consists of $b_2 b_3 \dots b_{k-1}$. So we have that j is the smallest index between 1 and k satisfying $b_1 \leqslant b_k < b_j$. In addition, $a_1 = y \leqslant x = b_j$. Hence $\begin{bmatrix} a_1 & a_j & a_k \\ b_1 & b_j & b_k \end{bmatrix}$ is a peak.

Subcase B: Assume y is an inserted letter, say b_i for some i. Let b_m be the value which bumped b_i from the first row. So $b_m < b_i \leqslant x = b_j$. Also we must have $b_m \leqslant b_k$ as otherwise $b_k < b_m < x$ and in this case b_k would bump an entry strictly smaller than $x = b_j$. Now two cases arise: $m < j$ and $m > j$. When $m > j$, we have $a_j < a_m$. We use the relations $b_m \leqslant b_k < x = b_j < a_j < a_m$ and $b_m < b_i$ to show that $\begin{bmatrix} a_i & a_m & a_k \\ b_i & b_m & b_k \end{bmatrix}$ is a valley. When $m < j$, we claim that $\begin{bmatrix} a_m & a_j & a_k \\ b_m & b_j & b_k \end{bmatrix}$

is a peak. First observe that $a_m \leqslant b_j$. Since $m < j$, $x = b_j$ is inserted after b_m. If $a_m > b_j$ then b_j would bump an entry weakly larger than y and the shape of T_{k-1} becomes non-hook. This contradicts the minimality of k. Hence $a_m \leqslant b_j$. Also note that j is the smallest index between m and k satisfying $b_m \leqslant b_k < b_j$ as otherwise this would contradict the choice of y or x. Hence the claim is true.

Case 2: Let x be a recorded letter say a_j for $1 < j \leqslant k-1$. This implies $y = b_i$ for some i as y can no longer be the recording letter a_1.

Subcase A: $i \leqslant j$**.** Let b_m be the value which bumps b_i from the first row. Then we must have $m \geqslant j$. If $m < j$, then b_i would be placed at position $(2,1)$ of T_m. Since $x = a_j$ is placed in the first row, b_j must bump a letter from the first row. That letter would bump b_i from position $(2,1)$ of T_j. This contradicts that $y = b_i$. Now we have the relations $b_m \leqslant b_k < x = a_j \leqslant a_m$ and $b_m < b_i$. Hence $\begin{bmatrix} a_i & a_m & a_k \\ b_i & b_m & b_k \end{bmatrix}$ is a valley.

Subcase B: $i > j$**.** Since $x = a_j$ is placed in the first row, b_j must bump a letter from the first row. This letter must be an inserted letter since a_1 is already placed in the first column and hence a bumped recorded letter would create a non-hook shape. This would contradict the minimality of k. Let b_t with $t < j$ be the value bumped by b_j. So $b_t > b_j$. Let b_m denote the value that bumps $y = b_i$. Here $m > i$ but $b_m < b_i$. Observe that $b_i < b_t$, as b_i and b_t are in the first column. We also have $b_m \leqslant b_k$ otherwise b_k would bump something smaller than $x = a_j$. Moreover, $b_k < a_j \leqslant a_i \leqslant a_m$. Therefore $b_m \leqslant b_k < a_m$ and $b_t > b_m$, which shows that $\begin{bmatrix} a_t & a_m & a_k \\ b_t & b_m & b_k \end{bmatrix}$ is a valley.

Proof of backward direction $\Leftarrow$:

Now we shall prove that the shape of T_G is non-hook if G has either a valley or a peak. We start by proving the result for the case of a valley.

Suppose $\mathcal{A}_G$ contains a **valley** $\begin{bmatrix} a_i & a_j & a_k \\ b_i & b_j & b_k \end{bmatrix}$. We may assume that there is no peak or valley in the first $k-1$ columns of $\mathcal{A}_G$ and that T_{k-1} has hook shape. We consider two cases.

Case 1: Assume that b_i is present in the first row of T_{j-1}. Since $b_i > b_j$, b_j bumps an element, say x, from the first row of T_{j-1}. So $b_j < x \leqslant b_i$. Since b_j bumps a letter in the first row and since by assumption T_j has hook shape, it follows that a_j must be in the first row of T_j. Note that a_j

must also be in the first row of T_{k-1}. This is because if an element say b_ℓ (insertion letter) bumps a_j from the first row before the insertion of b_k, then T_ℓ has non-hook shape since $a_j \geqslant a_1$, which is greater or equal to the letter in cell $(2,1)$.

Since we have $b_j \leqslant b_k < a_j$, b_k bumps an element (which lies in the first row of T_{k-1}), say y. Then $b_j < y \leqslant a_j$. We claim that $x \leqslant y$. If $y < x$, note that y was not in T_{j-1} when b_j was inserted, since otherwise b_j would have bumped y. So $b_j < y < x \leqslant b_i < a_i < a_j$. This shows that y must be an inserted letter, say b_ℓ with $j < \ell < k$, and we have a valley formed by columns i, j, ℓ. This is a contradiction to our assumption. Therefore we must have $x \leqslant y$. In this case the shape of T_k becomes non-hook, because the entry in cell $(2,1)$ of T_{k-1} is less than or equal to x and so y must be placed in the $(2,2)$ position of T_k.

Case 2: Assume that b_i is not present in the first row of T_{j-1}. Let x be the element in T_{j-1} in the position where b_i was originally inserted. Since $x < b_i$ and x is inserted after step i, x must be an inserted letter, say b_ℓ with $i < \ell < j$. We claim that $b_\ell > b_j$. If not, we have $b_\ell \leqslant b_j$ and $\begin{bmatrix} a_i & a_\ell & a_j \\ b_i & b_\ell & b_j \end{bmatrix}$ is a valley since $b_j < b_i < a_i \leqslant a_\ell$. This is a contradiction. Hence $b_\ell > b_j$. This implies that b_j must bump an element from the first row of T_{j-1}. If z is that element, then $b_j < z \leqslant b_\ell$. Also, since b_j bumps an element, a_j must be in the first row in T_j. By the same arguments as in Case 1, a_j must be in the first row in T_{k-1}. Since by the valley condition $b_k < a_j$, b_k bumps an element in T_{k-1}. Call this element w. We claim that $z \leqslant w$. If $w < z$, note that w was not in T_{j-1} since then $b_j \leqslant b_k < w < z$ and hence b_j would have bumped w instead of z in T_{j-1}. If w is an inserted letter b_m with $j < m < k$, then $\begin{bmatrix} a_i & a_j & a_m \\ b_i & b_j & b_m \end{bmatrix}$ forms a valley as $b_m = w < z \leqslant b_\ell < a_\ell \leqslant a_j$. This is a contradiction. If w is a recorded letter, then $w \geqslant a_j \geqslant a_\ell > b_\ell \geqslant z$, contradicting the assumption that $w < z$. This proves $z \leqslant w$. Hence w must be placed in position $(2,2)$ of T_k. This implies that the shape of T_k is non-hook.

Considering the above cases, we conclude that T_G has non-hook shape when $\mathcal{A}_G$ has a valley.

Suppose $\mathcal{A}_G$ contains a **peak** $\begin{bmatrix} a_i & a_j & a_k \\ b_i & b_j & b_k \end{bmatrix}$. As before, we may assume that there is no valley or peak in first $k-1$ columns of $\mathcal{A}_G$ and that T_{k-1} has hook shape.

Claim: b_j cannot be bumped from the first row before the k-th step.

Proof: Assume that b_j is bumped from the first row before the k-th column is inserted. This would create a non-hook shape as $b_j \geqslant a_i \geqslant a_1$. This contradicts the fact that T_{k-1} has hook shape. Hence we have proved the claim.

Since b_j is in the first row of T_{k-1} and $b_k < b_j$, b_k must bump an element, say z. So $b_k < z \leqslant b_j$.

Case 1: Suppose b_i is not present in the first row of T_{k-1}. Let y be the entry in position $(2,1)$ of T_{k-1}. Then $y \leqslant b_i$. Also we have $b_i \leqslant b_k < z$. Since $y \leqslant z$, z would be placed at position $(2,2)$ of T_k, hence the shape of T_k becomes non-hook.

Case 2: Assume b_i is present in the first row of T_{k-1}.

Subcase A: b_i is placed at the end of the first row of T_{i-1}. If $z = a_\ell$, then $z \geqslant a_1$ and T_k has non-hook shape since the element in position $(2,1)$ in T_{k-1} is smaller or equal to a_1.

Now consider the case when $z = b_\ell$ for some ℓ. If $\ell \leqslant j$, consider the array $\begin{bmatrix} a_i & a_\ell & a_j & a_k \\ b_i & b_\ell & b_j & b_k \end{bmatrix}$. Note that indeed $i < \ell$. Namely, $z = b_\ell$ implies $b_i < b_\ell$ since $b_i \leqslant b_k$ and $b_k < z$. This implies that $i < \ell$; otherwise, b_i would bump a value from the first row of T_{i-1}. We have $b_i \leqslant b_k < z = b_\ell$. By definition of the peak $\begin{bmatrix} a_i & a_j & a_k \\ b_i & b_j & b_k \end{bmatrix}$, we have $a_i \leqslant b_\ell = z$. Note that by the definition of a peak $j = \ell$. Again, $y \leqslant z$ implies that shape of T_k is non-hook.

Now let us consider the case when $\ell > j$. If $b_\ell = b_j$, then b_j would be bumped by b_k instead of b_ℓ, which is a contradiction. If $b_\ell < b_j$, then $\begin{bmatrix} a_i & a_j & a_\ell \\ b_i & b_j & b_\ell \end{bmatrix}$ becomes a peak. Observe that j is minimal due to the minimality condition of the peak $\begin{bmatrix} a_i & a_j & a_k \\ b_i & b_j & b_k \end{bmatrix}$ and the inequality $b_k < b_\ell$. This contradicts our assumption that there should not be any other peak in the first k columns of $\mathcal{A}_G$.

Subcase B: b_i bumps an element from the first row of T_{i-1} when inserted. Then a_i is placed in the first row of T_i. Let u be the value bumped by b_i when inserted to T_{i-1} and let z be the value bumped by b_k. So, $b_i < u$ and $b_k < z$. Notice that the entry in position $(2,1)$ of T_{k-1} is less than or equal to u. So, if $u \leqslant z$, the shape of T_k becomes non-hook.

On the contrary, suppose $u > z$. Then z is not in the first row of T_{i-1} since otherwise b_i would bump z instead of u as $b_i \leqslant b_k < z < u$. This contradicts the definition of u. Hence z is inserted after the i-th step. As b_i bumps u from the first row of T_{i-1}, u is weakly less than a_i. As z is inserted after the i-th step, it must be an inserted letter i.e. $z = b_\ell$ for some $i < \ell < k$. Now either $z < a_i$ or $z \geqslant a_i$.

Assume that $z < a_i$. We prove that there does not exists an inserted letter b_t such that $i < t < k$ and $b_i \leqslant b_t < a_i$. Assume that there exists such an inserted letter b_t, where t is the smallest possible index. Observe that when b_t is inserted it bumps an element strictly right of b_i and weakly left of a_i in the arm of T_{t-1}. Denote this element by w. From the minimality of t, we have w is present in the first row of T_{i-1} and is strictly to the right of u. Thus, w is weakly larger than u, and when w is bumped, it will be weakly larger than the value in the $(2,1)$ cell of T_{t-1}. This would contradict T_{k-1} being hook shaped. Therefore no such inserted letter b_t exists. Observe that z satisfies the condition of b_t namely $z = b_\ell$ where $i < \ell < k$ and $b_i \leqslant b_\ell < a_i$. By our claim this is impossible.

Next consider the case $z \geqslant a_i$. Note that $a_1 \geqslant u$ as both of them are placed in first column. Together with $u > z \geqslant a_i$ we get $a_1 > a_i$, which is not possible. Therefore the case $u > z$ does not arise.

Considering all the cases, we proved that the shape of T_k is non-hook when $\mathcal{A}_G$ has a peak. This completes the proof. □

Remark 4.2.2. *Theorem 4.2.1 is the analogue to the statement for RSK that the shape of a word w under RSK is a single row if and only if w is weakly increasing.*

Remark 4.2.3. *In analogy with Schensted's result for the RSK insertion that the length of the longest increasing subsequence of a word w gives the length of the longest row in the Young tableaux under RSK, one might suspect that the longest PV-free subsequence of a Burge array gives the size of the largest hook in $\mathsf{sh}(T_G)$. However, this is not true as the following counterexample shows. Take the graph G with Burge array*

$$\mathcal{A}_G = \begin{bmatrix} 4 & 8 & 8 & 9 & 9 \\ 1 & 3 & 2 & 5 & 2 \end{bmatrix}.$$

The tableau under the Burge correspondence is

$$T_G = \begin{array}{|c|c|c|}\hline 1 & 2 & 2 \\ \hline 3 & 5 & 9 \\ \hline 4 & 8 \\ \cline{1-2} 8 & 9 \\ \cline{1-2}\end{array},$$

so that $\mathsf{sh}(T_G) = (3,3,2,2)$*. However, the subsequence*

$$\begin{bmatrix} 4 & 8 & 9 & 9 \\ 1 & 3 & 5 & 2 \end{bmatrix}$$

is PV-free and has hook shape $(4,1,1,1,1)$*, which is larger than the biggest hook* $(3,1,1,1)$ *in* $\mathsf{sh}(T_G)$*.*

A *star graph* is a graph where one vertex i is connected to all other vertices by an edge and no other edges exist in the graph.

Corollary 4.2.2. *All star graphs are hook-graphs.*

Proof. Assuming that the vertices of the star graph are labelled $1, 2, \ldots, n$ and the vertex connected to all other vertices is vertex i, the Burge array is

$$\begin{bmatrix} i & i & \ldots & i & i+1 & i+2 & \ldots & n \\ i-1 & i-2 & \ldots & 1 & i & i & \ldots & i \end{bmatrix},$$

which is PV-free. $\square$

4.3. Crystal Structure on hook-graphs

We review the crystal structure on semistandard Young tableaux in Section 4.3.1 and then define the new crystal structure on hook-graphs in Section 4.3.2.

4.3.1. Review of crystal structure on semistandard Young tableaux.

Definition 4.3.1. *Let T be a semistandard Young tableau. The* reading word *of T denoted by $R(T)$ is obtained by reading the entries within a row from left to right starting with the bottommost row. The* i-th reading word *of T denoted by $R_i(T)$ is the induced subword of $R(T)$ containing only the entries i and $i+1$.*

DEFINITION 4.3.2. *Let ω be a word with length n over the alphabet $[m]$. A* Knuth move *on ω is one of the following transformations:*

(1) $\omega_1 \dots bca \dots \omega_n \longrightarrow \omega_1 \dots bac \dots \omega_n$ *if* $a < b \leqslant c$*,*

(2) $\omega_1 \dots bac \dots \omega_n \longrightarrow \omega_1 \dots bca \dots \omega_n$ *if* $a < b \leqslant c$*,*

(3) $\omega_1 \dots acb \dots \omega_n \longrightarrow \omega_1 \dots cab \dots \omega_n$ *if* $a \leqslant b < c$*,*

(4) $\omega_1 \dots cab \dots \omega_n \longrightarrow \omega_1 \dots acb \dots \omega_n$ *if* $a \leqslant b < c$*.*

Two words ω and ν are said to be Knuth equivalent *if they differ by a sequence of Knuth moves.*

It is well-known that ω and ν are Knuth equivalent if and only if $P(\omega) = P(\nu)$, that is, their insertion tableaux under Schensted insertion are equal. In addition, it is also known that the crystal operators f_i and e_i on words preserve Knuth equivalence. Thus, in order to define the crystal operators on semistandard Young tableaux it suffices to look at their reading words.

DEFINITION 4.3.3. *Let T be a semistandard Young tableau in $\mathrm{Tab}_m(\lambda)$. Assign a ')' to every i in $R_i(T)$ and a '(' to every $i+1$ in $R_i(T)$. Successively pair every '(' that is directly left of a ')' which we call an* i-pair *and remove the i-paired terms. Continue this process until no more terms can be i-paired.*

The lowering operator f_i *for $1 \leqslant i < m$ acts on T as follows:*

(1) If there are no unpaired ')' terms left, then f_i annihilates T.

(2) Otherwise locate the i in T corresponding to the rightmost unpaired ')' of $R_i(T)$ and replace it with an $i+1$.

The raising operator e_i *for $1 \leqslant i < m$ acts on T as follows:*

(1) If there are no unpaired '(' terms left, then e_i annihilates T.

(2) Otherwise locate the $i+1$ in T corresponding to the leftmost unpaired '(' of $R_i(T)$ and replace it with an i.

The weight $\mathsf{wt}(T) = (a_1, a_2, \dots, a_m)$ *is an m-tuple such that a_i is the number of letters i in T.*

The crystal lowering and raising operators f_i and e_i for $1 \leqslant i < m$ together with the weight function wt define a type A_{m-1} crystal structure on $\mathrm{Tab}_m(\lambda)$. The vertices of the crystal are the elements in $\mathrm{Tab}_m(\lambda)$ for a fixed partition λ. There is an edge labelled i from $T \in \mathrm{Tab}_m(\lambda)$ to

$T' \in \mathrm{Tab}_m(\lambda)$ if $f_i(T) = T'$. Note that f_i and e_i are partial inverses, that is, if $f_i(T) = T'$ then $e_i(T') = T$ and vice versa.

4.3.2. Crystal structure on hook-graphs. In this section, we assume that G is a hook-graph or equivalently by Theorem 4.2.1 that $\mathcal{A}_G$ is a PV-free Burge array.

DEFINITION 4.3.4. *The i-th reading word of $\mathcal{A}_G$, denoted by $\tilde{R}_i(\mathcal{A}_G)$, is obtained by the following algorithm:*

(1) Let a_k denote the leftmost $i+1$ in the top row of $\mathcal{A}_G$. If $k = 1$ or $b_{k-1} \leqslant b_k$, then let a_k be the first letter of $\tilde{R}_i(\mathcal{A}_G)$.

(2) Read all other i's and $(i+1)$'s in $\mathcal{A}_G$ from left to right while appending the corresponding value to $\tilde{R}_i(\mathcal{A}_G)$.

EXAMPLE 4.3.1. *Let $\mathcal{A}_G = \begin{bmatrix} 3 & 3 & 4 \\ 2 & 1 & 3 \end{bmatrix}$. Then $\tilde{R}_1 = 21$, $\tilde{R}_2 = 3233$, and $\tilde{R}_3 = 4333$. For $\mathcal{A}_G = \begin{bmatrix} 3 & 4 \\ 2 & 1 \end{bmatrix}$, we have $\tilde{R}_3 = 34$.*

REMARK 4.3.1. *Note that except for the column in $\mathcal{A}_G$ containing a_k as in (1) of Definition 4.3.4, each column of $\mathcal{A}_G$ contains either i or $i+1$, but not both. Hence the algorithm to construct the reading word in Definition 4.3.4 is well-defined. Indeed, if $\mathcal{A}_G$ contains the column $\begin{bmatrix} i+1 \\ i \end{bmatrix}$, then it must be the leftmost column containing $i+1$ in the top row since by the definition of a Burge array the bottom row is decreasing for equal top row elements. Hence a_k is this leftmost $i+1$ and either $k = 1$ or $a_{k-1} \leqslant i$ and $b_{k-1} < i = b_k$, so that a_k is chosen as the first letter of $\tilde{R}_i(\mathcal{A}_G)$.*

DEFINITION 4.3.5. *Assign a ')' to every i in $\tilde{R}_i(\mathcal{A}_G)$ and a '(' to every $i+1$ in $\tilde{R}_i(\mathcal{A}_G)$. Successively pair every '(' that is directly left of a ')', called an i-pair, and remove the paired terms. Continue this process until no more terms can be paired.*

The operator $\tilde{f}_i$ acts on $\mathcal{A}_G$ as follows:

(1) If there are no unpaired ')' terms left, then $\tilde{f}_i$ annihilates $\mathcal{A}_G$ denoted by $\tilde{f}_i(\mathcal{A}_G) = 0$.

(2) *Otherwise locate the i in $\mathcal{A}_G$ corresponding to the rightmost unpaired ')' and denote it by x.*

   (a) *If there is no $i+1$ in the same column as x, then $\tilde{f}_i$ changes x in $\mathcal{A}_G$ to an $i+1$.*

   (b) *If there is an $i+1$ in the same column as x, then x is on the bottom row of $\mathcal{A}_G$. Let k be the index such that $b_k = x$. Let ℓ be the smallest index such that $b_\ell \leqslant b_{\ell+1} \leqslant \cdots \leqslant b_{k-1}$. Let $\ell \leqslant m \leqslant k$ be the largest index such that $b_m < a_\ell$. In the top row of $\mathcal{A}_G$ replace a_{k-1} with an $i+1$ and replace a_s with a_{s+1} for $\ell \leqslant s \leqslant k-2$. In the bottom row of $\mathcal{A}_G$ replace b_m with a_ℓ and replace b_k with b_m. (Remark: Observe that in this case $k \neq 1$ as otherwise the $i+1$ and i in this column would form an i-pair in $\tilde{R}_i$. Thus, this operation is well-defined.) This procedure is illustrated in Figure 4.4.*

$$\begin{bmatrix} \dots a_\ell & a_{\ell+1} & \dots & a_{m-1} & a_m & a_{m+1} & \dots & a_{k-1} & i+1 & \dots \\ \dots b_\ell & b_{\ell+1} & \dots & b_{m-1} & b_m & b_{m+1} & \dots & b_{k-1} & i & \dots \end{bmatrix}$$
$$\downarrow \tilde{f}_i$$
$$\begin{bmatrix} \dots a_{\ell+1} & a_{\ell+2} & \dots & a_m & a_{m+1} & a_{m+2} & \dots & i+1 & i+1 & \dots \\ \dots b_\ell & b_{\ell+1} & \dots & b_{m-1} & a_\ell & b_{m+1} & \dots & b_{k-1} & b_m & \dots \end{bmatrix}$$

FIGURE 4.4. Action of $\tilde{f}_i$ in Case (2b).

The operator $\tilde{e}_i$ acts on $\mathcal{A}_G$ as follows:

(1) *If there are no unpaired '(' terms left, then $\tilde{e}_i$ annihilates $\mathcal{A}_G$ denoted by $\tilde{e}_i(\mathcal{A}_G) = 0$.*

(2) *Otherwise locate the $i+1$ in $\mathcal{A}_G$ corresponding to the leftmost unpaired '(' and denote it by x.*

   (a) *If x is in the top row of $\mathcal{A}_G$ and there is an $i+1$ directly to the left of it, then let k be the index such that $a_k = x$. Let ℓ be the smallest index such that $b_\ell \leqslant b_{\ell+1} \leqslant \cdots \leqslant b_{k-1}$. Let $\ell \leqslant m \leqslant k$ be the smallest index such that $b_k < b_m$. In the top row of $\mathcal{A}_G$ replace a_ℓ with b_m and replace a_s with a_{s-1} for $\ell+1 \leqslant s \leqslant k-1$. In the bottom row of $\mathcal{A}_G$ replace b_m with b_k and replace b_k with an i.*

   (b) *Otherwise, $\tilde{e}_i$ changes x in $\mathcal{A}_G$ to an i.*

EXAMPLE 4.3.2. *Examples of crystals on Burge arrays are given in Figure 4.5. To illustrate the crystal operators* $\tilde{f}_i$ *of Definition 4.3.5, consider* $\tilde{f}_2$ *on* $\mathcal{A}_G = \begin{bmatrix} 2 & 3 & 4 \\ 1 & 2 & 3 \end{bmatrix}$. *In this case* $\tilde{R}_2(\mathcal{A}_G) =$ 3223, x *is the* 2 *in column two of* $\mathcal{A}_G$, $k = 2$, $\ell = 1$, *and* $m = 1$. *We obtain* $\tilde{f}_2(\mathcal{A}_G) = \begin{bmatrix} 3 & 3 & 4 \\ 2 & 1 & 3 \end{bmatrix}$.
For $\tilde{f}_3$ *on* $\mathcal{A}_G$ *we have* $x = 3$, $k = 3$, $\ell = 1$, $m = 1$, *and* $\tilde{f}_3(\mathcal{A}_G) = \begin{bmatrix} 3 & 4 & 4 \\ 2 & 2 & 1 \end{bmatrix}$.

The fact that a non-annihilated $\tilde{f}_i(\mathcal{A}_G)$ (resp. $\tilde{e}_i(\mathcal{A}_G)$) is a PV-free Burge array or even a valid Burge array will be shown as a consequence of Proposition 4.3.1.

LEMMA 4.3.1. $\tilde{R}_i(\mathcal{A}_G)$ *has at most one* i*-pair.*

PROOF. Assume that $\tilde{R}_i(\mathcal{A}_G)$ has at least two i-pairs. This implies that $\mathcal{A}_G$ contains at least two $(i+1)$'s. Let j be the index of the column containing the leftmost $i+1$ and k be the index of the column containing the second leftmost $i+1$. We break into cases based on the position of the $(i+1)$'s in columns j and k.

Case 1: Assume that $a_j = i+1$ and $a_k = i+1$. This implies that a_k is the second leftmost $i+1$ in $\tilde{R}_i(\mathcal{A}_G)$. Since $\mathcal{A}_G$ is assumed to have at least two i-pairs, there must exist $\ell > k$ such that $b_\ell = i$. The subarray $\begin{bmatrix} a_j & a_k & a_\ell \\ b_j & b_k & b_\ell \end{bmatrix} = \begin{bmatrix} i+1 & i+1 & a_\ell \\ b_j & b_k & i \end{bmatrix}$ is then a valley as $b_k \leqslant i = b_\ell < i+1 = a_k$ and $b_k < b_j$. This contradicts $\mathcal{A}_G$ being a PV-free Burge array.

Case 2: Assume that $a_j = i+1$ and $b_k = i+1$. This once again implies that b_k is the second leftmost $i+1$ in $\tilde{R}_i(\mathcal{A}_G)$. As $\mathcal{A}_G$ contains at least two i-pairs, there must exist $\ell > k$ such that $b_\ell = i$. Let $j < s < \ell$ be the leftmost index such that $b_j \leqslant i = b_\ell < b_s$. Note that such an s exists as k satisfies the desired conditions. The subarray $\begin{bmatrix} a_j & a_s & a_\ell \\ b_j & b_s & b_\ell \end{bmatrix} = \begin{bmatrix} i+1 & a_s & a_\ell \\ b_j & b_s & i \end{bmatrix}$ is a peak as $b_j \leqslant i = b_\ell < b_s$ and $a_j = i+1 \leqslant b_s$. This contradicts $\mathcal{A}_G$ being a PV-free Burge array.

Case 3: Assume that $b_j = i+1$ and $b_k = i+1$. This implies that b_j is the leftmost $i+1$ in $\tilde{R}_i(\mathcal{A}_G)$. To have at least two i-pairs, $\mathcal{A}_G$ must contain columns ℓ and m such that $j < \ell < m$ and

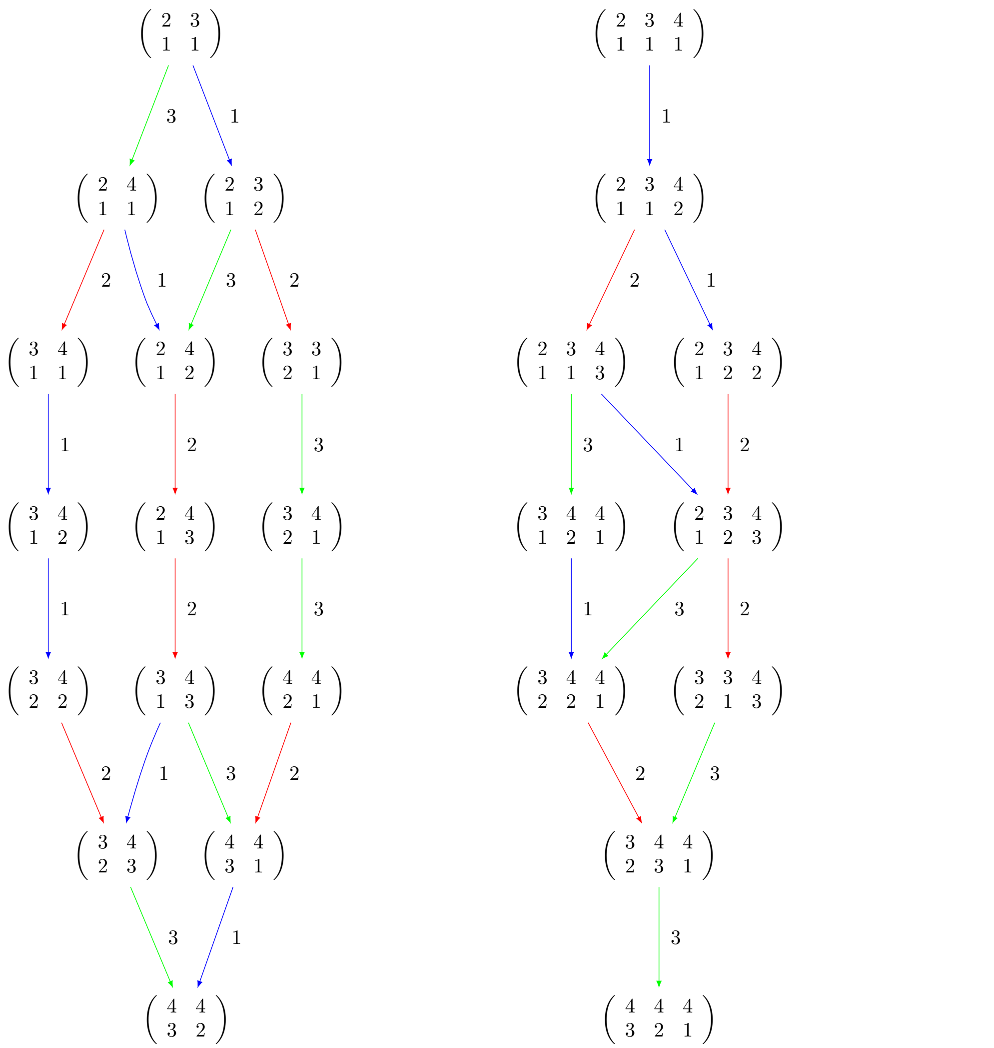

(A) Crystal of Burge arrays of shape $(2,1,1)$ with letters in $\{1,2,3,4\}$. (B) Crystal of Burge arrays of shape $(3,1,1,1)$ with letters in $\{1,2,3,4\}$.

FIGURE 4.5. Examples of crystals on Burge arrays.

$b_\ell = b_m = i$. The subarray $\begin{bmatrix} a_j & a_\ell & a_m \\ b_j & b_\ell & b_m \end{bmatrix} = \begin{bmatrix} a_j & a_\ell & a_m \\ i+1 & i & i \end{bmatrix}$ is a valley as $b_\ell = i \leqslant i = b_m < a_\ell$ and $b_\ell = i < i+1 = b_j$. This contradicts $\mathcal{A}_G$ being a PV-free Burge array. $\square$

LEMMA 4.3.2. *Let T_G be the threshold tableau associated to $\mathcal{A}_G$ under the Burge correspondence. Then $\tilde{R}_i(\mathcal{A}_G)$ is Knuth equivalent to $R_i(T_G)$.*

Proof. Since T_G is a hook tableau, $R_i(T_G)$ has at most one i-pair. Thus by Lemma 4.3.1 it suffices to prove that $\tilde{R}_i(\mathcal{A}_G)$ has an i-pair if and only if $R_i(T_G)$ has an i-pair, since the content of T_G and $\mathcal{A}_G$ are the same.

Assume that $\tilde{R}_i(\mathcal{A}_G)$ has an i-pair. Let k be the index of the column containing the $i+1$ that is in the i-pair. First assume that $a_k = i+1$. If $k = 1$, then a_k is recorded in the leg of T_G and $R_i(T_G)$ has an i-pair. If $b_{k-1} \leqslant b_k$ then b_k, when inserted, does not bump an element. Otherwise it would bump an element greater than the element bumped by b_{k-1} which would create a non-hook shape. Thus, a_k is recorded in the leg of T_G and $R_i(T_G)$ has an i-pair. If $b_{k-1} > b_k$, then in order for $\tilde{R}_i(\mathcal{A}_G)$ to have an i-pair, there must exist $\ell > k$ such that $b_\ell = i$. The subarray $\begin{bmatrix} a_{k-1} & a_k & a_\ell \\ b_{k-1} & b_k & b_\ell \end{bmatrix} = \begin{bmatrix} a_{k-1} & i+1 & a_\ell \\ b_{k-1} & b_k & i \end{bmatrix}$ is a valley as $b_k \leqslant i = b_\ell < i+1 = a_k$ and $b_{k-1} > b_k$ which is a contradiction. Next assume that $b_k = i+1$. In order for $\tilde{R}_i(\mathcal{A}_G)$ to have an i-pair, there must exist $\ell > k$ such that $b_\ell = i$. This implies that some $i+1$ must be bumped into the leg by an insertion letter whose index is at most ℓ. Thus, T_G has an $i+1$ in its leg and $R_i(T_G)$ has an i-pair. Thus, $R_i(T_G)$ has an i-pair whenever $\tilde{R}_i(\mathcal{A}_G)$ has an i-pair.

Assume that $R_i(T_G)$ has an i-pair. This implies that T_G has an $i+1$ in its leg. If the $i+1$ in the leg corresponds to a recording letter a_j for some j, then b_j does not bump an element when inserted. Otherwise $a_j = i+1$ would get placed in the first row of T_G and cannot be bumped into the leg as $a_1 \leqslant a_j$. This implies that either $j = 1$ or $b_{j-1} \leqslant b_j$. In either case, $\tilde{R}_i(\mathcal{A}_G)$ contains an i-pair. Assume the $i+1$ in the leg corresponds to an insertion letter b_j. Since b_j must be bumped into the leg and be i-paired with some i, there exists $j < k$ such that $b_k = i$. This implies that $\tilde{R}_i(\mathcal{A}_G)$ contains an i-pair. Thus, $\tilde{R}_i(\mathcal{A}_G)$ has an i-pair whenever $R_i(T_G)$ has an i-pair. $\square$

Proposition 4.3.1. *Let $\mathcal{A}_G$ be a PV-free Burge array and let T_G be its associated threshold tableau.*

(1) If $\tilde{f}_i(\mathcal{A}_G) \neq 0$, then $\tilde{f}_i(\mathcal{A}_G) = \mathcal{A}'_G$, where $\mathcal{A}'_G$ is the associated Burge array of $f_i(T_G)$.

(2) If $\tilde{e}_i(\mathcal{A}_G) \neq 0$, then $\tilde{e}_i(\mathcal{A}_G) = \tilde{\mathcal{A}}_G$, where $\tilde{\mathcal{A}}_G$ is the associated Burge array of $e_i(T_G)$.

Proof. As $\tilde{f}_i$ and $\tilde{e}_i$ are clearly partial inverses, it suffices to just prove part (1). From Lemma 4.3.2, we have that $f_i(T_G)$ is not annihilated. Let s be the column index of the rightmost i in $\mathcal{A}_G$ and denote this rightmost i by $\bar{i}$. We claim that $\bar{i}$ corresponds to the rightmost i in $R_i(T_G)$. If

$b_s = \bar{i}$, then $\bar{i}$ is inserted into the arm to the right of all preexisting i's when column s is inserted and will remain the rightmost i by the properties of Schensted row insertions. If $a_s = \bar{i}$ and $a_{s-1} = i$, then when column s is inserted b_s will bump an element from the arm. As T_G is hook-shaped, $a_s = \bar{i}$ will be recorded into the arm to the right of all preexisting i's and will remain the rightmost i. If $a_s = \bar{i}$ and $a_{s-1} \neq i$, then a_s is the only i in $\mathcal{A}_G$ and is trivially the rightmost i in $R_i(T_G)$ which proves our claim. As $f_i(T_G)$ is not annihilated and T_G is hook-shaped, $\bar{i}$ is the rightmost unpaired i of T_G and is changed to an $i+1$ by f_i.

Let r be the column index of the last column of $\mathcal{A}_G$. We denote by S_t the tableau obtained by reverse inserting columns $t+1$ through r of $f_i(T_G)$ and T_t the tableau obtained by inserting columns 1 through t of $\mathcal{A}_G$. We first assume that $r > s$ and prove that columns $s+1$ through r are the same in both arrays so that we may take r to be the same as s later in the proof. More specifically using induction, we will prove that for $s+1 \leqslant t \leqslant r$ column t of $\mathcal{A}'_G$ is the same as column t in $\mathcal{A}_G$ and $S_{t-1} = f_i(T_{t-1})$.

Let ℓ and a be the largest entries in the leg and arm of $T_r = T_G$, respectively. Note that ℓ and a are also the largest entries in the leg and arm of $S_r = f_i(T_G)$, respectively, as $r > s$. We break into subcases depending on whether $\ell > a$ or $\ell \leqslant a$.

When $\ell > a$, the column $[\ell, a]^T$ is obtained by reverse inserting both T_r and S_r implying the r-th column of $\mathcal{A}'_G$ is the same as the r-th column of $\mathcal{A}_G$. We claim that $\ell > i+1$. This is clearly true if $\bar{i}$ is in the leg of T_G as we assume $r > s$. If $\bar{i}$ is in the arm of T_r, then $a \geqslant i+1$ as a is to the right of $\bar{i}$ and $\bar{i}$ is the rightmost i in T_r. Hence the claim is true, and $\bar{i}$ remains the rightmost unpaired i in T_{r-1}. Thus, f_i acts on T_{r-1} by changing $\bar{i}$ to an $i+1$ which is precisely S_{r-1}.

When $\ell \leqslant a$, a is removed from T_r and a number which we denote by b_r is reverse inserted. This implies that the r-th column of $\mathcal{A}_G$ is $[a, b_r]^T$. Similarly, reverse inserting a column from S_r, a is removed from S_r and a number which we denote by c_r is reverse inserted. Note that b_r and c_r are equal and are in the same cell of their corresponding tableau except if an i and $i+1$ lie in the arm of S_r and the $(2,1)$ cell of S_r is an $i+1$. If an i and $i+1$ lie in the arm of S_r, then the value of the $(2,1)$ entry in T_r cannot be $\bar{i}$ as this would contradict $\bar{i}$ being the rightmost unpaired i of T_r. Thus, if an i and $i+1$ lie in the arm of S_r and the $(2,1)$ cell of S_r is an $i+1$, then the $(2,1)$ cell of T_r is an $i+1$. However, this would imply $b_r = i$ as it would need to bump an $i+1$ so that a is in the arm of T_r, an $i+1$ is in the $(2,1)$ cell, and the i in the arm is not bumped. This contradicts $r > s$. Therefore the r-th column of $\mathcal{A}_G$ and $\mathcal{A}'_G$ match. As $b_r \neq i$, $\bar{i}$ is still the rightmost unpaired i of T_{r-1} and $f_i(T_{r-1}) = S_{r-1}$. Assume that column t of $\mathcal{A}'_G$ is the same as column t in $\mathcal{A}_G$ and $S_{t-1} = f_i(T_{t-1})$ for some $s+1 < t \leqslant r$. Repeating the argument in the base case, we see that this holds for the case $t-1$ as well.

From the definition of $\tilde{f}_i$, we have that the columns $s+1$ through r of $\tilde{f}_i(\mathcal{A}_G)$ are the same as the columns $s+1$ through r of $\mathcal{A}_G$. By the previous paragraph, these columns are also equal to columns $s+1$ through r of $\mathcal{A}'_G$. We now assume that $r = s$ and prove that the columns 1 through s of $\tilde{f}_i(\mathcal{A}_G)$ and $\mathcal{A}'_G$ are equal by breaking into cases based off the position of $\bar{i}$ in T_s.

Case 1: $\bar{i}$ is in the leg of T_s.

Since $\bar{i}$ is the rightmost unpaired i of T_s, this implies that T_s does not contain any other i except for $\bar{i}$. Also in order for $\bar{i}$ to be in column s of $\mathcal{A}_G$, we must have $a_s = \bar{i}$. Thus, the column obtained from T_s by reverse inserting is of the form $[\bar{i}, a]^T$ where a is the largest value in the arm of T_s. In S_s, $\bar{i}$ is replaced with an $i+1$. Thus, the column obtained from S_s by reverse inserting is of the form $[i+1, a]^T$. We see that T_{s-1} and S_{s-1} are equal implying columns 1 through $s-1$ of $\mathcal{A}_G$ and $\mathcal{A}'_G$ are equal. Note that as $\bar{i}$ is the only i in $\mathcal{A}_G$ and $a_s = \bar{i}$, we have $\tilde{f}_i$ acts by changing $\bar{i}$ to an $i+1$ in $\mathcal{A}_G$. This is precisely the form of $\mathcal{A}'_G$ implying $\tilde{f}_i(\mathcal{A}_G) = \mathcal{A}'_G$.

Case 2: $\bar{i}$ is in the arm of T_s.

Let ℓ and a be the largest elements in the leg and arm of T_s, respectively. We break into subcases.

Assume $\bar{i} \geqslant \ell$. In order for $\bar{i}$ to be in the s-th column of $\mathcal{A}_G$, $\bar{i}$ must be a; otherwise the column reverse inserted from T_s would be $[a, \bar{i}]^T$. This implies $\bar{i}$ must bump an entry in the arm of T_{s-1} into its leg which would contradict $\bar{i} \geqslant \ell$. In particular, this implies that $a = \bar{i} \geqslant \ell$. Furthermore, the column obtained from T_s when reverse inserting is of the form $[\bar{i}, b_s]^T$, where b_s is the largest element in the arm of T_s strictly less than the entry in the cell $(2,1)$. Since $\bar{i}$ is the largest value in T_s, the $i+1$ in S_s created by applying f_i to T_s is also the largest value. Thus, the column obtained from S_s when reverse inserting is of the form $[i+1, c_s]^T$, where c_s is the largest element in the arm of S_s strictly less than the entry in the cell $(2,1)$. Since $f_i(T_s) = S_s$, we have $b_s = c_s$ and $T_{s-1} = S_{s-1}$. Thus, columns 1 through $s-1$ of $\mathcal{A}_G$ are identical to the corresponding columns of

$\mathcal{A}'_G$. As $\bar{i}$ is the rightmost i in $\mathcal{A}_G$ and is in the top row, it is also the rightmost unpaired i in $\mathcal{A}_G$. Thus, $\tilde{f}_i$ acts by changing $\bar{i}$ to an $i+1$ in $\mathcal{A}_G$. Thus, $\tilde{f}_i(\mathcal{A}_G) = \mathcal{A}'_G$.

Assume now that $\ell > a$ and $\ell \neq i+1$. In order for $\bar{i}$ to be in the s-th column of $\mathcal{A}_G$, $\bar{i}$ must be equal to a. When reversing the Burge correspondence of T_s, the column obtained is then of the form $[\ell, \bar{i}]^T$. From our assumption, we also have $\ell > i+1$ which implies that the column obtained from S_s when reversing the Burge correspondence is $[\ell, i+1]^T$. Observe that $T_{s-1} = S_{s-1}$ which forces columns 1 through $s-1$ of $\mathcal{A}_G$ and $\mathcal{A}'_G$ to be equal. We prove that $\bar{i}$ is the rightmost unpaired i in $\mathcal{A}_G$. For there to be a hope that this claim is not true, then there must exist either a column $[i+1, b_j]^T$ with $b_j \neq i$ or $[a_j, i+1]^T$ in $\mathcal{A}_G$. Note that there can only be one column with an $i+1$ in the top row; otherwise it would form a valley with columns $[i+1, b_j]^T$ and $[\ell, \bar{i}]^T$. If there exists a column of the form $[i+1, b_j]^T$, then in order for $\bar{i}$ to be unpaired in T_s there must be an i in a column $j+1$ through $s-1$ or a column of the form $[i, b_{j'}]^T$. Note that if there is an i in columns $j+1$ through $s-1$ this would imply $\bar{i}$ is the rightmost unpaired i of $\mathcal{A}_G$. If there is no i in columns $j+1$ through $s-1$, we must then have that column $j-1$ is of the form $[i, b_{j-1}]^T$. If $b_{j-1} > b_j$, then $\begin{bmatrix} i & i+1 & \ell \\ b_{j-1} & b_j & \bar{i} \end{bmatrix}$ is a valley implying $b_{j-1} \leqslant b_j$. Thus, if there exists a column of the form $[i+1, b_j]^T$ with no i's in columns j through $s-1$, then $\bar{i}$ must be the rightmost unpaired i. If there exists a column of the form $[a_j, i+1]^T$ with no i's in columns j through $s-1$, this would imply $\bar{i}$ when inserted would bump an element from the arm of T_s contradicting that ℓ is in the leg of T_s. Thus, if there exists a column of the form $[a_j, i+1]^T$, then there exists an i in columns j through $s-1$. Therefore, $\bar{i}$ is the rightmost unpaired i of $\mathcal{A}_G$ and $\tilde{f}_i$ acts by changing $\bar{i}$ to an $i+1$ in the s-th column. This is precisely $\mathcal{A}'_G$.

Assume that $\ell > a$ and $\ell = i+1$. In order for $\bar{i}$ to be in column s of $\mathcal{A}_G$, a must be precisely $\bar{i}$. When reversing the Burge correspondence of T_s, the column obtained is then of the form $[\ell = i+1, \bar{i}]^T$. Since $\ell = i+1$ came from the leg of T_s, there must exist an i somewhere in columns 1 through $s-1$; otherwise $\bar{i}$ would not be the rightmost unpaired i in T_s. Thus, $\bar{i}$ is also the rightmost unpaired i of $\mathcal{A}_G$. Let x be the value in the $(2,1)$ position of T_s and let y be the rightmost element in the arm of T_s that is strictly less than x. Note that $x < i+1 = \ell$; otherwise T_s would have shape $(1,1)$ and $R_i(T_s) = i+1\,i$. This implies $y \neq i$. We also have y is not an element in the top row of $\mathcal{A}_G$. Otherwise if $a_m = y$ for some m, then $x > y \geqslant a_1$ which contradicts x being in the $(2,1)$ cell. Thus, $y = b_m$ for some $1 \leqslant m \leqslant s-1$.

Assume now that x is a recording letter. As x lies in the $(2,1)$ cell of T_s, we must have $x = a_1$. This implies $b_1 \leqslant b_2 \leqslant \cdots \leqslant b_s = \bar{i}$ and $a_1 < a_2 < \cdots < a_s = \ell$. Recall that in S_s, $b_s = \bar{i}$ is replaced with an $i+1$. Hence, when reverse inserting a column from S_s, the $i+1$ that replaced $\bar{i}$ is removed, $y = b_m$ is replaced by $x = a_1$, and the rest of the entries in the leg are shifted up. Thus column s of $\mathcal{A}'_G$ is of the form $[i+1, b_m]^T$. We see that S_{s-1} is then associated to the Burge array $\begin{bmatrix} a_2 & a_3 & \ldots & a_m & a_{m+1} & a_{m+2} & \ldots & a_s = \ell = i+1 \\ b_1 & b_2 & \ldots & b_{m-1} & a_1 & b_{m+1} & \ldots & b_{s-1} \end{bmatrix}$ which mimics the action of $\tilde{f}_i$ on $\mathcal{A}_G$ as $b_1 \leqslant \cdots \leqslant b_{s-1}$ and b_m is the rightmost entry such that $b_m < a_1$.

Assume now that x lies in the bottom row of $\mathcal{A}_G$. This implies that there exists b_n that bumped x in T_{n-1} to the $(2,1)$ cell. Note that $b_{n-1} > b_n$; otherwise $\begin{bmatrix} a_z & a_{n-1} & a_n \\ x & b_{n-1} & b_n \end{bmatrix}$ would form a valley in $\mathcal{A}_G$. Since x is the value in the $(2,1)$ cell, $b_n \leqslant b_{n+1} \leqslant \cdots \leqslant b_s = \bar{i}$ in $\mathcal{A}_G$. We also have $b_{n+1} \geqslant a_n$. Otherwise $\begin{bmatrix} a_z & a_n & a_{n+1} \\ x & b_n & b_{n+1} \end{bmatrix}$ would form a valley. Thus, b_n is the largest element in the bottom row from column n to $s-1$ such that $b_n < a_n$ which implies $m = n$. Moreover, $a_n < \cdots < a_s = \ell$ are all in the legs of both of T_s and S_s. As S_s differs from T_s by changing $\bar{i}$ to an $i+1$, we have that reversing the Burge correspondence removes the $i+1$ from the arm of S_s, b_n is replaced by x, and the rest of the leg entries are shifted up. Thus column s of $\mathcal{A}'_G$ is $[i+1, b_n]^T$. As b_n bumped x out, we see that x is in the cell that it was originally inserted into. We see that reverse the Burge correspondence for S_{s-1} up to S_{n-1}, we get the columns $\begin{bmatrix} a_{n+1} & a_{n+2} & \ldots & a_{s-1} & a_s = \ell = i+1 \\ a_n & b_{n+1} & \ldots & b_{s-2} & b_{s-1} \end{bmatrix}$ and S_{n-1} is equal to T_{n-1} as x is in its original cell. These changes to $\mathcal{A}_G$ are seen to be the same as $\tilde{f}_i$ as n is the leftmost column index such that $b_n \leqslant \cdots \leqslant b_{s-1}$ and n is the rightmost column index between n and $s-1$ such that $b_n < a_n$.

Assume that $\bar{i} < \ell \leqslant a$ and the $(2,1)$ cell of T_s is not an $i+1$. Let x be the value in the $(2,1)$ position of T_s and let y be the rightmost element in the arm of T_s that is strictly less than x. Note that for $\bar{i}$ to be in the s-th column of $\mathcal{A}_G$, y must equal $\bar{i}$. As x is not equal to $i+1$, we have also $i+1 < x$. When reversing the Burge correspondence of T_s and S_s the columns obtained are $[a, \bar{i}]^T$ and $[a, i+1]^T$ respectively where the $i+1$ reverse bumped from S_s was the $i+1$ created by f_i. We have T_{s-1} and S_{s-1} are equal implying columns 1 through $s-1$ of $\mathcal{A}_G$ and $\mathcal{A}'_G$ are the same. Note that there cannot be an $i+1$ in columns 1 through $s-1$. Otherwise there would either be an $i+1$ in the leg of T_{s-1} which would contradict $x > i+1$ or $i+1$ is in the arm of T_{s-1} in which case $\bar{i}$ would bump an $i+1$ instead of x. Thus, $\bar{i}$ is the rightmost unpaired i of $\mathcal{A}_G$ and $\tilde{f}_i$ changes $\bar{i}$ to an $i+1$.

Assume that $\bar{i} < \ell \leqslant a$ and the $(2,1)$ cell of T_s is an $i+1$. Let $x = i+1$ be the value in the $(2,1)$ cell of T_s and y be the rightmost element in the arm of T_s that is strictly less than x. For $\bar{i}$ to be in the s-th column of $\mathcal{A}_G$, y must equal $\bar{i}$. As column s in $\mathcal{A}_G$ is of the form $[a,\bar{i}]^T$, $\bar{i}$ bumps $i+1$ from the arm of T_{s-1}. Since x is bumped into the cell $(2,1)$, we have $x = b_n$ for some n. Observe that no i can be strictly between columns n through s in $\mathcal{A}_G$; otherwise T_{s-1} would contain an $i+1$ in its leg. From this observation and the fact that $\bar{i}$ is the rightmost unpaired i in T_G, there must exist an i somewhere in columns 1 through $n-1$ in $\mathcal{A}_G$.

Let m be the column of the index of the second rightmost i in $\mathcal{A}_G$ which by the reasoning above satisfies $m < n$. We claim that i must be the insertion letter in column m, i.e. $b_m = i$. If $a_m = i$, then b_m must have bumped an element in T_{m-1} when inserted; otherwise an i would be present in the leg of T_{s-1}. Let b_z be the element bumped by b_m. This implies b_z is in the leg of T_{m-1}; however, $b_z < a_z \leqslant a_m = i < i+1$ which would be a contradiction. Thus our claim that $b_m = i$ holds. We also have $a_m \neq i+1$ as $\tilde{R}_i(\mathcal{A}_G)$ can have at most one i-pair by Lemma 4.3.1. From these two facts, b_m can not have bumped an element b_u when inserted into T_{m-1}. Otherwise $\begin{bmatrix} a_u & a_m & a \\ b_u & b_m & \bar{i} \end{bmatrix}$ would be a valley. As $y = \bar{i}$ is turned into an $i+1$ in S_s, the rightmost element in the arm of S_s that is strictly less than $x = i+1$ is b_m. Thus, the column reverse inserted from S_s is $[a, b_m = i]^T$ while the column reverse inserted from T_s is $[a,\bar{i}]^T$. This implies the s-th columns of $\mathcal{A}_G$ and $\mathcal{A}'_G$ are the same, but S_{s-1} differs from T_{s-1}. Note that columns $m+1$ through $s-1$ of both $\mathcal{A}_G$ and $\mathcal{A}'_G$ are the same as the reverse insertions of T_s and S_s in these steps do not involve b_m or the $i+1$ created by f_i respectively. As b_m did not bump an element when inserted into T_{m-1}, we have a_m is in the leg of both T_m and S_m and is the largest entry. We see $[a_m, b_m]^T$ is reverse inserted from T_m and $[a_m, i+1]^T$ is reverse inserted from S_m and $S_{s-1} = T_{s-1}$. Thus, the only difference between $\mathcal{A}_G$ and $\mathcal{A}'_G$ is that b_m is changed to an $i+1$ in $\mathcal{A}_G$. Note that b_m is the rightmost unpaired i in $\mathcal{A}_G$

since it is the second rightmost i and $\bar{i}$ is i-paired with the b_n. Thus, $\tilde{f}_i$ acts by changing b_m in $\mathcal{A}_G$ to an $i+1$ which is precisely $\mathcal{A}'_G$. $\square$

Corollary 4.3.1. *Let C_m be the set of all PV-free Burge arrays with entries at most m. Then C_m together with the operators $\tilde{f}_i$ and $\tilde{e}_i$ forms a Stembridge crystal of type A_{m-1}.*

Proof. The Burge correspondence is a crystal isomorphism between C_m and $\bigsqcup_{\substack{\lambda \text{ hook-shaped,} \\ \text{threshold}}} \mathrm{Tab}_m(\lambda)$ by Proposition 4.3.1, where $\mathrm{Tab}_m(\lambda)$ is the set of all semistandard Young tableaux of shape λ and entries at most m together with the usual crystal operators as in Definition 4.3.3. Since $\mathrm{Tab}_m(\lambda)$ forms a Stembridge crystal, so does C_m. $\square$

Corollary 4.3.2. *Let $\mathcal{A}_G$ be a PV-free Burge array corresponding to a graph G on n vertices. Then $\mathcal{A}_G$ is highest weight if and only if G is star-shaped (up to singletons) such that the central vertex is labelled 1 and the other vertices have labels $\{2, \ldots, n\}$.*

For a crystal C, an element $b \in C$ is called *extremal* if either $f_i(b) = 0$ or $e_i(b) = 0$ for each i in the index set and its weight is in the Weyl orbit of the highest weight element in the crystal component (see [**50**]). Let the weight of the highest weight vector $u \in C$ (which satisfies $e_i(u) = 0$ for all i) be $\mathsf{wt}(u) = \lambda$. The weight of the extremal vectors are permutations of λ. The tableaux under the Burge correspondence are threshold shapes. Hence, by the definition of threshold graphs, the extremal vectors of the crystal correspond to threshold graphs under the Burge correspondence.

CHAPTER 5

Promotion and growth diagrams for fans of Dyck paths and vacillating tableaux

This chapter is based on work in collaboration with Stephan Pfannerer, Anne Schilling, and Mary Claire Simone in [**71**].

5.1. Crystal bases

In this section we give further background knowledge on crystal bases. In section 5.1.1 we introduce the crystals corresponding to the spin representation in type B and the vector representation in type B and C. In section 5.1.2 we define virtual crystals and provide the virtual crystals for the spin and vector representation of type B_r into type C_r. In 5.1.3 we discuss the highest weight elements of weight zeros for the relevant crystals. We finish in Sections 5.1.4 and 5.1.5 by defining promotion on crystals via the crystal commutor and local rules respectively.

5.1.1. Background on crystals. Here we define certain crystals for the root systems B_r and C_r explicitly. Let $\mathbf{e}_i \in \mathbb{Z}^r$ be the i-th unit vector with 1 in position i and 0 everywhere else.

Definition 5.1.1. *The spin crystal of type B_r, denoted by $\mathcal{B}_{\mathsf{spin}}$, consists of all r-tuples $\epsilon = (\epsilon_1, \epsilon_2, \ldots, \epsilon_r)$, where $\epsilon_i \in \{\pm\}$. The weight of ϵ is*

$$\mathsf{wt}(\epsilon) = \frac{1}{2}\sum_{i=1}^{r} \epsilon_i \mathbf{e}_i.$$

The crystal operator f_r annihilates ϵ unless $\epsilon_r = +$. If $\epsilon_r = +$, f_r acts on ϵ by changing ϵ_r from $+$ to $-$ and leaving all other entries unchanged. The crystal operator f_i for $1 \leqslant i < r$ annihilates ϵ unless $\epsilon_i = +$ and $\epsilon_{i+1} = -$. In the latter case, f_i acts on ϵ by changing ϵ_i to $-$ and ϵ_{i+1} to $+$. Similarly, the crystal operator e_r annihilates ϵ unless $\epsilon_r = -$. If $\epsilon_r = -$, e_r acts on ϵ by changing ϵ_r from $-$ to $+$. The crystal operator e_i for $1 \leqslant i < r$ annihilates ϵ unless $\epsilon_i = -$ and $\epsilon_{i+1} = +$. In the latter case, e_i acts on ϵ by changing ϵ_i to $+$ and ϵ_{i+1} to $-$.

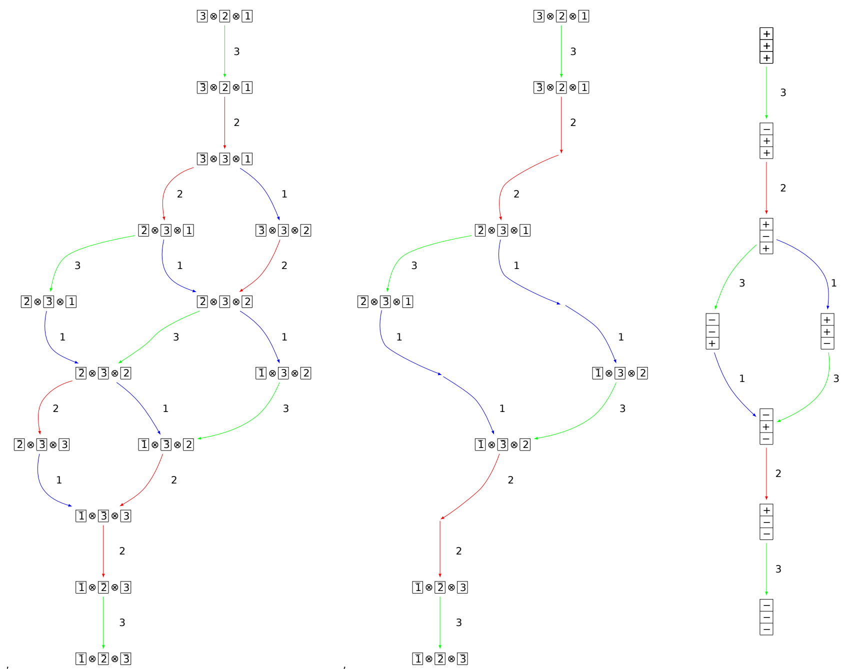

FIGURE 5.1. Left: One component of the crystal $\widehat{\mathcal{V}} = \mathcal{C}_{\square}^{\otimes 3}$ of type C_3. Middle: The virtual crystal $\mathcal{V}$ inside $\widehat{\mathcal{V}}$ of type B_3. Right: The spin crystal $\mathcal{B}_{\mathsf{spin}}$ of type B_3.

The crystal $\mathcal{B}_{\mathsf{spin}}$ of type B_3 is depicted in Figure 5.1.

DEFINITION 5.1.2. *Here we define the crystals for the vector representation of type B_r and C_r.*

(1) *The crystal $\mathcal{C}_{\square}$ of type C_r consists of the elements $\{1, 2, \ldots, r, \overline{r}, \ldots, \overline{2}, \overline{1}\}$. The crystal operator f_i for $1 \leqslant i < r$ maps i to $i+1$, maps $\overline{i+1}$ to $\overline{i}$ and annihilates all other elements. The crystal operator f_r maps r to $\overline{r}$ and annihilates all other elements. Similarly, the crystal operator e_i for $1 \leqslant i < r$ maps $i+1$ to i, maps $\overline{i}$ to $\overline{i+1}$ and annihilates all other elements. The crystal operator e_r maps $\overline{r}$ to r and annihilates all other elements. Furthermore, $\mathsf{wt}(i) = \mathbf{e}_i$ and $\mathsf{wt}(\overline{i}) = -\mathbf{e}_i$.*

(2) *The crystal $\mathcal{B}_{\square}$ of type B_r consists of the elements $\{1, 2, \ldots, r, 0, \overline{r}, \ldots, \overline{2}, \overline{1}\}$. The crystal operator f_i for $1 \leqslant i < r$ maps i to $i+1$, maps $\overline{i+1}$ to $\overline{i}$ and annihilates all other elements. The crystal operator f_r maps r to 0, 0 to $\overline{r}$ and annihilates all other elements. Similarly, the crystal operator e_i for $1 \leqslant i < r$ maps $i+1$ to i, maps $\overline{i}$ to $\overline{i+1}$ and annihilates all other elements. The crystal operator e_r maps $\overline{r}$ to 0, 0 to r and annihilates all other elements. Furthermore, $\mathsf{wt}(i) = \mathbf{e}_i$ and $\mathsf{wt}(\overline{i}) = -\mathbf{e}_i$ for $i \neq 0$ and $\mathsf{wt}(0) = 0$.*

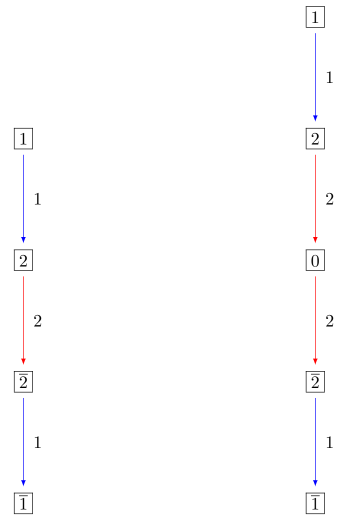

FIGURE 5.2. Left: The crystal $\mathcal{C}_\square$ of type C_2. Right: The crystal $\mathcal{B}_\square$ of type B_2.

The crystals $\mathcal{C}_\square$ for type C_2 and $\mathcal{B}_\square$ for type B_2 are depicted in Figure 5.2.

5.1.2. Virtual crystals. In this paper, we utilize virtual crystals to construct Fomin growth diagrams and the promotion operators for type B_r using results for type C_r. Hence let us briefly review the set-up for virtual crystals. Let $X \hookrightarrow Y$ be an embedding of Lie algebras such that the fundamental weights ω_i and simple roots α_i map as follows

$$\omega_i^X \mapsto \gamma_i \sum_{j \in \sigma(i)} \omega_j^Y,$$

$$\alpha_i^X \mapsto \gamma_i \sum_{j \in \sigma(i)} \alpha_j^Y.$$

Here γ_i is a multiplication factor, $\sigma \colon I^X \to I^Y / \operatorname{aut}$ is a bijection and aut is an automorphism on the Dynkin diagram for Y.

Let $\widehat{\mathcal{V}}$ be an ambient crystal associated to the Lie algebra Y. In [**16**, Chapter 5] it is assumed that $\widehat{\mathcal{V}}$ is a crystal for a simply-laced root system. However, in general it may be assumed that $\widehat{\mathcal{V}}$ is a crystal corresponding to a quantum group representation (which is the case in our setting).

DEFINITION 5.1.3. *If there is an embedding of Lie algebras $X \hookrightarrow Y$, then $\mathcal{V} \subseteq \widehat{\mathcal{V}}$ is a* virtual crystal *for the root system Φ^X if*

V1. *The ambient crystal $\widehat{\mathcal{V}}$ is a Stembridge crystal or a crystal associated to a representation for the root system Φ^Y with crystal operators $\widehat{e}_i$, $\widehat{f}_i$, $\widehat{\varepsilon}_i$, $\widehat{\varphi}_i$ for $i \in I^Y$ and weight function $\widehat{\mathsf{wt}}$.*

V2. *If $b \in \mathcal{V}$ and $i \in I^X$, then $\widehat{\varepsilon}_j(b)$ has the same value for all $j \in \sigma(i)$ and that value is a multiple of γ_i. The same is true for $\widehat{\varphi}_j(b)$.*

V3. *The subset $\mathcal{V} \sqcup \{\emptyset\} \subseteq \widehat{\mathcal{V}} \sqcup \{\emptyset\}$ is closed under the virtual crystal operators*

$$e_i := \prod_{j \in \sigma(i)} \widehat{e}_j^{\gamma_i} \quad \textit{and} \quad f_i := \prod_{j \in \sigma(i)} \widehat{f}_j^{\gamma_i}.$$

Furthermore, for all $b \in \mathcal{V}$

$$\varepsilon_i(b) = \max\{k \geqslant 0 \mid e_i^k(b) \neq \emptyset\} \quad \textit{and} \quad \varphi_i(b) = \max\{k \geqslant 0 \mid f_i^k(b) \neq \emptyset\}.$$

The tensor product of two virtual crystals for the same embedding $X \hookrightarrow Y$ is again a virtual crystal (see for example [**16**, Theorem 5.8]).

5.1.2.1. *Virtual crystal $B_r \hookrightarrow C_r$ spin to vector.* We will now apply the theory of virtual crystals to the embedding $B_r \hookrightarrow C_r$. In this setting $I^{C_r} = I^{B_r} = \{1, 2, \ldots, r\}$, $\sigma(i) = \{i\}$, $\gamma_i = 2$ for $1 \leqslant i < r$ and $\gamma_r = 1$. We consider as the ambient crystal

$$\widehat{\mathcal{V}} = \mathcal{C}_{\square}^{\otimes r}.$$

Define an ordering $<$ on the set $[r] \cup [\bar{r}]$ as follows:

$$1 < 2 < \cdots < r < \bar{r} < \cdots < \bar{1}.$$

Denote by $|\cdot|$ the map from $[r] \cup [\bar{r}]$ to $[r]$ that sends letters to their corresponding unbarred values.

Definition 5.1.4. *Let $\mathcal{V} \subseteq \widehat{\mathcal{V}}$ be given by*

$$\mathcal{V} := \{v_r \otimes v_{r-1} \otimes \cdots \otimes v_1 \in \widehat{\mathcal{V}} \mid v_i > v_j \textit{ and } |v_i| \neq |v_j| \textit{ for all } i > j\}.$$

Let $f_i = \widehat{f}_i^2$, $e_i = \widehat{e}_i^2$ for $1 \leqslant i < r$ and $f_r = \widehat{f}_r$, $e_r = \widehat{e}_r$.

Lemma 5.1.1. *$\mathcal{V} \sqcup \{\emptyset\}$ is closed under the operators f_i and e_i for $1 \leqslant i \leqslant r$.*

PROOF. Let $v = v_r \otimes v_{r-1} \otimes \cdots \otimes v_1 \in \mathcal{V}$. We break into cases depending on the value of i.

Assume that $i = r$. By the definition of $\mathcal{V}$, v must either contain an r or $\bar{r}$, but not both. If v contains an r, then this r must be to the left of all other unbarred letters and to the right of all barred letters. As f_r changes the r to a $\bar{r}$, $f_r(v)$ is still in $\mathcal{V}$. If v contains an $\bar{r}$, then $f_r(v) = \emptyset \in \mathcal{V} \sqcup \{\emptyset\}$.

Assume that $i \neq r$. Note that the conditions imposed on v imply that there exists exactly two indices j and k such that $|v_j| = i$ and $|v_k| = i+1$. By the ordering imposed on v, v can only be in the following forms:

- $\cdots \otimes i+1 \otimes i \otimes \cdots$
- $\cdots \otimes \bar{i} \otimes \overline{i+1} \otimes \cdots$
- $\cdots \otimes \bar{i} \otimes \cdots \otimes i+1 \otimes \cdots$
- $\cdots \otimes \overline{i+1} \otimes \cdots \otimes i \otimes \cdots$

For the first three cases, $f_i(v) = \emptyset$. When v is of the form $\cdots \otimes \overline{i+1} \otimes \cdots \otimes i \otimes \cdots$, f_i replaces the $\overline{i+1}$ with $\bar{i}$ and the i with $i+1$. Since v does not contain an $\bar{i}$ nor an $i+1$, $f_i(v)$ is an element of $\mathcal{V}$.

The fact that $e_i(v) \in \mathcal{V}$ for all $i \in 1 \leqslant i \leqslant r$ follows similarly. Thus, $\mathcal{V}$ is closed under the operators f_i and e_i. □

LEMMA 5.1.2. *All elements of $\mathcal{V}$ are in the connected component of $\widehat{\mathcal{V}}$ with highest weight element $r \otimes r-1 \otimes \cdots \otimes 1$.*

PROOF. Clearly $r \otimes r-1 \otimes \cdots \otimes 1$ is a highest weight element of $\widehat{\mathcal{V}}$ and the only element in $\mathcal{V}$ without any barred letters.

Consider $v = v_r \otimes \cdots \otimes v_1 \in \mathcal{V}$ containing a barred letter. Observe that the number of barred letters in $e_i(v)$ is at most the number of barred letters in v whenever $e_i(v) \neq \emptyset$. Since $\widehat{\mathcal{V}}$ is finite and $\mathcal{V}$ is closed under e_i, it suffices to show that $e_i(v) \neq \emptyset$ for some i. Let v_j denote the rightmost tensor factor in v that is a barred letter, and let $i = |v_j|$. We break into cases depending on the value of i.

If $i = r$, then $v_j = \bar{r}$ and v cannot contain an r. This implies that $e_r(v) \neq \emptyset$ as it acts on v by replacing v_j by r. The number of barred letters has decreased by one.

If $i \neq r$, then $v_j = \bar{i}$. As v_j is the rightmost barred letter in v, v must be of the form $\cdots \otimes \bar{i} \otimes \cdots \otimes i+1 \otimes \cdots$. Thus, e_i acts by changing $\bar{i}$ to $\overline{i+1}$ and $i+1$ to i. Note that the rightmost barred letter is closer to $\bar{r}$. $\square$

Definition 5.1.5. *Let $\Psi \colon \mathcal{B}_{\mathsf{spin}} \to \mathcal{V}$ be the map*

$$\Psi(\epsilon_1 \epsilon_2 \cdots \epsilon_r) = v_r \otimes v_{r-1} \otimes \cdots \otimes v_1,$$

where $v_r > v_{r-1} > \cdots > v_1$ such that if $\epsilon_i = +$ then v contains an i and if $\epsilon_i = -$ then v contains an $\bar{i}$ for all $1 \leqslant i \leqslant r$.

Lemma 5.1.3. *The map Ψ is a bijective map that intertwines the crystal operators on $\mathcal{B}_{\mathsf{spin}}$ and $\mathcal{V}$.*

Proof. From the definition of Ψ, it is clearly bijective. Let $\epsilon = \epsilon_1 \epsilon_2 \cdots \epsilon_r \in \mathcal{B}_{\mathsf{spin}}$. Since the raising and lowering operators of a crystal are partial inverses, it suffices to prove that $f_i(\epsilon) \neq \emptyset$ if and only if $f_i(\Psi(\epsilon)) \neq \emptyset$ and $\Psi(f_i(\epsilon)) = f_i(\Psi(\epsilon))$ whenever $f_i(\epsilon) \neq \emptyset$.

Assume that $f_i(\Psi(\epsilon)) \neq \emptyset$. If $i = r$, then $\Psi(\epsilon)$ contains an r implying $\epsilon_r = +$. Therefore $f_r(\epsilon) \neq \emptyset$. If $i \neq r$, then ϵ contains both an i and an $\overline{i+1}$. Thus, $\epsilon_i = +$ and $\epsilon_{i+1} = -$ implying $f_i(\epsilon) \neq \emptyset$.

Assume that $f_i(\epsilon) \neq \emptyset$. If $i = r$, then $\epsilon_r = +$ and f_r acts on ϵ by replacing ϵ_r with a $-$. This implies that $\Psi(f_r(\epsilon))$ can be obtained from $\Psi(\epsilon)$ by changing the r to $\bar{r}$, which agrees with the action of f_r. Therefore $\Psi(f_r(\epsilon)) = f_r(\Psi(\epsilon))$. If $i \neq r$, then ϵ_i must be a $+$ and ϵ_{i+1} must be a $-$. Thus, f_i swaps the signs of ϵ_i and ϵ_{i+1}. Since $\epsilon_i = +$ and $\epsilon_{i+1} = -$, $\Psi(\epsilon)$ must contain both an $\overline{i+1}$ and an i. This implies $\Psi(f_i(\epsilon))$ can be obtained from $\Psi(\epsilon)$ by replacing the $\overline{i+1}$ with $\bar{i}$ and the i with $i+1$. Observe that f_i acts on $\Psi(\epsilon)$ in exactly the same manner. Hence, $\Psi(f_i(\epsilon)) = f_i(\Psi(\epsilon))$. $\square$

Proposition 5.1.1. *$\mathcal{V}$ is a virtual crystal for the embedding of Lie algebras $B_r \hookrightarrow C_r$.*

Proof. The ambient crystal $\widehat{\mathcal{V}}$ is a crystal coming from a representation (see for example [**16**]), ensuring **V1**. Using Lemmas 5.1.1 and 5.1.3, we have $\Psi(\mathcal{B}_{\mathsf{spin}}) = \mathcal{V}$ is closed under the crystal operators f_i and e_i. Since $\mathcal{B}_{\mathsf{spin}}$ and $\widehat{\mathcal{V}}$ are both seminormal, the string lengths of $\mathcal{B}_{\mathsf{spin}}$ are the same as the string lengths in $\mathcal{V}$, showing **V3**. It is also not hard to see from Definition 5.1.4, that $\widehat{\varphi}_i(v), \widehat{\varepsilon}_i(v) \in 2\mathbb{Z}$ for $v \in \mathcal{V}$ and $1 \leqslant i < r$, proving **V2**. $\square$

An example of the virtual crystal construction for $\mathcal{B}_{\mathsf{spin}}$ is given in Figure 5.1. The virtual crystal of this section also follows from [**51**]. An affine version of this virtual crystal construction (which implies the one in this section) has appeared in [**33**, Lemma 4.2].

5.1.2.2. *Virtual crystal $B_r \hookrightarrow C_r$ vector to vector.* The crystal $\mathcal{B}_\square$ of Definition 5.1.2 can be realized as a virtual crystal inside the ambient crystal $\widehat{\mathcal{V}} = \mathcal{C}_\square^{\otimes 2}$.

Definition 5.1.6. *Define $\mathcal{V} \subseteq \widehat{\mathcal{V}} = \mathcal{C}_\square^{\otimes 2}$ of type C_r as*

$$\mathcal{V} = \{a \otimes a \mid 1 \leqslant a \leqslant r\} \cup \{\overline{a} \otimes \overline{a} \mid 1 \leqslant a \leqslant r\} \cup \{r \otimes \overline{r}\}$$

with $f_i = \widehat{f}_i^2$, $e_i = \widehat{e}_i^2$ for $1 \leqslant i < r$ and $f_r = \widehat{f}_r$, $e_r = \widehat{e}_r$.

Lemma 5.1.4. *$\mathcal{V} \sqcup \{\emptyset\}$ of Definition 5.1.6 is closed under the operators f_i and e_i for $1 \leqslant i \leqslant r$ and all elements in $\mathcal{V}$ are in the connected component of $\widehat{\mathcal{V}}$ with highest weight $1 \otimes 1$.*

Proof. We leave this to the reader to check. $\square$

Definition 5.1.7. *Let $\Psi \colon \mathcal{B}_\square \to \mathcal{V}$ be the map $\Psi(a) = a \otimes a$ and $\Psi(\overline{a}) = \overline{a} \otimes \overline{a}$ for $1 \leqslant a \leqslant r$ and $\Psi(0) = r \otimes \overline{r}$.*

Lemma 5.1.5. *The map Ψ of Definition 5.1.7 is a bijective map that intertwines the crystal operators on $\mathcal{B}_\square$ and $\mathcal{V}$.*

Proof. We leave this to the reader to check. $\square$

Proposition 5.1.2. *$\mathcal{V}$ of Definition 5.1.6 is a virtual crystal for the embedding of Lie algebras $B_r \hookrightarrow C_r$.*

Proof. We leave this to the reader to check. $\square$

An example of the virtual crystal construction for $\mathcal{B}_\square$ is given in Figure 5.3. The virtual crystal of this section also follows from [**51**]. An affine version of this virtual crystal construction (which implies the one in this section) has appeared in [**33**, Theorem 4.8].

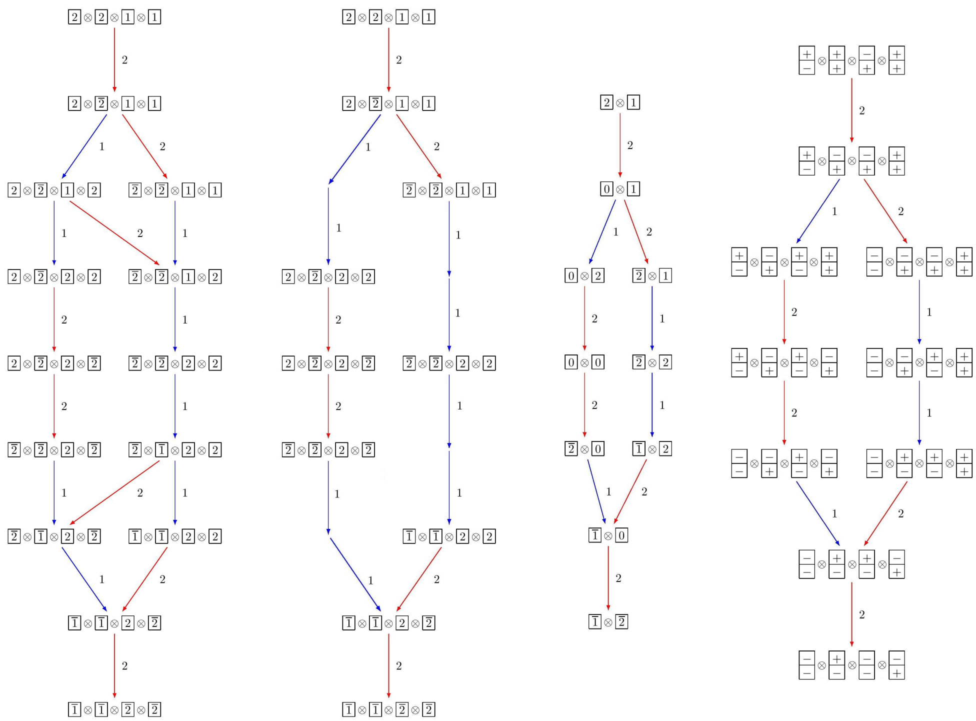

FIGURE 5.3. Far Left: One connected component $\widehat{\mathcal{S}}$ of the crystal $\widehat{\mathcal{V}}^{\otimes 2} = (\mathcal{C}_{\square}^{\otimes 2})^{\otimes 2}$ of type C_2. Middle Left: The connected component $\mathcal{S}$ of the virtual crystal $\mathcal{V}^{\otimes 2}$ inside $\mathcal{S}$ induced by Definition 5.1.6. Middle Right: The corresponding connected component $\mathcal{T}$ of the crystal $\mathcal{B}_{\square}^{\otimes 2}$ of type B_2 that corresponds to $\mathcal{S}$ under the embedding given in Definition 5.1.7. Far Right: The connected component $\mathcal{U}$ of $(\mathcal{B}_{\mathsf{spin}} \otimes \mathcal{B}_{\mathsf{spin}})^{\otimes 2}$ of type B_2 corresponding to $\mathcal{T}$ under the isomorphism given in Figure 5.4.

5.1.3. Highest weights of weight zero. A weight $\lambda \in \Lambda$ is called *minuscule* if $\langle \lambda, \alpha^\vee \rangle \in \{0, \pm 1\}$ for all coroots $\alpha^\vee$. A crystal $\mathcal{B}$ is called *minuscule* if $\mathsf{wt}(b)$ is minuscule for all $b \in \mathcal{B}$. Note that $\mathcal{B}_{\mathsf{spin}}$ is a minuscule crystal (see for example [**16**, Chapter 5.4]).

A weight λ is called *dominant* if $\langle \lambda, \alpha_i^\vee \rangle \geqslant 0$ for all $i \in I$. Let $\Lambda^+ \subseteq \Lambda$ denote the set of all dominant weights. Except for spin weights, dominant weights can be identified with partitions, where the fundamental weight ω_h corresponds to a column of height h in the partition. In this chapter we will identify partitions that differ by trailing zeroes. That is, $(3, 2, 0, 0)$ is identified with the partition $(3, 2)$.

Let $\mathcal{B}_1, \mathcal{B}_2, \ldots, \mathcal{B}_n$ be minuscule crystals. For any highest weight element

$$u = u_n \otimes \cdots \otimes u_1 \in \mathcal{B}_n \otimes \cdots \otimes \mathcal{B}_1$$

we may bijectively associate a sequence of dominant weights $\emptyset = \mu^0, \mu^1, \dots, \mu^n$, where $\mu^q := \sum_{i=1}^{q} \mathsf{wt}(u_i)$. The final weight $\mu := \mu^n$ of such a sequence is also the weight of the crystal element u. If μ is zero, u is a *highest weight element of weight zero*.

Note that the number of highest weight elements of weight zero in a tensor product of crystals is equal to the dimension of the invariant subspace, see for example [**75**, **97**].

5.1.3.1. *Oscillating tableaux.* Oscillating tableaux were introduced by Sundaram [**92**].

DEFINITION 5.1.8 (Sundaram [**92**]). *An* r-symplectic oscillating tableau O *of length* n *and shape* μ *is a sequence of partitions*

$$\mathsf{O} = (\emptyset = \mu^0, \mu^1, \dots, \mu^n = \mu)$$

such that the Ferrers diagrams of two consecutive partitions differ by exactly one cell, and each partition μ^i *has at most* r *nonzero parts.*

The r-symplectic oscillating tableaux of length n and shape μ are in bijection with highest weight elements in $\mathcal{C}_{\square}^{\otimes n}$ of type C_r and weight μ. This can be seen by induction on n. For $n = 1$, the only highest weight element is 1 and the only oscillating tableau is $(\emptyset, \square)$. Suppose the claim is true for $n-1$. If $u = b \otimes u_0 \in \mathcal{C}_{\square}^{\otimes n}$ is highest weight, then $u_0 \in \mathcal{C}_{\square}^{\otimes(n-1)}$ must be highest weight and hence by induction corresponds to an oscillating tableau $(\emptyset = \mu^0, \mu^1, \dots, \mu^{n-1})$. The element b is either an unbarred or barred letter. If b is the unbarred letter a, μ^n differs from μ^{n-1} by a box in row a. If b is the barred letter $\overline{a}$, μ^n has one less box in row a than μ^{n-1}. More precisely, for a highest weight element $b_n \otimes \cdots \otimes b_1 \in \mathcal{C}_{\square}^{\otimes n}$, the corresponding oscillating tableau satisfies $\mu^q = \sum_{i=1}^{q} \mathsf{wt}(b_i)$. This map can be reversed and it is not hard to see that the result is a highest weight element using the tensor product rule.

5.1.3.2. *r-fans of Dyck paths.* Next we relate highest weight elements of weight zero in $\mathcal{B}_{\mathsf{spin}}^{\otimes n}$ of type B_r and r-fans of Dyck paths.

DEFINITION 5.1.9. *An* r-fan of Dyck paths F *of length* n *is a sequence*

$$\mathsf{F} = (\emptyset = \mu^0, \mu^1, \dots, \mu^n = \emptyset)$$

of partitions μ^i with at most r parts such that the Ferrers diagram of two consecutive partitions differs by exactly one cell in each part. In other words, μ^i differs from μ^{i+1} by $(\pm 1, \pm 1, \ldots, \pm 1)$ for $0 \leqslant i < n$.

EXAMPLE 5.1.1. *For $r = 3$ and $n = 4$, the following is a 3-fan of Dyck paths*

$$\mathsf{F} = ((000), (111), (220), (111), (000)).$$

Since $\mathcal{B}_{\mathsf{spin}}$ of type B_r is minuscule, by the above discussion $\epsilon = \epsilon_n \otimes \cdots \otimes \epsilon_1 \in \mathcal{B}_{\mathsf{spin}}^{\otimes n}$ is highest weight if and only if $\sum_{i=1}^{q} \mathsf{wt}(\epsilon_i)$ is dominant for all $1 \leqslant q \leqslant n$. Hence highest weight elements of weight zero can be identified with an r-fan of Dyck paths of length n: the j-th entry of ϵ_i is $+$ if and only if the j-th Dyck path has an North-step at position i. In particular, for a highest weight element ϵ of weight zero, the sequence of dominant weights $\mu^q := \sum_{i=1}^{q} 2\mathsf{wt}(\epsilon_i)$ for $0 \leqslant q \leqslant n$ defines an r-fan of Dyck paths consistent with Definition 5.1.9.

A similar bijection was given in [**66**].

EXAMPLE 5.1.2. *The 3-fan of Dyck paths of Example 5.1.1 corresponds to the element*

$$\epsilon = (-,-,-) \otimes (-,-,+) \otimes (+,+,-) \otimes (+,+,+) \in \mathcal{B}_{\mathsf{spin}}^{\otimes 4}.$$

Following Definition 5.1.5, we obtain an embedding from the set of r-fans of Dyck paths into the set of oscillating tableaux.

DEFINITION 5.1.10. *For an r-fan of Dyck paths $\mathsf{F} = (\emptyset = \lambda^0, \lambda^1, \ldots, \lambda^n = \emptyset)$ we define the oscillating tableau $\iota_{F \to O}(\mathsf{F}) = (\emptyset = \mu^0, \ldots, \mu^{rn} = \emptyset)$ as follows. Let $v^t = \Psi(\lambda^t - \lambda^{t-1})$ for $1 \leqslant t \leqslant n$ with Ψ as in Definition 5.1.5. Then*

$$\mu^{tr+s} = \lambda^t + \sum_{i=1}^{s} \mathsf{wt}(v_i^{t+1}) \qquad \text{for } 0 \leqslant t < n,\ 0 \leqslant s < r.$$

5.1.3.3. *Vacillating tableaux.* Next we define *vacillating tableaux* which correspond to highest weight elements in $\mathcal{B}_{\square}^{\otimes n}$ of type B_r.

DEFINITION 5.1.11. *A* $(2r+1)$-orthogonal vacillating tableau *of length n is a sequence of partitions $\mathsf{V} = (\emptyset = \lambda^0, \ldots, \lambda^n)$ such that:*

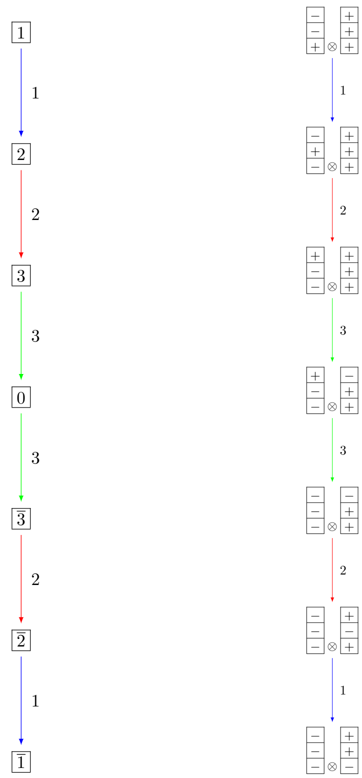

FIGURE 5.4. Left: $\mathcal{B}_\square$ of type B_3, Right: The component in $\mathcal{B}_{\mathsf{spin}} \otimes \mathcal{B}_{\mathsf{spin}}$ of type B_3 isomorphic to $\mathcal{B}_\square$.

(i) λ^i *has at most* r *parts.*

(ii) Two consecutive partitions either differ by a box or are equal.

(iii) If two consecutive partitions are equal, then all their r *parts are greater than* 0*.*

We call λ^n *the* weight *of* V*.*

A highest weight element $u = u_n \otimes \cdots \otimes u_1 \in \mathcal{B}_\square^{\otimes n}$ of type B_r corresponds to the $(2r+1)$-vacillating tableau $(\emptyset = \lambda^0, \lambda^1, \ldots, \lambda^n)$, where $\lambda^q = \sum_{i=1}^q \mathsf{wt}(u_i)$.

Note that $\mathcal{B}_\square$ is not minuscule. The crystal $\mathcal{B}_\square$ is isomorphic to the component with highest weight element $(+,-,\ldots,-) \otimes (+,\ldots,+)$ in $\mathcal{B}_{\mathsf{spin}} \otimes \mathcal{B}_{\mathsf{spin}}$, see Figure 5.4. From this we obtain a map from the set of vacillating tableaux of weight zero and length n into the set of fans of Dyck paths of length $2n$ that we now explain. Denote by $\mathbf{1}$ the vector $\mathbf{e}_1 + \mathbf{e}_2 + \cdots + \mathbf{e}_r$ and write $\rho < \nu$ if $\nu = \rho + \mathbf{e}_i$ for some i.

DEFINITION 5.1.12. *For a vacillating tableau of weight zero* $\mathsf{V} = (\emptyset = \lambda^0, \dots, \lambda^n = \emptyset)$ *we define the fan of Dyck paths* $\iota_{V \to F}(\mathsf{V}) = (\emptyset = \mu^0, \dots, \mu^{2n} = \emptyset)$ *as follows:*

$$\mu^{2i} = 2 \cdot \lambda^i$$

$$\mu^{2i-1} = \begin{cases} 2 \cdot \lambda^{i-1} + \mathbf{1} & \text{if } \lambda^{i-1} < \lambda^i, \\ 2 \cdot \lambda^i + \mathbf{1} & \text{if } \lambda^{i-1} > \lambda^i, \\ 2 \cdot \lambda^{i-1} + \mathbf{1} - 2\mathbf{e}_r & \text{if } \lambda^{i-1} = \lambda^i. \end{cases}$$

Similarly, following Definition 5.1.7, we obtain an embedding from the set of vacillating tableaux of weight zero into the set of oscillating tableaux.

DEFINITION 5.1.13. *For a vacillating tableau of weight zero* $\mathsf{V} = (\emptyset = \lambda^0, \dots, \lambda^n = \emptyset)$ *we define the oscillating tableau* $\iota_{V \to O}(\mathsf{V}) = (\emptyset = \mu^0, \dots, \mu^{2n} = \emptyset)$ *as follows:*

$$\mu^{2i} = 2 \cdot \lambda^i$$

$$\mu^{2i-1} = \lambda^{i-1} + \lambda^i + \begin{cases} 0 & \text{if } \lambda^{i-1} \neq \lambda^i, \\ -\mathbf{e}_r & \text{if } \lambda^{i-1} = \lambda^i. \end{cases}$$

5.1.4. Promotion via crystal commutor. For finite crystals B_λ of classical type of highest weight λ, Henriques and Kamnitzer [**41**] introduced the crystal commutor as follows. Let $\eta_{B_\lambda} \colon B_\lambda \to B_\lambda$ be the Lusztig involution, which maps the highest weight vector to the lowest weight vector and interchanges the crystal operators f_i with $e_{i'}$, where $w_0(\alpha_i) = -\alpha_{i'}$ under the longest element w_0. This can be extended to tensor products of such crystals by mapping each connected component to itself using the above. Then the *crystal commutor* is defined as

$$\sigma \colon B_\lambda \otimes B_\mu \to B_\mu \otimes B_\lambda$$
$$b \otimes c \mapsto \eta_{B_\mu \otimes B_\lambda}(\eta_{B_\mu}(c) \otimes \eta_{B_\lambda}(b)).$$

If we want to emphasize the crystals involved, we write $\sigma_{A,B} \colon A \otimes B \to B \otimes A$.

Following [**31**, **97**, **98**], we define the promotion operator using the crystal commutor.

Definition 5.1.14. *Let C be a crystal and $u \in C^{\otimes n}$ a highest weight element. Then* promotion pr *on u is defined as $\sigma_{C^{\otimes n-1},C}(u)$.*

Remark 5.1.1. *Note that inverse promotion is given by $\sigma_{C,C^{\otimes n-1}}(u)$. The conventions in the literature about what is called promotion and what is called inverse promotion are not always consistent. Our convention here agrees with the definition of promotion on posets that removes the letters 1 and slides letters (see for example [**6**, **88**]). The convention here is the opposite of the convention on tableaux which removes the largest letter and uses jeu de taquin slides (see for example [**8**, **78**]).*

Example 5.1.3. *Consider the crystal $C = B_\square$ of type A_2 (see [**16**]). Then*

$$u = 1 \otimes 3 \otimes 2 \otimes 2 \otimes 1 \otimes 1 \in C^{\otimes 6}$$

is highest weight and

$$\sigma_{C^{\otimes 5},C}(u) = 2 \otimes 1 \otimes 3 \otimes 1 \otimes 2 \otimes 1.$$

The recording tableaux for the RSK insertion of the words 132211 *and* 213121 *(from right to left) are*

$$\begin{array}{|c|c|c|}\hline 1 & 2 & 6 \\ \hline 3 & 4 \\ \cline{1-2} 5 \\ \cline{1-1}\end{array} \qquad \text{and} \qquad \begin{array}{|c|c|c|}\hline 1 & 3 & 5 \\ \hline 2 & 6 \\ \cline{1-2} 4 \\ \cline{1-1}\end{array}$$

which are related by the usual (inverse) promotion operator (removing the letter 1, doing jeu-de-taquin slides, filling the empty cell with the largest letter plus one and subtracting 1 from all entries) on standard tableaux.

Example 5.1.4. *Promotion on the element ϵ in Example 5.1.2 is*

$$\sigma_{\mathcal{B}_{\mathsf{spin}}^{\otimes 3},\mathcal{B}_{\mathsf{spin}}}(\epsilon) = (-,-,-) \otimes (-,+,+) \otimes (+,-,-) \otimes (+,+,+).$$

Note that if $\Psi \colon C \to \mathcal{V} \subseteq \widehat{\mathcal{V}}$ is a virtual embedding, then

$$\Psi \circ \sigma_{C^{\otimes n-1},C} = \sigma_{\widehat{\mathcal{V}}^{\otimes n-1},\widehat{\mathcal{V}}} \circ \Psi \tag{5.1.1}$$

by Axioms V2 and V3 in Definition 5.1.3 as long as the folding σ and the multiplication factors γ_i respect the map $w_0(\alpha_i) = -\alpha_{i'}$. This is the case for the virtualizations in this paper.

5.1.5. Promotion via local rules. Adapting local rules of van Leeuwen [**94**], Lenart [**60**] gave a combinatorial realization of the crystal commutor $\sigma_{A,B}$ by constructing an equivalent bijection between the highest weight elements of $A \otimes B$ and $B \otimes A$ respectively. The *local rules* of Lenart [**60**] can be stated as follows: four weight vectors $\lambda, \mu, \kappa, \nu \in \Lambda$ depicted in a square diagram $\begin{tikzcd} \lambda \arrow[r, dash] \arrow[d, dash] & \nu \arrow[d, dash] \\ \kappa \arrow[r, dash] & \mu \end{tikzcd}$ satisfy the local rule, if $\mu = \mathrm{dom}_W(\kappa + \nu - \lambda)$, where W is the Weyl group of the root system Φ underlying A and B. Furthermore, $\mathrm{dom}_W(\rho)$ is the dominant weight in the Weyl orbit of ρ.

Theorem 5.1.1 ([**60**, Theorem 4.4]). *Let A and B be crystals embedded into tensor products $A_\ell \otimes \cdots \otimes A_1$ and $B_k \otimes \cdots \otimes B_1$ of crystals of minuscule representations, respectively. Let $w = w_{k+\ell} \otimes \cdots \otimes w_1$ be a highest weight element in $A \otimes B$ with corresponding tableau $(\emptyset = \mu^0, \mu^1, \ldots, \mu^{k+\ell} = \mu)$ Then $\sigma_{A,B}(w)$ can be computed as follows. Create a $k \times \ell$ grid of squares as in (5.1.2), labelling the edges along the left border with $w_1, \ldots, w_k$ and the edges along the top border with $w_{k+1}, \ldots, w_{k+\ell}$:*

(5.1.2)
$$\begin{tikzcd}
\mu^k \arrow[r, "w_{k+1}"] & \cdot \arrow[r, dotted, dash] & \cdot \arrow[r, "w_{k+\ell}"] & \mu^{k+\ell} \\
\mu^{k-1} \arrow[r] \arrow[u, "w_k"] & \cdot \arrow[r, dotted, dash] \arrow[u] & \cdot \arrow[r] \arrow[u] & \cdot \arrow[u, "\hat{w}_{k+\ell}"'] \\
\mu^1 \arrow[r] \arrow[u, dotted, dash] & \cdot \arrow[r, dotted, dash] \arrow[u, dotted, dash] & \cdot \arrow[r] \arrow[u, dotted, dash] & \cdot \arrow[u, dotted, dash] \\
\mu^0 \arrow[r, "\hat{w}_1"'] \arrow[u, "w_1"] & \hat{\mu}^1 \arrow[r, dotted, dash] \arrow[u] & \hat{\mu}^{\ell-1} \arrow[r, "\hat{w}_\ell"'] \arrow[u] & \hat{\mu}^\ell \arrow[u, "\hat{w}_{1+\ell}"']
\end{tikzcd}$$

For each square use the local rule to compute the weight vectors on the square's corners. Given a horizontal edge from κ to μ in the jth column, label the edge by the element in A_j with weight $\mu - \kappa$. Similarly, given a vertical edge from μ to ν in the ith row, label the edge by the element in B_i with weight $\nu - \mu$. The labels $\hat{w}_{k+\ell} \ldots \hat{w}_1$ of the edges along the right and the bottom border of the grid then form $\sigma_{A,B}(w)$ with corresponding tableau $(\emptyset = \mu^0, \hat{\mu}^1, \ldots, \hat{\mu}^{k+\ell-1}, \mu^{k+\ell} = \mu)$.

1. Calculate promotion over and over again using a calculation schema	**2.** Cut and glue the schema to obtain a square	**3.** Fill all cells according to a function Φ with integers	**4.** Interpret the filled square as adjacency matrix of a graph	**5.** Read the chord diagram from the adjacency matrix.
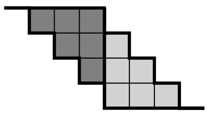	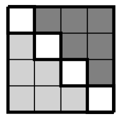	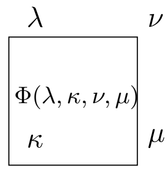	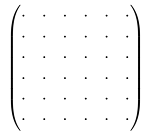	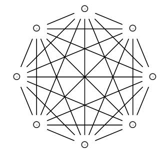

FIGURE 5.5. Overview of the steps in our map

EXAMPLE 5.1.5. *Performing Lenart's local rules on the elements in Example 5.1.3 gives*

$$\begin{tikzcd}
(1,0,0) \arrow[r, "1"] & (2,0,0) \arrow[r, "2"] & (2,1,0) \arrow[r, "2"] & (2,2,0) \arrow[r, "3"] & (2,2,1) \arrow[r, "1"] & (3,2,1) \\
(0,0,0) \arrow[r, "1"'] \arrow[u, "1"] & (1,0,0) \arrow[r, "2"'] \arrow[u, "1"] & (1,1,0) \arrow[r, "1"'] \arrow[u, "1"] & (2,1,0) \arrow[r, "3"'] \arrow[u, "2"] & (2,1,1) \arrow[r, "1"'] \arrow[u, "2"] & (3,1,1) \arrow[u, "2"']
\end{tikzcd}$$

which recovers $\sigma_{C^{\otimes 5},C}(1 \otimes 3 \otimes 2 \otimes 2 \otimes 1 \otimes 1) = 2 \otimes 1 \otimes 3 \otimes 1 \otimes 2 \otimes 1$.

5.2. Chord diagrams

In this section, we give the various filling rules and methods to construct maps from highest weight elements of weight zero to chord diagrams. In Section 5.2.1 we define a construction that involves building an adjacency matrix via promotion. In Section 5.2.2 we define another construction that involves Fomin growth diagrams.

5.2.1. Promotion matrices.

In this section we summarize the method developed in [**74**] to obtain a map from highest weight words of weight zero to chord diagrams that intertwines promotion and rotation.

We start with the definition of chord diagrams and their rotation.

DEFINITION 5.2.1. *A chord diagram of size n is a graph with n vertices depicted on a circle which are labelled $1, \dots, n$ in counter-clockwise orientation.*

The rotation of a chord diagram is obtained by rotating all edges clockwise by $\frac{2\pi}{n}$ around the center of the diagram.

In our setting all chord diagrams are undirected graphs with possibly multiple edges between the same two vertices. We can therefore identify chord diagrams with their *adjacency matrix*. The adjacency matrix is a symmetric $n \times n$ matrix $M = (m_{ij})_{1 \leqslant i,j \leqslant n}$ with non-negative integer entries and m_{ij} denotes the number of edges between vertex i and vertex j.

Proposition 5.2.1 ([**74**]). *Let M be the adjacency matrix of a chord diagram G. Denote by $\operatorname{rot} M$ the toroidal shift of M, that is, the matrix obtained from M by first cutting the top row and pasting it to the bottom and then cutting the leftmost column and pasting it to the right.*

Then $\operatorname{rot} M$ is the adjacency matrix corresponding to the rotation of G.

Let us now outline the idea to construct such a rotation and promotion intertwining map and then provide the details on the individual steps on the examples of oscillating tableaux, r-fans of Dyck paths and vacillating tableaux. A visual guideline can be seen in Figure 5.5.

Construction 5.2.1. *The construction is given as follows:*

Step 1: *Iteratively calculate promotion of a highest weight word of weight zero and length n using Lenart's schema* (5.1.2) *a total of n times.*

Step 2: *Group the results into a square grid, called the* promotion matrix*.*

Step 3: *Fill the cells of the square grid with certain non-negative integers according to a filling rule Φ that only depends on the four corners of the cells in the schema* (5.1.2)*.*

Step 4: *Regard the filling as the adjacency matrix of a graph, which is the chord diagram.*

We now discuss the filling rules in the various cases. Note that the filling rules are new even in the case of oscillating tableaux as the proofs in [**75**] did not follow this construction.

5.2.1.1. *Chord diagrams for oscillating tableaux.* Recall that the Weyl group of type C_r is the hyperoctahedral group $\mathfrak{H}_r$ of signed permutations of $\{\pm 1, \pm 2, \ldots, \pm r\}$. Weights are elements in $\mathbb{Z}^r$ and dominant weights are weakly decreasing integer vectors with non-negative entries (or equivalently partitions). Thus, the dominant representative $\operatorname{dom}_{\mathfrak{H}_r}(\lambda)$ of a weight λ is obtained by sorting the absolute values of its entries into weakly decreasing order.

We slightly modify Lenart's schema for the crystal commutor (5.1.2) by omitting edge labels as only the weights on the corners are needed. Additionally, given an oscillating tableau $\mathsf{O} =$

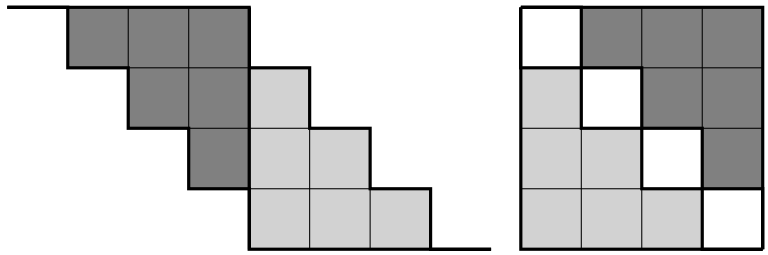

FIGURE 5.6. The transformation into a promotion matrix. The highlighted part is cut away and glued on the left.

$(\emptyset = \mu^0, \mu^1, \dots, \mu^n = \mu)$, we start each row with the zero weight $\emptyset$ and end each row with the weight μ, which makes it easier to iteratively use this schema to calculate promotion. This way the promotion of the oscillating tableau $\mathsf{O} = (\emptyset = \mu^0, \mu^1, \dots, \mu^n = \mu)$ is the unique sequence $(\emptyset = \hat{\mu}^0, \hat{\mu}^1, \dots, \hat{\mu}^n = \mu)$, such that all squares in the diagram

satisfy the local rule of Section 5.1.5.

Using this schema we iteratively calculate promotion a total of n times and depict the results in a diagram as seen in Figure 5.6 on the left. This diagram consists of n promotion schemas glued together. As $\mathsf{pr}^n = \mathsf{id}$, the labels on the top and the bottom row must be equal to $\mu^0, \dots, \mu^n$.

We now transform this diagram by copying everything to the right of the n-th column into the triangular empty space on the left, see Figure 5.6. In this way the labels on the right corners of the n-th column are duplicated. We obtain an $n \times n$ grid, where each corner of a cell is labelled with a dominant weight and the labels on the top and bottom border are equal and the labels on the left and right border are equal. This grid is called the *promotion matrix* of O.

To obtain an adjacency matrix, we fill the cells of this diagram with non-negative integers according to the following rule.

Definition 5.2.2. *The* filling rule *for oscillating tableaux is*

$$\Phi(\lambda,\kappa,\nu,\mu) = \begin{cases} 1 & \text{if } \kappa+\nu-\lambda \text{ contains a negative entry,} \\ 0 & \text{else,} \end{cases} \tag{5.2.1}$$

where the cells are labelled as depicted below:

$$\begin{array}{ccc} \lambda & & \nu \\ & \boxed{\Phi(\lambda,\kappa,\nu,\mu)} & \\ \kappa & & \mu \end{array} . \tag{5.2.2}$$

Definition 5.2.3. *Denote by* M_O *the function that maps an* r*-symplectic oscillating tableau of length* n *to an* $n \times n$ *adjacency matrix using Construction 5.2.1 and the filling rule* (5.2.1).

Next, we generalize the above construction for r-fans of Dyck paths and vacillating tableaux.

5.2.1.2. *Chord diagrams for* r*-fans of Dyck paths.* Given an r-fan of Dyck paths $\mathsf{F} = (\emptyset = \mu^0, \mu^1, \ldots, \mu^n = \emptyset)$, we construct an adjacency matrix via Construction 5.2.1 using the following filling rule:

Definition 5.2.4. *The* filling rule *for fans of Dyck paths is*

$$\Phi(\lambda,\kappa,\nu,\mu) = \text{number of negative entries in } \kappa+\nu-\lambda, \tag{5.2.3}$$

where the cells are labelled as in (5.2.2).

Remark 5.2.1. *Note that for oscillating tableaux at most one negative entry can occur. Thus the filling rule* (5.2.3) *for fans of Dyck paths is a natural generalization of the rule* (5.2.1).

Definition 5.2.5. *Denote by* M_F *the function that maps an* r*-fan of Dyck paths of length* n *to an* $n \times n$ *adjacency matrix using Construction 5.2.1 and the filling rule* (5.2.3).

Example 5.2.1. *Consider the following fan corresponding to the sequence of vectors* $\mathsf{F} = (000, 111, 222, 311, 422, 331, 222, 111, 000)$.

(1) We apply promotion a total of $n = 8$ *times, to obtain the full orbit.*

000 111 222 311 422 331 222 111 000
000 111 200 311 220 111 000 111 000
000 111 222 311 220 111 222 111 000
000 111 200 111 200 311 200 111 000
000 111 220 311 422 311 222 111 000
000 111 220 331 220 311 200 111 000
000 111 222 111 220 111 220 111 000
000 111 000 111 200 311 220 111 000
000 111 222 311 422 331 222 111 000 .

(2) We group the results into the promotion matrix and fill the cells of the square grid according to Φ. For better readability we omitted zeros.

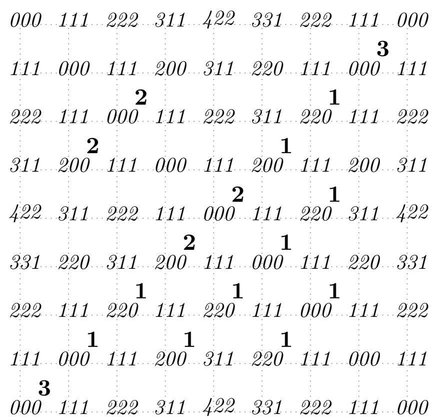

(3) Regard the filling as the adjacency matrix of a graph, the chord diagram.

$$
\mathsf{M}_F(\mathsf{F}) = \begin{pmatrix}
0 & 0 & 0 & 0 & 0 & 0 & 0 & 3 \\
0 & 0 & 2 & 0 & 0 & 0 & 1 & 0 \\
0 & 2 & 0 & 0 & 0 & 1 & 0 & 0 \\
0 & 0 & 0 & 0 & 2 & 0 & 1 & 0 \\
0 & 0 & 0 & 2 & 0 & 1 & 0 & 0 \\
0 & 0 & 1 & 0 & 1 & 0 & 1 & 0 \\
0 & 1 & 0 & 1 & 0 & 1 & 0 & 0 \\
3 & 0 & 0 & 0 & 0 & 0 & 0 & 0
\end{pmatrix}
$$

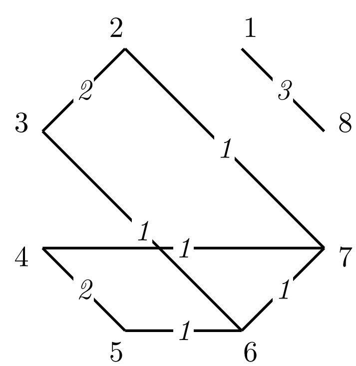

5.2.1.3. *Chord diagrams for vacillating tableaux.* Note that $\mathcal{B}_\square$ is not minuscule and thus Theorem 5.1.1 is not directly applicable. Using Definition 5.1.7 we can embed $\mathcal{B}_\square$ in $\mathcal{C}_\square^{\otimes 2}$ which gives a map $\iota_{V\to O}$ from vacillating tableaux to oscillating tableaux of twice the length which commutes with the crystal commutor. That is

$$\iota_{V\to O}\circ \mathsf{pr}_{\mathcal{B}_\square} = \iota_{V\to O}\circ \sigma_{\mathcal{B}_\square^{\otimes n-1},\mathcal{B}_\square} = \sigma_{(\mathcal{C}_\square^{\otimes 2})^{\otimes n-1},\mathcal{C}_\square^{\otimes 2}}\circ \iota_{V\to O}. \tag{5.2.4}$$

This follows directly from the properties of virtualization.

Let V be a vacillating tableau of length n and weight zero. Let $\mathsf{O} = (\emptyset = \mu^0, \mu^1, \ldots, \mu^{2n} = \emptyset)$ be the corresponding oscillating tableau using $\iota_{V\to O}$. Then we obtain the promotion of V using the following schema

(5.2.5)

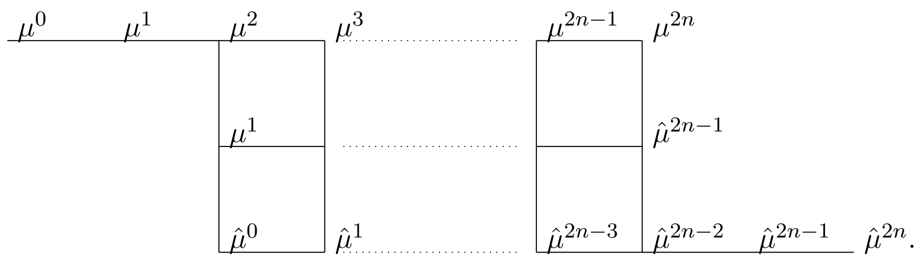

Following Construction 5.2.1, we apply promotion a total of n times and use the cut-and-glue procedure to obtain a $2n \times 2n$ square. We fill the squares using the filling rule for oscillating tableaux as given by (5.2.1).

To obtain an $n \times n$ adjacency matrix, we subdivide the $2n \times 2n$ matrix into 2×2 blocks and take the sum of each block.

Definition 5.2.6. *Denote by* $\mathsf{M}_{V\to O}$ *the function that maps a vacillating tableau* V *of weight zero of length* n *to an* $n \times n$ *adjacency matrix using* $\iota_{V\to O}$*, Schema* (5.2.5)*, Construction 5.2.1, filling rule* (5.2.1)*, and block sums.*

Example 5.2.2. *Consider the vacillating tableau of length* 9

$$\mathsf{V} = (000, 100, 200, 210, 211, 111, 111, 110, 100, 000).$$

We first embed V *into an oscillating tableau using the bijection* Ψ *from* $\mathcal{B}_\square$ *to* $\mathcal{V}$ *given in Definition 5.1.7. Specifically, we use* Ψ *to establish a correspondence between the highest weight element* *in* $\mathcal{B}_{\square}^{\otimes 9}$ *associated to* V *and a highest weight element in* $(\mathcal{C}_{\square}^{\otimes 2})^{\otimes 9}$*, from which we obtain* $\iota_{V\to O}(\mathsf{V})$ *as*

$$\iota_{V\to O}(\mathsf{V}) = (000, 100, 200, 300, 400, 410, 420, 421, 422, 322, 222, 221,$$
$$222, 221, 220, 210, 200, 100, 000).$$

(1) *We apply promotion a total of* $n = 9$ *times on the above schema* ($2n = 18$ *times on the oscillating tableau* $\iota_{V\to O}(\mathsf{V})$)*, to obtain the full orbit. Below we show all* 9 *applications of promotion.*

000 100 200 300 400 410 420 421 422 322 222 221 222 221 220 210 200 100 000
100 200 300 310 320 321 322 222 221 220 221 220 221 211 210 110 100
000 100 200 210 220 221 222 221 220 221 222 221 222 221 220 210 200 100 000
100 110 210 211 221 220 221 222 322 321 322 321 320 310 300 200 100
000 100 200 210 220 221 222 322 422 421 422 421 420 410 400 300 200 100 000
100 110 210 211 221 321 421 420 421 420 421 411 410 310 210 110 100
000 100 200 210 220 320 420 421 422 421 422 421 420 320 220 210 200 100 000
100 110 210 310 410 411 421 420 421 420 421 321 221 211 210 110 100
000 100 200 300 400 410 420 421 422 421 422 322 222 221 220 210 200 100 000
100 200 300 310 320 321 322 321 322 222 221 220 221 211 210 110 100
000 100 200 210 220 221 222 221 222 221 220 221 222 221 220 210 200 100 000
100 110 210 211 221 220 221 220 221 222 322 321 320 310 300 200 100
000 100 200 210 220 221 222 221 222 322 422 421 420 410 400 300 200 100 000
100 110 210 211 221 220 221 321 421 420 421 411 410 310 210 110 100
000 100 200 210 220 221 222 322 422 421 422 421 420 320 220 210 200 100 000
100 110 210 211 221 321 421 420 421 420 421 321 221 211 210 110 100
000 100 200 210 220 320 420 421 422 421 422 322 222 221 220 210 200 100 000
100 110 210 310 410 411 421 420 421 321 221 220 221 211 210 110 100
000 100 200 300 400 410 420 421 422 322 222 221 222 221 220 210 200 100 000

(2) *We group the results into the promotion matrix and fill the cells of the square grid according to* Φ *in* (5.2.1)*. For better readability, we subdivided the diagram into* 2×2 *blocks and took the sum of the entries in each block, as well as omitted the zeros.*

000		200		400		420		422		222		222		220		200		000
											1		**1**					
200		000		200		220		222		220		222		222		220		200
									2									
400		200		000		200		220		222		422		422		420		400
													1		**1**			
420		220		200		000		200		220		420		422		422		420
															1		**1**	
422		222		220		200		000		200		400		420		422		422
			2															
222		220		222		220		200		000		200		220		222		222
	1																**1**	
222		222		422		420		400		200		000		200		220		222
	1				**1**													
220		222		422		422		420		220		200		000		200		220
					1		**1**											
200		220		420		422		422		222		220		200		000		200
							1				**1**							
000		200		400		420		422		222		222		220		200		000

(2) Regard the filling as the adjacency matrix of a graph, the chord diagram.

$$\mathsf{M}_{V\to O}(\mathsf{V}) = \begin{pmatrix} 0&0&0&0&0&1&1&0&0\\ 0&0&0&0&2&0&0&0&0\\ 0&0&0&0&0&0&1&1&0\\ 0&0&0&0&0&0&0&1&1\\ 0&2&0&0&0&0&0&0&0\\ 1&0&0&0&0&0&0&0&1\\ 1&0&1&0&0&0&0&0&0\\ 0&0&1&1&0&0&0&0&0\\ 0&0&0&1&0&1&0&0&0 \end{pmatrix}$$

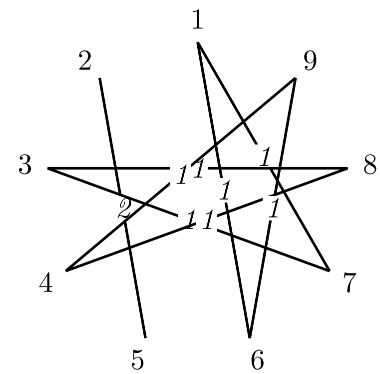

Alternatively, we may obtain an adjacency matrix by embedding $\mathcal{B}_{\Box}$ as a connected component of $\mathcal{B}_{\mathsf{spin}}^{\otimes 2}$ (see Section 5.1.3.3). As discussed in Definition 5.1.12, this embedding gives rise to the map $\iota_{V\to F}$ from vascillating tableaux to r-fans of Dyck paths of twice the length. From the r-fans of Dyck paths, we apply M_F to obtain a $2n \times 2n$ matrix. Subdividing this matrix into 2×2 blocks and taking block sums produces an $n \times n$ adjacency matrix for vascillating tableaux.

Definition 5.2.7. *Denote by* $\mathsf{M}_{V\to F}$ *the function that maps a vascillating tableau* V *of weight zero and length n to an* $n \times n$ *adjacency matrix using* $\iota_{V\to F}$*, Construction 5.2.1, filling rule* (5.2.3), *and block sums.*

5.2.1.4. *Promotion and rotation.* For the various maps M_X with $X \in \{O, F, V \to O, V \to F\}$ constructed in this section, we obtain the following main result.

Proposition 5.2.2. *The map* M_X *for* $X \in \{O, F, V \to O, V \to F\}$ *intertwines promotion and rotation, that is*

$$\mathsf{M}_X \circ \mathsf{pr} = \mathrm{rot} \circ \mathsf{M}_X.$$

Proof. Let T be either a fan of Dyck paths, an oscillating tableau of weight zero or a vacillating tableau of weight zero of length n and denote by $\widehat{\mathsf{T}}$ its promotion.

For $0 \leqslant i, j < n$ let $\mu^{i,j}$ be the $(j-i)$-th entry of $\mathsf{pr}^i(\mathsf{T})$, where indexing starts with zero and is understood modulo n. For $1 \leqslant i, j \leqslant n$ denote by $m_{i,j}$ the entry in the i-th row and j-th column of $\mathsf{M}_X(\mathsf{T})$. Similarly, denote by $\widehat{\mu}^{i,j}$ the $(j-i)$-th entry of $\mathsf{pr}^i(\widehat{\mathsf{T}})$ and by $\widehat{m}_{i,j}$ the i-th row and j-th column of $\mathsf{M}_X(\widehat{\mathsf{T}})$.

In all of our constructions $m_{i,j}$ depends on the four partitions $\mu^{i-1,j-1}$, $\mu^{i,j-1}$, $\mu^{i-1,j}$ and $\mu^{i,j}$ via some function $m_{i,j} = \widetilde{\Phi}(\mu^{i-1,j-1}, \mu^{i,j-1}, \mu^{i-1,j}, \mu^{i,j})$. Analogously we have $\widehat{m}_{i,j} = \widetilde{\Phi}(\widehat{\mu}^{i-1,j-1}, \widehat{\mu}^{i,j-1}, \widehat{\mu}^{i-1,j}, \widehat{\mu}^{i,j})$.

A simple calculation gives

$$\begin{aligned}\widehat{m}_{i,j} &= \widetilde{\Phi}(\widehat{\mu}^{i-1,j-1}, \widehat{\mu}^{i,j-1}, \widehat{\mu}^{i-1,j}, \widehat{\mu}^{i,j})\\ &= \widetilde{\Phi}(\mu^{i,j}, \mu^{i+1,j}, \mu^{i,j+1}, \mu^{i+1,j+1}) = m_{i+1,j+1},\end{aligned}$$

where indices are understood modulo n. Thus, $\mathsf{M}_X(\widehat{\mathsf{T}}) = \mathrm{rot}(\mathsf{M}_X(\mathsf{T}))$. $\square$

Note that the promotion matrix $\mathsf{M}_X(\mathsf{T})$ is sometimes referred to as the *promotion-evacuation diagram* of T as it also encodes information about the evacuation of T. Following [**75**], a generalization of Schützenberger's evacuation operator can be defined on crystals as follows.

Definition 5.2.8. *Let C be a crystal and $u \in C^{\otimes n}$ a highest weight element. Then* evacuation evac *on u is defined as*

$$(1_{C^{\otimes n-2}} \otimes \mathsf{pr}) \circ \cdots \circ (1_C \otimes \mathsf{pr}) \circ \mathsf{pr}(u),$$

where $(1_{C^{\otimes n-m}} \otimes \mathsf{pr})(w_n \otimes \cdots \otimes w_2 \otimes w_1) = w_n \otimes \cdots \otimes w_{m+1} \otimes \mathsf{pr}(w_m \otimes \cdots \otimes w_1)$.

Given a tableau T corresponding to a highest weight element u, we denote by $\mathsf{evac}(\mathsf{T})$ the tableau associated to the highest weight element $\mathsf{evac}(u)$.

Proposition 5.2.3. *The map M_X for $X \in \{O, F, V \to O, V \to F\}$ intertwines evacuation and the anti-transpose, that is*

$$\mathsf{M}_X \circ \mathsf{evac} = \mathrm{antr} \circ \mathsf{M}_X,$$

where the anti-transpose antr *of a matrix is its transpose over its anti-diagonal.*

Proof. Let T be either a fan of Dyck paths, an oscillating tableau of weight zero, or a vacillating tableau of weight zero of length n. From the definition of evac and the construction of M_X, we have that $\mathsf{evac}(\mathsf{T})$ is precisely the tableau obtained by reading the right border of M_X from bottom to top. Note that in order to prove the statement for $\mathsf{M}_{V\to O}$ it suffices to show it for M_O as Ψ intertwines

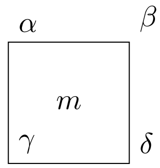

FIGURE 5.7. A cell of a growth diagram filled with a non-negative integer m

$\sigma_{\mathcal{B}_\square^{\otimes m},\mathcal{B}_\square}$ and $\sigma_{(\mathcal{C}_\square^{\otimes 2})^{\otimes m},\mathcal{C}_\square^{\otimes 2}}$ for all $m \geqslant 1$ by Equation (5.1.1), where Ψ is the virtualization map given in Definition 5.1.7. Similarly, in order to prove the statement for $\mathsf{M}_{V\to F}$ it suffices to prove it for M_F.

Consider partitions $\lambda, \kappa, \nu, \mu$ labelling the corner of a cell in M_X as in (5.2.2), where $X \in \{O, F\}$. By [**94**, Lemma 4.1.2], we have $\mu = \mathrm{dom}_W(\kappa + \nu - \lambda)$ if and only if $\lambda = \mathrm{dom}_W(\kappa + \nu - \mu)$ as $\mathcal{B}_{\mathsf{spin}}$ and $\mathcal{C}_\square$ are minuscule. This implies that partitions labelling the corners of every cell in $\mathsf{M}_X \circ \mathsf{evac}$ and $\mathrm{antr} \circ \mathsf{M}_X$ are equal.

To complete the proof we show that filling rules $\Phi(\lambda, \kappa, \nu, \mu)$ given in (5.2.1) and (5.2.3) satisfy $\Phi(\lambda, \kappa, \nu, \mu) = \Phi(\mu, \kappa, \nu, \lambda)$. As partitions connected by a vertical or horizontal edge in M_O differ by exactly one box, we have that $\Phi(\lambda, \kappa, \nu, \mu) = 1$ if and only if $\lambda = \mu = (\lambda_1, \dots, \lambda_i, 0, \dots, 0)$, $\lambda_i = 1$ for some i, and $\kappa = \nu = (\lambda_1, \dots, \lambda_{i-1}, 0, 0, \dots, 0)$. Thus, the filling rule for oscillating tableaux satisfies $\Phi(\lambda, \kappa, \nu, \mu) = \Phi(\mu, \kappa, \nu, \lambda)$. By a similar argument the filling rule for fans of Dyck paths also satisfies the desired symmetry. $\square$

5.2.2. Fomin growth diagrams. Generally speaking, a *Fomin growth diagram* is a means to bijectively map sequences of partitions satisfying certain constraints to fillings of a Ferrers shape with non-negative integers [**30, 54, 80, 95**]. In this setting, we draw the Ferrers shape in French notation (to fix how the growth diagrams are arranged).

To map a filling of a Ferrers shape to a sequence of partitions we iteratively label all corners of cells of the shape with partitions by certain local rules. Given a cell, where already all three partitions on the left and bottom corners are known, the forward rules determine the fourth partition on the top right corner based on the filling of the cell. Conversely, given the three partitions on the top and right corners of a cell, the backwards rules determine the last partition and the filling of the cell. When defining the local rules we label the cells as seen in Figure 5.7.

For partitions δ and α, we define their union $\delta \cup \alpha$ to be the partition containing $\delta_i + \alpha_i$ cells in row i, where δ_i and α_i denote the number of cells in row i of δ and α respectively. Recall that we pad partitions with 0's if necessary. We denote $\delta \cup \delta$ by 2δ. We define the intersection of two partitions $\delta \cap \alpha$ to be the partition containing $\min\{\delta_i, \alpha_i\}$ cells in row i.

We begin by describing the local rules for a filling of a Ferrers shape with at most one 1 in each row and in each column and 0's everywhere else (omitted for readability). Moreover, we require that any two adjacent partitions in the labelling of our growth diagram (for example, $\gamma \to \alpha$ and $\gamma \to \delta$ in Figure 5.7) must either coincide or the one at the head of the arrow is obtained from the other by adding a unit vector. We record the local forward rules and local backward rules for this case of 0/1 filling, which are stated explicitly in [**54**, p. 4-5].

Given a 0/1 filling of a Ferrers shape and partitions labelling the bottom and left side of the Ferrers shape, we apply the following *local forward rules* to complete the labelling.

- (F1) If $\gamma = \delta = \alpha$, and there is no 1 in the cell, then $\beta = \gamma$.
- (F2) If $\gamma = \delta \neq \alpha$, then $\beta = \alpha$.
- (F3) If $\gamma = \alpha \neq \delta$, then $\beta = \delta$.
- (F4) If γ, δ, α are pairwise different, then $\beta = \delta \cup \alpha$.
- (F5) If $\gamma \neq \delta = \alpha$, then β is formed by adding a square to the $(k+1)$-st row of $\delta = \alpha$, given that $\delta = \alpha$ and γ differ in the k-th row.
- (F6) If $\gamma = \delta = \alpha$, and if there is a 1 in the cell, then β is formed by adding a square to the first row of $\gamma = \delta = \alpha$.

Given a Ferrers shape and partitions labelling the top and right side, we apply the following *local backward rules* to complete the labelling and recover the filling.

- (B1) If $\beta = \delta = \alpha$, then $\gamma = \beta$.
- (B2) If $\beta = \delta \neq \alpha$, then $\gamma = \alpha$.
- (B3) If $\beta = \alpha \neq \delta$, then $\gamma = \delta$.
- (B4) If β, δ, α are pairwise different, then $\gamma = \delta \cap \alpha$.
- (B5) If $\beta \neq \delta = \alpha$, then γ is formed by deleting a square from the $(k-1)$-st row of $\delta = \alpha$, given that $\delta = \alpha$ and β differ in the k-th row with $k \geqslant 2$.

(B6) If $\beta \neq \delta = \alpha$, and if β and $\delta = \alpha$ differ in the first row, then $\gamma = \delta = \alpha$ and the cell is filled with a 1.

Construction 5.2.2 ([**75**]). *Let $\mathsf{O} = (\emptyset = \mu^0, \mu^1, \dots, \mu^n = \emptyset)$ be an oscillating tableau. The associated triangular growth diagram is the Ferrers shape $(n-1, n-2, \dots, 2, 1, 0)$. Label the cells according to the following specification:*

(1) Label the north-east corners of the cells on the main diagonal from the top-left to the bottom-right with the partitions in O.

(2) For each $i \in \{0, \dots, n-1\}$ label the corner on the first subdiagonal adjacent to the labels μ^i and μ^{i+1} with the partition $\mu^i \cap \mu^{i+1}$.

(3) Use the backwards rules B1-B6 to obtain all other labels and the fillings of the cells.

We denote by $\mathsf{G}_O(\mathsf{O})$ the symmetric $n \times n$ matrix one obtains from the filling of the growth diagram by putting zeros in the unfilled cells and along the diagonal and completing this to a symmetric matrix.

Starting from a filling of a growth diagram one obtains the oscillating tableau by setting all vectors on corners on the bottom and left border of the diagram to be the empty partition and applying the forwards growth rules F1-F6.

Next, we will extend these local rules to any filling of a Ferrers shape with non-negative integers.

5.2.3. Fomin growth diagrams: Burge Rule. Given a filling of a Ferrers shape $(\lambda_1, \dots, \lambda_\ell)$ with non-negative integers, we produce a "blow up" construction of the original shape for the Burge variant which contains south-east chains of 1's, as done by [**54**]. We begin by separating entries. If a cell is filled with a positive entry m, we replace the cell with an $m \times m$ grid of cells with 1's along the diagonal (from top-left to bottom-right). If there exist several nonzero entries in one column, we arrange the grids of cells also from top-left to bottom-right, so that the 1's form a south-east chain in each column. We make the same arrangements for the rows, also establishing a south-east chain in each row. The resulting blow up Ferrers diagram then contains c_j columns in the original j-th column, where c_j is equal to the sum of the entries in column j or 1 if the j-th column contains only 0's, and r_i rows in the original i-th row, where r_i is equal to the sum of the entries in row i or 1 if the i-th row contains only 0's. See Figure 5.8.

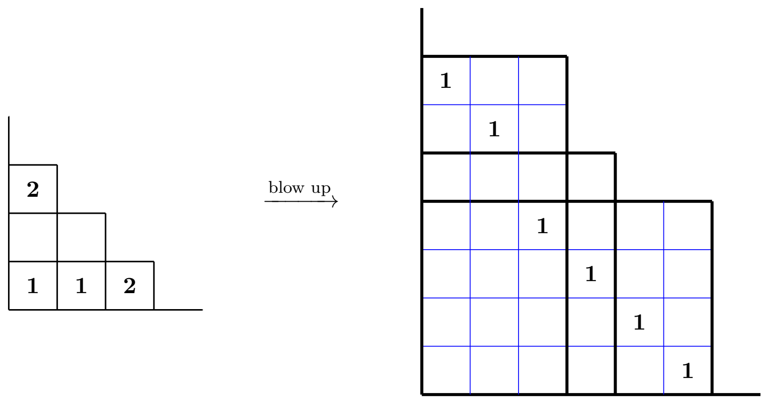

FIGURE 5.8. An example of the blow up construction for Burge rules replacing positive integer entries with south-east chains of 1's in each column and row.

Since the filling of the blow up growth diagram consists of 1's and 0's, we now apply the forward local rules. To start, we label all of the corners of the cells on the left side and the bottom side of the blow up growth diagram by $\emptyset$. Then we apply the forward local rules to determine the partition labels of the other corners, using the 0/1 filling and partitions defined in previous iterations of the forward local rule. Finally, we "shrink back" the labelled blow up growth diagram to obtain a labelling of the original Ferrers diagram by only considering the partitions labelling positions $\{(c_1 + \cdots + c_j, r_i + \cdots + r_\ell) \mid 1 \leqslant i \leqslant \ell, 1 \leqslant j \leqslant \lambda_{\ell-i+1}\}$. These positions are precisely the intersections of the bolded black lines in Figure 5.8. To shrink back, we ignore the labels on intersections involving any blue lines in the blow up growth diagram and assign the partition labelling $(c_1 + \cdots + c_j, r_i + \cdots + r_\ell)$ to the position $(j, \ell - i + 1)$ in the original Ferrers diagram. The resulting labelling has the property that partitions on adjacent corners differ by a vertical strip [**54**, Theorem 11].

We now describe the direct Burge forward and backwards rules [**54**, Section 4.4]. Consider a cell filled by a non-negative integer m, and labelled by the partitions γ, δ, α, where $\gamma \subset \delta$ and $\gamma \subset \alpha$, α/γ and δ/γ are vertical strips. Moreover, denote by $\mathbb{1}_A$ the truth function

$$\mathbb{1}_A = \begin{cases} 1 & \text{if } A \text{ is true,} \\ 0 & \text{otherwise.} \end{cases}$$

Then β is determined by the following procedure:

Burge F0: Set CARRY $:= m$ and $i := 1$.

Burge F1: Set $\beta_i := \max\{\delta_i, \alpha_i\} + \min\{\mathbb{1}_{\gamma_i=\delta_i=\alpha_i}, \text{CARRY}\}$

Burge F2: If $\beta_i = 0$, then stop and return $\beta = (\beta_1, \beta_2, \dots, \beta_{i-1})$. If not, then set CARRY $:=$ CARRY $- \min\{\mathbb{1}_{\gamma_i=\delta_i=\alpha_i}, \text{CARRY}\} + \min\{\delta_i, \alpha_i\} - \gamma_i$ and $i := i+1$ and go to F1.

Note that this algorithm is reversible. Given β, δ, α such that β/δ and β/α are vertical strips, the backwards algorithm is defined by the following rules:

Burge B0: Set $i := \max\{j \mid \beta_j \text{ is positive}\}$ and CARRY $:= 0$.

Burge B1: Set $\gamma_i := \min\{\delta_i, \alpha_i\} - \min\{\mathbb{1}_{\gamma_i=\alpha_i=\beta_i}, \text{CARRY}\}$.

Burge B2: Set CARRY $:=$ CARRY $- \min\{\mathbb{1}_{\beta_i=\delta_i=\alpha_i}, \text{CARRY}\} + \beta_i - \max\{\delta_i, \alpha_i\}$ and $i := i-1$. If $i = 0$, then stop and return $\gamma = (\gamma_1, \gamma_2, \dots)$ and $m =$ CARRY. If not, got to B1.

Construction 5.2.3. *Let $\mathsf{F} = (\emptyset = \mu^0, \mu^1, \dots, \mu^n = \emptyset)$ be an r-fan of Dyck paths. The associated triangular growth diagram is the Ferrers shape $(n-1, n-2, \dots, 2, 1, 0)$. Label the cells according to the following specification:*

(1) Label the north-east corners of the cells on the main diagonal from the top-left to the bottom-right with the partitions in F.

(2) For each $i \in \{0, \dots, n-1\}$ label the corner on the first subdiagonal adjacent to the labels μ^i and μ^{i+1} with the partition $\mu^i \cap \mu^{i+1}$.

(3) Use the backwards rules Burge B0, B1 and B2 to obtain all other labels and the fillings of the cells.

We denote by $\mathsf{G}_F(\mathsf{F})$ the symmetric $n \times n$ matrix one obtains from the filling of the growth diagram by putting zeros in the unfilled cells and along the diagonal and completing this to a symmetric matrix.

Starting from a filling of a growth diagram one obtains the r-fan by filling the cells of a growth diagram, setting all vectors on corners on the bottom and left border of the diagram to be the empty partition and applying the forwards growth rules Burge F0-F2.

An example is given in Figure 5.9.

5.2.4. Fomin growth diagrams: RSK Rule. Given a filling of a Ferrers shape $(\lambda_1, \dots, \lambda_\ell)$ with non-negative integers, we produce a "blow up" construction of the original shape for the RSK

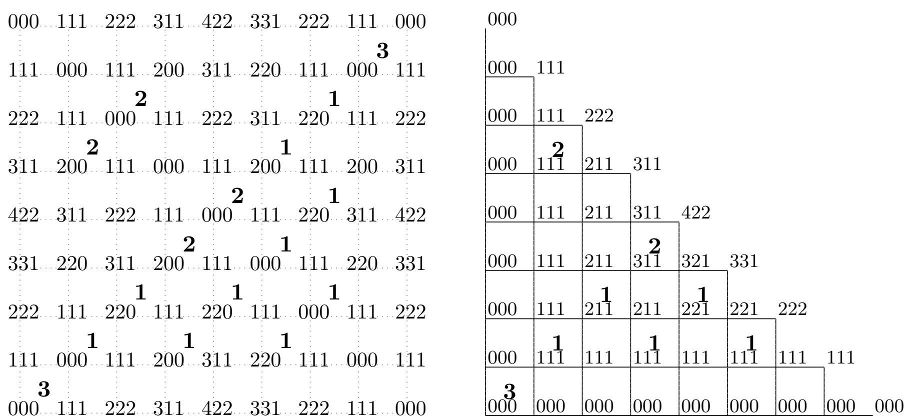

FIGURE 5.9. On the left the filled promotion matrix of $\mathsf{F} = (000, 111, 222, 311, 422, 331, 222, 111, 000)$. On the right the triangular growth diagram for the same fan.

variant which contains north-east chains of 1's, as done by [**54**]. We begin by separating entries. If a cell is filled with positive entry m, we replace the cell with an $m \times m$ grid of cells with 1's along the off-diagonal (from bottom-left to top-right). If there exist several nonzero entries in one column, we arrange the grids of cells also from bottom-left to top-right, so that the 1's form a north-east chain in each column. We make the same arrangements for the rows, also establishing a north-east chain in each row. The resulting blow up Ferrers diagram then contains c_j columns in the original j-th column, where c_j is equal to the sum of the entries in column j or 1 if the j-th column contains only 0's, and r_i rows in the original i-th row, where r_i is equal to the sum of the entries in row i or 1 if the i-th row contains only 0's.

Since the filling of the blow up growth diagram consists of 1's and 0's, we now apply the forward local rules. To start, we label all of the corners of the cells on the left side and the bottom side of the blow up growth diagram by $\emptyset$. Then, we apply the forward local rules to determine the partition labels of the other corners, using the 0/1 filling and partitions defined in previous iterations of the forward local rule. Finally, we "shrink back" the labelled blow up growth diagram to obtain a labelling of the original Ferrers diagram by only partitions labelling positions $\{(c_1 + \cdots + c_j, r_i + \cdots + r_\ell) \mid 1 \leqslant i \leqslant \ell, 1 \leqslant j \leqslant \lambda_{\ell-i+1}\}$. To shrink back, we assign the partition labelling $(c_1 + \cdots + c_j, r_i + \cdots + r_\ell)$ in the blow up growth diagram to the position $(j, \ell - i + 1)$ in the original Ferrers diagram. The resulting labelling has the property that partitions on adjacent corners differ by a horizontal strip [**54**, Theorem 7].

The direct RSK forward rules are as follows [**54**, Section 4.1]: Consider a cell as in Figure 5.7 filled by a non-negative integer m, and labelled by the partitions γ, δ, α, where $\gamma \subset \delta$ and $\gamma \subset \alpha$, α/γ and δ/γ are horizontal strips. Then β is determined by the following procedure:

RSK F0: Set CARRY $:= m$ and $i := 1$.

RSK F1: Set $\beta_i := \max\{\delta_i, \alpha_i\} + \text{CARRY}$

RSK F2: If $\beta_i = 0$, then stop and return $\beta = (\beta_1, \beta_2, \dots, \beta_{i-1})$. If not, then set CARRY $:= \min\{\delta_i, \alpha_i\} - \gamma_i$ and $i := i + 1$ and go to F1.

Note that this algorithm is reversible. Given β, δ, α such that β/δ and β/α are horizontal strips, the backwards algorithm is defined by the following rules:

RSK B0: Set $i := \max\{j \mid \beta_j \text{ is positive}\}$ and CARRY $:= 0$.

RSK B1: Set $\gamma_i := \min\{\delta_i, \alpha_i\} - \text{CARRY}$.

RSK B2: Set CARRY $:= \beta_i - \max\{\delta_i, \alpha_i\}$ and $i := i - 1$. If $i = 0$, then stop and return $\gamma = (\gamma_1, \gamma_2, \dots)$ and $m = \text{CARRY}$. If not, got to B1.

Construction 5.2.4. *Let $\mathsf{V} = (\emptyset = \mu^0, \mu^1, \dots, \mu^n = \emptyset)$ be a vacillating tableau of weight zero. The associated triangular growth diagram is the Ferrers shape $(n-1, n-2, \dots, 2, 1, 0)$. Label the cells according to the following specification:*

(1) Label the north-east corners of the cells on the main diagonal from the top-left to the bottom-right with the partitions $2\mu^i$.

(2) For each $i \in \{0, \dots, n-1\}$ label the corner on the first subdiagonal adjacent to the labels $2\mu^i$ and $2\mu^{i+1}$ with the partition $2(\mu^i \cap \mu^{i+1})$ when $\mu^i \neq \mu^{i+1}$ and the partition obtained by removing a cell from the final row of $2\mu^i$ when $\mu^i = \mu^{i+1}$.

(3) Use the backwards rules RSK B0, B1 and B2 to obtain all other labels and the fillings of the cells.

We denote by $\mathsf{G}_V(\mathsf{V})$ the symmetric $n \times n$ matrix one obtains from the filling of the growth diagram by putting zeros in the unfilled cells and along the diagonal and completing this to a symmetric matrix.

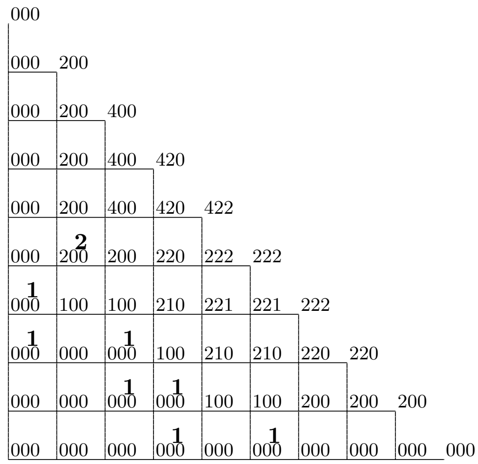

FIGURE 5.10. The triangular growth diagram for the vacillating tableau $\mathsf{V} = (000, 100, 200, 210, 211, 111, 111, 110, 100, 000)$.

Starting from a filling of a growth diagram one obtains the vacillating tableau by setting all vectors on corners on the bottom and left border of the diagram to be the empty partition and applying the forwards growth rules RSK F0-F2.

The triangular growth diagram of the vacillating tableau from Example 5.2.2 is depicted in Figure 5.10.

5.3. Main results

In this section, we state and prove our main results for oscillating tableaux, fans of Dyck paths, and vacillating tableaux. In particular, we show in Theorems 5.3.1, 5.3.2 and 5.3.3 that the fillings of the growth diagrams coincide with the fillings of the promotion–evacuation diagrams. This in turn shows that the maps M_F, $\mathsf{M}_{V\to O}$ and $\mathsf{M}_{V\to F}$ are injective. Having these injective maps to chord diagrams gives a first step towards a diagrammatic basis for the invariant subspaces. In Section 5.3.4, we give various new cyclic sieving phenomena associate to the promotion action.

We start by the following notation used later in this section. Let $M = (a_{i,j})_{i,j=1}^{kn}$ be a $kn \times kn$ matrix. It will often be convenient to consider M as the block matrix $(B_{i,j}^{(k)})_{i,j=1}^{n}$, where $B_{i,j}^{(k)}$ is the $k \times k$ matrix given by $(a_{p,q})_{p=k(i-1)+1,q=k(j-1)+1}^{ki,kj}$. We also follow the convention that for all $p, q > n$ we have $B_{p,q}^{(k)} \coloneqq B_{i,j}^{(k)}$, where $p \equiv i \mod n$ and $q \equiv j \mod n$.

Definition 5.3.1. *For a $kn \times kn$ matrix M with block matrix decomposition given by $(B_{i,j}^{(k)})_{i,j=1}^{n}$, denote by $\mathsf{blocksum}_k(M)$ the $n \times n$ matrix $(b_{i,j})_{i,j=1}^{n}$, where $b_{i,j}$ is equal to the sum of all entries in $B_{i,j}^{(k)}$.*

Given an $n \times n$ matrix $M = (a_{i,j})_{i,j=1}^{n}$, we recursively define its skewed partial row sums $r_{i,j}$ by setting $r_{i,i} = 0$ for all $1 \leqslant i \leqslant n$ and letting $r_{i,j+1} = r_{i,j} + a_{i,j}$ for $1 \leqslant j \leqslant n-1$. Note that as before, we use the convention that $a_{p,q} = a_{i,j}$ whenever $p \equiv i \mod n$ and $q \equiv j \mod n$. Similarly, the skewed partial column sums $c_{i,j}$ can be defined. Partial inverses to $\mathsf{blocksum}_k$ are given by $\mathsf{blowup}_k^{\mathsf{SE}}$ and $\mathsf{blowup}_k^{\mathsf{NE}}$ which we presently define.

Definition 5.3.2. *Let $M = (a_{i,j})_{i,j=1}^{n}$ be a matrix with non-negative integer entries such that for each row and for each column the sum of the entries is k. Let $r_{i,j}$ and $c_{i,j}$ be its skewed partial row and column sums respectively. Let $B_{i,j}^{SE}$ be the $k \times k$ matrix, where $B_{i,j}^{SE}$ is the zero-matrix if $a_{i,j} = 0$ and a zero-one-matrix if $a_{i,j} \neq 0$ consisting of 1's in positions $(r_{i,j}+1, c_{i,j}+1), \ldots, (r_{i,j} + a_{i,j}, c_{i,j} + a_{i,j})$ and zeros elsewhere. We define $\mathsf{blowup}^{\mathsf{SE}}(M)$ to be the block matrix $(B_{i,j}^{SE})_{i,j=1}^{n}$.*

Similarly, let $B_{i,j}^{NE}$ be the $k \times k$ matrix, where $B_{i,j}^{BE}$ is the zero-matrix if $a_{i,j} = 0$ and a zero-one-matrix if $a_{i,j} \neq 0$ consisting of 1's in positions $(k - r_{i,j}, k - c_{i,j} - a_{i,j} + 1), \ldots, (k - r_{i,j} - (a_{i,j} - 1), k - c_{i,j})$ and zeros elsewhere. We define $\mathsf{blowup}^{\mathsf{NE}}(M)$ to be the block matrix $(B_{i,j}^{NE})_{i,j=1}^{n}$.

Remark 5.3.1. *Note that $\mathsf{blowup}^{\mathsf{SE}}(M)$ and $\mathsf{blowup}^{\mathsf{NE}}(M)$ are the unique $kn \times kn$ zero-one-matrices whose $\mathsf{blocksum}_k$ equals M and for all $1 \leqslant i \leqslant n$, the nonzero entries in the matrices*

$$[B_{i,i}, B_{i,i+1}, B_{i,i+2}, \ldots, B_{i,i+n-1}] \qquad \textit{and}$$

$$[B_{i,i}, B_{i+1,i}, B_{i+2,i}, \ldots, B_{i+n-1,i}]$$

form a south-east chain or a north-east chain, respectively.

5.3.1. Results for oscillating tableaux. The next result was not stated explicitly in [**75**], but can be deduced from the proof in the paper.

Theorem 5.3.1. *For an oscillating tableau of weight zero O the fillings of the growth diagram (Construction 5.2.2) and the fillings of the promotion-evacuation (Construction 5.2.1) diagram coincide, that is*

$$\mathsf{G}_O(\mathsf{O}) = \mathsf{M}_O(\mathsf{O}).$$

Proof. This follows from the proof of [**75**, Corollary 6.17, Lemma 6.26]. □

5.3.2. Results for r-fans of Dyck paths. We state our main results.

Theorem 5.3.2. *For an r-fan of Dyck paths* F

$$\mathsf{G}_F(\mathsf{F}) = \mathsf{M}_F(\mathsf{F}).$$

In other words, the fillings of its growths diagram (Construction 5.2.3) and the fillings of the promotion-evacuation diagram coincide.

In particular we obtain the corollary:

Corollary 5.3.1. *The map M_F is injective.*

We now state and prove some results which are needed for the proof of Theorem 5.3.2.

Lemma 5.3.1. *Let F be an r-fan of Dyck paths of length n. Then*

$$\iota_{F\to O} \circ \mathsf{pr}_{\mathcal{B}_{\mathsf{spin}}}(\mathsf{F}) = \mathsf{pr}^r_{\mathcal{C}_\square} \circ \iota_{F\to O}(\mathsf{F}).$$

Proof. Let $\iota_{F\to O}(\mathsf{F}) = \mu = (\emptyset = \mu^{(0,0)}, \dots, \mu^{(0,rn)} = \emptyset)$. We first prove that $\mathsf{pr}^r_{\mathcal{C}_\square}(\mu) = \mathsf{pr}_{\mathcal{C}_\square^{\otimes r}}(\mu)$. Let $\mathsf{pr}^i_{\mathcal{C}_\square}(\mu) = (\emptyset = \mu^{(i,0)}, \dots, \mu^{(i,rn)} = \emptyset)$. From the definition of $\iota_{F\to O}$, we have $\mu^{(0,k)} = (1^k)$ for all $0 \leqslant k \leqslant r$ where (1^0) denotes the empty partition $\emptyset$. Using the local rules for promotion and induction, we see that the sequence of partitions $(\mu^{(k,0)}, \dots, \mu^{(k,r-k)})$ is equal to $((1^0), \dots, (1^{r-k}))$ for all $0 \leqslant k \leqslant r$. This implies the following equality

$$\begin{aligned}\mu &= ((1^0), (1^1), \dots, (1^r), \mu^{(0,r+1)}, \dots, \mu^{(0,rn)})\\ &= (\mu^{(r,0)}, \mu^{(r-1,1)}, \dots, \mu^{(0,r)}, \mu^{(0,r+1)}, \dots, \mu^{(0,rn)}).\end{aligned}$$

By a similar argument, the sequence of partitions $(\mu^{(k,rn-k)}, \dots, \mu^{(k,rn)})$ is equal to $((1^k), \dots, (1^0))$ for all $1 \leqslant k \leqslant r$ implying

$$\begin{aligned}\mathsf{pr}^r_{\mathcal{C}_\square}(\mu) &= (\mu^{(r,0)}, \mu^{(r,1)}, \dots, \mu^{(r,r(n-1)-1)}, (1^r), (1^r - 1), \dots, (1^0))\\ &= (\mu^{(r,0)}, \mu^{(r,1)}, \dots, \mu^{(r,rn-r-1)}, \mu^{(r,rn-r)}, \mu^{(r-1,rn-r-1)}, \dots, \mu^{(0,r)}).\end{aligned}$$

By Theorem 5.1.1, we obtain the desired equality

$$\begin{aligned}\mathsf{pr}_{\mathcal{C}_\square^{\otimes r}}(\mu) &= \mathsf{pr}_{\mathcal{C}_\square^{\otimes r}}(\mu^{(r,0)}, \mu^{(r-1,1)}, \dots, \mu^{(0,r)}, \mu^{(0,r+1)}, \dots, \mu^{(0,rn)}) \\ &= (\mu^{(r,0)}, \mu^{(r,1)}, \dots, \mu^{(r,r(n-1))}, \mu^{(r-1,r(n-1)+1)}, \dots, \mu^{(0,rn)}) \qquad = \mathsf{pr}^r_{\mathcal{C}_\square}(\mu).\end{aligned}$$

Let $w = w_n \otimes w_{n-1} \otimes \cdots \otimes w_1 \in \mathcal{B}_{\mathsf{spin}}^{\otimes n}$ and $v = v_{rn} \otimes v_{rn-1} \otimes \cdots \otimes v_1 \in (\mathcal{C}_\square^{\otimes r})^{\otimes n}$ be the highest weight crystal elements associated to F and μ, respectively. In order to show $\iota_{F\to O} \circ \mathsf{pr}_{\mathcal{B}_{\mathsf{spin}}}(\mathsf{F}) = \mathsf{pr}_{\mathcal{C}_\square^{\otimes r}}(\mu)$, it suffices to show that $\Psi(\mathsf{pr}_{\mathcal{B}_{\mathsf{spin}}}(w)) = \mathsf{pr}_{\mathcal{C}_\square^{\otimes r}}(v)$, where Ψ is the crystal isomorphism defined in Definition 5.1.5. Let $\mathcal{V} \subseteq \mathcal{C}_\square^{\otimes r}$ be the virtual crystal defined in Definition 5.1.4. As Ψ is a crystal isomorphism, we have $\Psi(\mathsf{pr}_{\mathcal{B}_{\mathsf{spin}}}(w)) = \mathsf{pr}_{\mathcal{V}}(\Psi(w)) = \mathsf{pr}_{\mathcal{V}}(v)$. As Lusztig's involution for crystals of type B_r and C_r interchanges the crystal operators f_i and e_i, the virtualization induced by the embedding $B_r \hookrightarrow C_r$ commutes with Lusztig's involution. In addition virtualization is preserved under tensor products (see for example [**16**, Theorem 5.8]). Thus, we have $\mathsf{pr}_{\mathcal{V}}(v) = \mathsf{pr}_{\mathcal{C}_\square^{\otimes r}}(v)$. $\square$

Lemma 5.3.2. *Let F be an r-fan of Dyck paths with length n, and let $(B_{i,j}^{(r)})_{i,j=1}^n$ be the block matrix decomposition of the $rn \times rn$ adjacency matrix $\mathsf{M}_O(\iota_{F\to O}\mathsf{F})$. Then for all $1 \leqslant i \leqslant n$, the nonzero entries in the matrices*

$$[B_{i,i+1}^{(r)}, B_{i,i+2}^{(r)}, \dots, B_{i,i+n-1}^{(r)}] \qquad \text{and}$$
$$[B_{i+1,i}^{(r)}, B_{i+2,i}^{(r)}, \dots, B_{i+n-1,i}^{(r)}]$$

form a south-east chain of r 1's.

Proof. By the definition of oscillating tableaux and the local rules for promotion, M_O is a zero-one matrix. From Lemma 5.3.1, Proposition 5.2.1, and Proposition 5.2.2, it suffices to prove that the nonzero entries in $[B_{n,n+1}^{(r)}, B_{n,n+2}^{(r)}, \dots, B_{n,2n-1}^{(r)}]$ and $[B_{2,1}^{(r)}, B_{3,1}^{(r)}, \dots, B_{n,1}^{(r)}]^T$ form a south-east chain. Recall that by construction, the Fomin growth diagram of $\iota_{F\to O}(\mathsf{F})$ is a triangle diagram with the entries of $\iota_{F\to O}(\mathsf{F})$ labelling its diagonal. As F is an r-fan of Dyck paths, the partition (1^r) sits at the corners $(r, r(n-1))$ and $(r(n-1), r)$ in the Fomin growth diagram of $\iota_{F\to O}(\mathsf{F})$. By Theorem 5.3.1, we have $\mathsf{M}_O(\iota_{F\to O}(\mathsf{F})) = \mathsf{G}_O(\iota_{F\to O}(\mathsf{F}))$. This implies that the filling of the leftmost r columns and bottommost r rows match $\mathsf{M}_O(\iota_{F\to O}(\mathsf{F}))$. As all the entries of $\mathsf{M}_O(\iota_{F\to O}(\mathsf{F}))$ are either 0 or 1, we have by [**54**, Theorem 2] that there are exactly r 1's forming a south-east chain in the leftmost r columns and in the bottommost r rows. $\square$

REMARK 5.3.2. *The proof of Lemma 5.3.2 implies that the diagonal block matrices* $B^{(r)}_{i,i}$ *of* $\mathsf{M}_O(\iota_{F\to O}\mathsf{F})$ *are all zero matrices.*

PROPOSITION 5.3.1. *Let* F *be an* r*-fan of Dyck paths of length* n*. Then*

$$\mathsf{M}_F(\mathsf{F}) = \mathsf{blocksum}_r(\mathsf{M}_O(\iota_{F\to O}(\mathsf{F}))).$$

Moreover,

$$\mathsf{blowup}^{\mathsf{SE}}_r(\mathsf{M}_F(\mathcal{F})) = \mathsf{M}_O(\iota_{F\to O}(\mathcal{F})).$$

PROOF. By Remark 5.3.2, the diagonal entries of $\mathsf{M}_F(\mathsf{F})$ and $\mathsf{blocksum}_r(\mathsf{M}_O(\iota_{F\to O}(\mathsf{F})))$ are all zero. Let $a_{i,j}$ with $i \neq j$ be the entry in $\mathsf{M}_F(\mathsf{F})$ that is the filling of the cell labelled by $\begin{array}{cc} \lambda & \nu \\ \boxed{\kappa} & \mu \end{array}$ in the promotion matrix of F. To show that the number of 1's appearing in $B^{(r)}_{i,j}$ of $\mathsf{M}_O(\iota_{F\to O}(\mathsf{F}))$ is also equal to $a_{i,j}$, we first compute $a_{i,j}$ for $i \neq j$. By Definition 5.2.3, $a_{i,j}$ is the number of negative entries in $\kappa + \nu - \lambda$. Since λ, ν and κ, μ are consecutive partitions in an r-fan of Dyck paths, we know that they differ by a vector of the form $(\pm 1, \ldots, \pm 1)$. We may write $\nu - \lambda$ and $\mu - \kappa$ as

$$\nu - \lambda = \mathbf{e}_{i_1} + \cdots + \mathbf{e}_{i_k} - \mathbf{e}_{i_{k+1}} - \cdots - \mathbf{e}_{i_r},$$

$$\mu - \kappa = \mathbf{e}_{j_1} + \cdots + \mathbf{e}_{j_m} - \mathbf{e}_{j_{m+1}} - \cdots - \mathbf{e}_{j_r},$$

where

$$\{i_1, \ldots, i_r\} = [r] = \{j_1, \ldots, j_r\},$$

$$i_1 < \cdots < i_k \text{ and } i_{k+1} > \cdots > i_r,$$

$$j_1 < \cdots < j_m \text{ and } j_{m+1} > \cdots > j_r.$$

By the definition of μ from the local rules of Lenart [**60**] (see Section 5.1.5), we have

$$\begin{aligned}\mu &= \mathrm{dom}_{\mathfrak{H}_r}(\kappa + \nu - \lambda)\\ &= \mathrm{dom}_{\mathfrak{H}_r}(\kappa + \mathbf{e}_{i_1} + \cdots + \mathbf{e}_{i_k} - \mathbf{e}_{i_{k+1}} - \cdots - \mathbf{e}_{i_r}).\end{aligned}$$

Recall that $\mathrm{dom}_{\mathfrak{H}_r}$ applied to a weight sorts the absolute values of the entries of the weight into weakly decreasing order. In particular, $\mathrm{dom}_{\mathfrak{H}_r}(\kappa + \mathbf{e}_{i_1} + \cdots + \mathbf{e}_{i_k} - \mathbf{e}_{i_{k+1}} - \cdots - \mathbf{e}_{i_r})$ will change all of the -1 entries of $\kappa + \mathbf{e}_{i_1} + \cdots + \mathbf{e}_{i_k} - \mathbf{e}_{i_{k+1}} - \cdots - \mathbf{e}_{i_r}$ to $+1$ and then sort all entries into weakly decreasing order (note that sorting will not change the number of cells). We thus have two equations for μ:

$$\begin{aligned}\mu &= \mathrm{dom}_{\mathfrak{H}_r}(\kappa + \mathbf{e}_{i_1} + \cdots + \mathbf{e}_{i_k} - \mathbf{e}_{i_{k+1}} - \cdots - \mathbf{e}_{i_r}) \\ &= \kappa + \mathbf{e}_{j_1} + \cdots + \mathbf{e}_{j_m} - \mathbf{e}_{j_{m+1}} - \cdots - \mathbf{e}_{j_r}.\end{aligned}$$

Therefore, $\mathrm{dom}_{\mathfrak{H}_r}$ changed $m-k$ negative entries in $\kappa+\nu-\lambda$ to $+1$ in μ, showing that $a_{i,j} = m-k$.

From the virtualization given in Definition 5.1.5, the partitions labelling the top of the first row of cells in $B_{i,j}^{(r)}$ are $\lambda, \lambda^{(1)}, \ldots, \lambda^{(r-1)}, \nu$, where $\lambda^{(\ell)} = \lambda + \mathbf{e}_{i_1} + \cdots \pm \mathbf{e}_{i_\ell}$. Similarly, the partitions labelling the bottom of the r-th row of cells in $B_{i,j}^{(r)}$ are $\kappa, \kappa^{(1)}, \ldots, \kappa^{(r-1)}, \mu$, where $\kappa^{(\ell)} = \kappa + \mathbf{e}_{j_1} + \cdots \pm \mathbf{e}_{j_\ell}$. In particular, we have

$$\begin{gathered}\lambda \subset \lambda^{(1)} \subset \cdots \subset \lambda^{(k-1)} \subset \lambda^{(k)} \supset \lambda^{(k+1)} \supset \cdots \supset \lambda^{(r-1)} \supset \nu, \\ \kappa \subset \kappa^{(1)} \subset \cdots \subset \kappa^{(m-1)} \subset \kappa^{(m)} \supset \kappa^{(m+1)} \supset \cdots \supset \kappa^{(r-1)} \supset \mu.\end{gathered}$$

Let $\begin{array}{cc}\lambda' & \nu' \\ \boxed{\kappa'} & \mu'\end{array}$ label a cell in the first row of $B_{i,j}^{(r)}$, and note that the pairs λ', ν' and κ', μ' differ by a unit vector since they are adjacent partitions in an oscillating tableau. It is impossible for the inclusions $\begin{array}{cc}\lambda' \subset & \nu' \\ \boxed{\kappa'} \supset & \mu'\end{array}$ since $\lambda' \subset \nu'$ implies $\kappa' + \nu' - \lambda' = \kappa' + \mathbf{e}_i$ for some i, and by definition $\mu' = \mathrm{dom}_{\mathfrak{H}_r}(\kappa' + \mathbf{e}_i) = \kappa' + \mathbf{e}_i$ which contradicts $\mu' \subset \kappa'$. When $\begin{array}{cc}\lambda' \supset & \nu' \\ \boxed{\kappa'} \subset & \mu'\end{array}$ occurs, we know that $\kappa' + \nu' - \lambda' = \kappa' - \mathbf{e}_i$ for some i since $\nu' \subset \lambda'$. Since $\kappa' \subset \mu' = \mathrm{dom}_{\mathfrak{H}_r}(\kappa' - \mathbf{e}_i)$, it must be that $\mu' = \kappa' + \mathbf{e}_i$ and therefore $\kappa' - \mathbf{e}_i$ contained a negative entry. Therefore, when $\lambda' \supset \nu'$ and $\kappa' \subset \mu'$ there is a 1 filling the cell. Conversely, when there is a 1 filling a cell labelled $\begin{array}{cc}\lambda' & \nu' \\ \boxed{\kappa'} & \mu'\end{array}$, then there is a negative in $\kappa' + \nu' - \lambda' = \kappa' \pm \mathbf{e}_i$ for some i, which is only possible when $\kappa' + \nu' - \lambda' = \kappa' - \mathbf{e}_i$. As a result, $\kappa' \subset \mu'$ and $\lambda' \supset \nu'$.

By Theorem 5.3.1, each row and each column in $\mathsf{M}_O(\iota_{F\to O}(\mathsf{F}))$ contains exactly one 1. Therefore there is at most one cell in the first row of $B^{(r)}_{i,j}$ where the containment between the top and bottom pairs of partitions is flipped. By the cases described above, containment between pairs of partitions labelling the bottom of the first row of cells in $B^{(r)}_{i,j}$ either exactly matches the containment between pairs of partitions labelling the top of the first row or the switch in containment in the bottom occurs immediately to the right of the switch in containment in the top. The same outcome is observed recursively in the remaining rows of cells in $B^{(r)}_{i,j}$. Since we already knew the labels of the bottom of the r-th row to be increasing up to $\kappa^{(m)}$, we conclude that the number of 1's appearing in $B^{(r)}_{i,j}$ is equal to $m-k$, which we showed above is equal to $a_{i,j}$. Therefore, $\mathsf{M}_F(\mathsf{F}) = \mathsf{blocksum}_r(\mathsf{M}_O(\iota_{F\to O}(\mathsf{F})))$. Further, since the 1's in $\mathsf{M}_O(\iota_{F\to O}(\mathsf{F}))$ form a south-east chain, by Remark 5.3.1 we have $\mathsf{blowup}^{\mathsf{SE}}_r(\mathsf{M}_F(\mathsf{F})) = \mathsf{M}_O(\iota_{F\to O}(\mathsf{F}))$. □

We can now prove Theorem 5.3.2.

Proof. Let $\mathsf{F} = (\mu^0, \ldots, \mu^n)$ be an r-fan of Dyck paths of length n. We have

$$\begin{aligned} \mathsf{M}_F(\mathsf{F}) &= \mathsf{blocksum}_r(\mathsf{M}_O(\iota_{F\to O}(\mathsf{F}))) && \text{by Proposition 5.3.1} \\ &= \mathsf{blocksum}_r(\mathsf{G}_O(\iota_{F\to O}(\mathsf{F}))) && \text{by Theorem 5.3.1.} \end{aligned}$$

It remains to show that $\mathsf{blocksum}_r(\mathsf{G}_O(\iota_{F\to O}(\mathsf{F}))) = \mathsf{G}_F(\mathsf{F})$. The diagonal entries of $\mathsf{blocksum}_r(\mathsf{G}_O(\iota_{F\to O}(\mathsf{F})))$ and $\mathsf{G}_F(\mathsf{F})$ are all zero by Remark 5.3.2 and by definition of G_F respectively. As G_O and G_F are symmetric matrices, it suffices to show that the lower triangular entries of $\mathsf{blocksum}_r(\mathsf{G}_O(\iota_{F\to O}(\mathsf{F})))$ and $\mathsf{G}_F(\mathsf{F})$ agree. Let G denote the triangular growth diagram associated with $\iota_{F\to O}(\mathsf{F})$. By the definition of $\iota_{F\to O}$ and Construction 5.2.2, the coordinate $(kr, (n-k)r)$ is labelled with partition μ^k for $0 \leqslant k \leqslant n$. As G has a 0/1 filling, the local rules guarantee that the partition ν^k labelling the coordinate $(kr, (n-k-1)r)$ of G is contained within the partition $\mu^k \cap \mu^{k+1}$ for $0 \leqslant k \leqslant n-1$. Moreover, $|\mu^k/\nu^k| + |\mu^{k+1}/\nu^k|$ is equal to the total number of 1's lying in either a column from $kr+1$ to $(k+1)r$ or in a row from $(n-k-1)r+1$ to $(n-k)r$. From Lemma 5.3.2 and the fact that G_O is symmetric, there exist exactly r such 1's which implies $|\mu^k/\nu^k| + |\mu^{k+1}/\nu^k| = r$. Since μ^k and μ^{k+1} differ by exactly k boxes, $\nu^k = \mu^k \cap \mu^{k+1}$ for all $0 \leqslant k \leqslant n-1$.

Let H denote the triangular growth diagram with filling given by the lower triangular entries of $\mathsf{blocksum}_r(\mathsf{G}_O(\iota_{F\to O}(\mathsf{F})))$ and local rules given by the Burge rules. From Lemma 5.3.2, $\mathsf{blowup}^{\mathsf{SE}}(\mathsf{blocksum}_r(\mathsf{G}_O(\iota_{F\to O}(\mathsf{F})))) = \mathsf{G}_O(\iota_{F\to O}(\mathsf{F}))$. A result by Krattenthaler [**54**] implies that the labellings of the hypotenuse of H are given by $(\mu^0, \nu^0, \mu^1, \ldots, \nu^{n-1}, \mu^n)$. As the Burge rules are injective and the growth diagram associated to F under Construction 5.2.3 has hypotenuse labelled by $(\mu^0, \mu^0 \cap \mu^1, \mu^1, \ldots, \mu^{n-1} \cap \mu^n, \mu^n)$, the lower triangular entries of $\mathsf{blocksum}_r(\mathsf{G}_O(\iota_{F\to O}(\mathsf{F})))$ and $\mathsf{G}_F(\mathsf{F})$ are equal. □

5.3.3. Results for vacillating tableaux. We state our main results.

THEOREM 5.3.3. *For a vacillating tableau* V

$$\mathsf{G}_V(\mathsf{V}) = \mathsf{M}_{V\to O}(\mathsf{V}) = \mathsf{M}_{V\to F}(\mathsf{V}).$$

In other words, the filling of the growth diagram (see Construction 5.2.4), the filling of the promotion matrix $\mathsf{M}_{V\to O}(\mathsf{V})$*, and the filling of the promotion matrix* $\mathsf{M}_{V\to F}(\mathsf{V})$ *coincide.*

In particular we obtain the corollary:

COROLLARY 5.3.2. *The maps* $\mathsf{M}_{V\to O}$ *and* $\mathsf{M}_{V\to F}$ *are injective.*

We will first prove the second equality in Theorem 5.3.3. To do so, we need the following lemma.

LEMMA 5.3.3. *We have the following:*

(i) $\mathsf{M}_{V\to O} = \mathsf{blocksum}_2 \circ \mathsf{M}_O \circ \iota_{V\to O}$.

(ii) Denote by E *the* $r \times r$ *identity matrix, then*

$$\mathsf{M}_{V\to F} + 2(r-1)E = \mathsf{blocksum}_2 \circ \mathsf{M}_F \circ \iota_{V\to F}.$$

PROOF. Let V be a vacillating tableau of length n and weight zero and let $X \in \{O, F\}$. Denote by $\mathsf{T} = (\emptyset = \mu^0, \mu^1, \ldots, \mu^{2n} = \emptyset)$ the corresponding oscillating tableau (resp. r-fan of Dyck path) to V using $\iota_{V\to X}$.

Recall that $\mathsf{M}_{V\to X}$ is defined using the Schema (5.2.5) to calculate promotion. Let $\hat{\hat{\mu}}^1, \dots, \hat{\hat{\mu}}^{2n-1}$ be the partitions in the middle row in of this schema.

Note that we have $\mu^2 = \hat{\mu}^{2n-2} = 2\mathbf{e}_1$ and

$$\mu^1 = \hat{\hat{\mu}}^1 = \hat{\hat{\mu}}^{2n-1} = \hat{\mu}^{2n-1} = \begin{cases} \mathbf{e}_1 & \text{if } X = O, \\ \mathbf{1} & \text{if } X = F. \end{cases}$$

It is easy to see that the squares

$$\begin{tikzcd} \mu^1 \arrow[r, dash] \arrow[d, dash] & \mu^2 \arrow[d, dash] \\ \emptyset \arrow[r, dash] & \hat{\hat{\mu}}^1 \end{tikzcd} \qquad \text{and} \qquad \begin{tikzcd} \hat{\hat{\mu}}^{2n-1} \arrow[r, dash] \arrow[d, dash] & \emptyset \arrow[d, dash] \\ \hat{\mu}^{2n-2} \arrow[r, dash] & \hat{\mu}^{2n-1} \end{tikzcd}$$

satisfy the local rule and

$$\Phi(\mu^1, \emptyset, \mu^2, \hat{\hat{\mu}}^1) = \Phi(\hat{\hat{\mu}}^{2n-1}, \hat{\mu}^{2n-2}, \emptyset, \hat{\mu}^{2n-1}) = \begin{cases} 0 & \text{if } X = O, \\ r-1 & \text{if } X = F. \end{cases}$$

Thus we have

$$\mathsf{pr}_X(\iota_{V\to X}(\mathsf{V})) = (\emptyset, \hat{\hat{\mu}}_1, \dots, \hat{\hat{\mu}}_{2n-1}, \emptyset)$$

and obtain $\mathsf{M}_{V\to X} + \mathbb{1}_{X=F} \cdot 2(r-1)E = \mathsf{blocksum}_2 \circ \mathsf{M}_X \circ \iota_{V\to X}$. □

The following relates the growth diagrams for $\iota_{V\to O}(\mathsf{V})$ and $\iota_{V\to F}(\mathsf{V})$.

Lemma 5.3.4. *Denote by S the $2r \times 2r$ block diagonal matrix consisting of r copies of the block* $\begin{bmatrix} 0 & 1 \\ 1 & 0 \end{bmatrix}$ *along the diagonal and zeros everywhere else. Then*

$$\mathsf{G}_F \circ \iota_{V\to F} = \mathsf{G}_O \circ \iota_{V\to O} + (r-1)S.$$

Proof. Let $\mathsf{V} = (\lambda^0, \dots, \lambda^n)$ be a vacillating tableau of weight zero. Denote with $\mathsf{O} = (\mu^0, \dots, \mu^{2n}) = \iota_{V\to O}(\mathsf{V})$ the corresponding oscillating tableaux and denote with $\mathsf{F} = (\nu^0, \dots, \nu^{2n}) = \iota_{V\to O}(F)$ the r-fan of Dyck paths.

Consider the portion of the growth diagram for the oscillating tableau involving only $(\mu^{2i-2}, \mu^{2i-1}, \mu^{2i})$ and the portion of the growth diagram for the fan of Dyck paths involving only $(\nu^{2i-2}, \nu^{2i-1}, \nu^{2i})$. We label the partitions as follows.

(5.3.1)

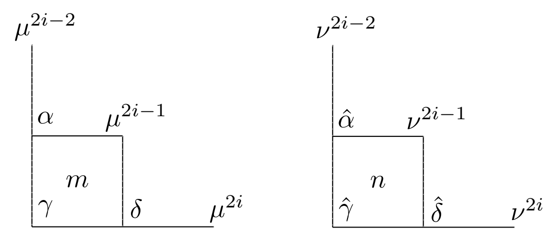

Claim: We have $\mu^{2i-2} = \nu^{2i-2}$, $\mu^{2i} = \nu^{2i}$, $\alpha = \hat{\alpha}$, $\gamma = \hat{\gamma}$, $\delta = \hat{\delta}$, $m = 0$ and $n = r-1$. Moreover all partitions on consecutive corners on the lower left border of the diagrams in (5.3.1) differ by at most one cell.

We consider the three cases $\lambda^{i-1} = \lambda^i$, $\lambda^{i-1} \subset \lambda^i$ and $\lambda^{i-1} \supset \lambda^i$.

By Definition 5.1.12, Construction 5.2.2, Definition 5.1.13 and Construction 5.2.3 we have

$$\mu^{2i-2} = \nu^{2i-2} = 2\lambda^{i-1}, \qquad \mu^{2i} = \nu^{2i} = 2\lambda^i,$$

$$\alpha = \mu^{2i-2} \cap \mu^{2i-1}, \qquad \delta = \mu^{2i-1} \cap \mu^{2i},$$

$$\hat{\alpha} = \nu^{2i-2} \cap \nu^{2i-1}, \qquad \hat{\delta} = \nu^{2i-1} \cap \nu^{2i}.$$

Case I. Assume $\lambda^{i-1} = \lambda^i$. In this case we have $\mu^{2i-1} = 2\lambda^i - \mathbf{e}_r$ and $\nu^{2i-1} = 2\lambda^i + \mathbf{1} - 2\mathbf{e}_r$ and get

$$\alpha = \delta = (2\lambda^i) \cap (2\lambda^i - \mathbf{e}_r) = 2\lambda^i - \mathbf{e}_r,$$

$$\hat{\alpha} = \hat{\delta} = (2\lambda^i) \cap (2\lambda^i + \mathbf{1} - 2\mathbf{e}_r) = 2\lambda^i - \mathbf{e}_r.$$

Using the backwards rules for growth diagrams we obtain

$$\gamma = \hat{\gamma} = 2\lambda^i - \mathbf{e}_r, \quad m = 0 \quad \text{and} \quad n = r - 1.$$

Case II. Assume $\lambda^{i-1} \subset \lambda^i$. In this case we have $\mu^{2i-1} = \lambda^{i-1} + \lambda^i$ and $\nu^{2i-1} = 2\lambda^{i-1} + \mathbf{1}$. Furthermore we obtain

$$\alpha = (2\lambda^{i-1}) \cap (\lambda^{i-1} + \lambda^i) = 2\lambda^{i-1},$$

$$\hat{\alpha} = (2\lambda^{i-1}) \cap (2\lambda^{i-1} + \mathbf{1}) = 2\lambda^{i-1},$$

$$\delta = (\lambda^{i-1} + \lambda^i) \cap (2\lambda^i) = \lambda^{i-1} + \lambda^i,$$

$$\hat{\delta} = (2\lambda^{i-1} + \mathbf{1}) \cap (2\lambda^i) = \lambda^{i-1} + \lambda^i.$$

Using the backwards rules for growth diagrams we obtain

$$\gamma = \hat{\gamma} = 2\lambda^{i-1}, \quad m = 0 \quad \text{and} \quad n = r - 1.$$

Case III. Assume $\lambda^{i-1} \supset \lambda^i$. This case is symmetric to Case II.

This proves the claim.

The rest of the growth diagrams must agree, as the Burge growth rules and Fomin growth rules agree in the case where labels on consecutive corners differ by at most one cell. $\square$

Note that Lemma 5.3.4 implies

$$\mathsf{blocksum}_2 \circ \mathsf{G}_F \circ \iota_{V \to F} = \mathsf{blocksum}_2 \circ \mathsf{G}_O \circ \iota_{V \to O} + 2(r-1)E. \tag{5.3.2}$$

Now we can prove the second identity of Theorem 5.3.3.

Proof. We have

$$\begin{aligned}
\mathsf{M}_{V \to O} &= \mathsf{blocksum}_2 \circ \mathsf{M}_O \circ \iota_{V \to O} && \text{by Lemma 5.3.3 (i)} \\
&= \mathsf{blocksum}_2 \circ \mathsf{G}_O \circ \iota_{V \to O} && \text{by Theorem 5.3.1} \\
&= \mathsf{blocksum}_2 \circ \mathsf{G}_F \circ \iota_{V \to F} - 2(r-1)E && \text{by Equation (5.3.2)} \\
&= \mathsf{blocksum}_2 \circ \mathsf{M}_F \circ \iota_{V \to F} - 2(r-1)E && \text{by Theorem 5.3.2} \\
&= \mathsf{M}_{V \to F} && \text{by Lemma 5.3.3 (ii).}
\end{aligned}$$

$\square$

It is possible to invert Lemma 5.3.3 (i) as follows.

Lemma 5.3.5. *Let* V *be a vacillating tableau of weight zero with length* n*, and let* $(B^{(2)}_{i,j})^n_{i,j=1}$ *be the block matrix decomposition of the* $2n \times 2n$ *adjacency matrix* $\mathsf{M}_O(\iota_{V\to O}\mathsf{V})$*. Then for all* $1 \leqslant i \leqslant n$*, the nonzero entries in the matrices*

$$[B^{(2)}_{i,i+1}, B^{(2)}_{i,i+2}, \dots, B^{(2)}_{i,i+n-1}] \qquad \text{and}$$
$$[B^{(2)}_{i+1,i}, B^{(2)}_{i+2,i}, \dots, B^{(2)}_{i+n-1,i}]$$

form a north-east chain. In particular, we have

$$\mathsf{blowup}^{\mathsf{NE}}_2 \circ \mathsf{M}_{V\to O} = \mathsf{M}_O \circ \iota_{V\to O}.$$

Proof. From Propositions 5.2.1 and 5.2.2, it suffices to prove that the nonzero entries in $[B^{(2)}_{n,n+1}, B^{(2)}_{n,n+2}, \dots, B^{(2)}_{n,2n-1}]$ and $[B^{(2)}_{2,1}, B^{(2)}_{3,1}, \dots, B^{(2)}_{n,1}]^T$ form a south-east chain. Recall that by construction, the Fomin growth diagram of $\iota_{V\to O}(\mathsf{V})$ is a triangle diagram with the entries of $\iota_{V\to O}(\mathsf{V})$ labelling its diagonal. As V is a vacillating tableau of weight zero, the partition (2) sits at the corners $(2, 2(n-1))$ and $(2(n-1), 2)$ in the Fomin growth diagram of $\iota_{V\to O}(\mathsf{V})$. By Theorem 5.3.1, we have $\mathsf{M}_O(\iota_{V\to O}(\mathsf{V})) = \mathsf{G}_O(\iota_{V\to O}(\mathsf{V}))$. This implies that the filling of the first 2 columns and first 2 rows match $\mathsf{M}_O(\iota_{V\to O}(\mathsf{V}))$. As all the entries of $\mathsf{M}_O(\iota_{V\to O}(\mathsf{V}))$ are either 0 or 1, we have that all the nonzero entries in the first 2 rows and the first 2 rows form a north-east chain by [**54**, Theorem 2]. $\square$

We can now prove the first part of Theorem 5.3.3.

Proof. Putting together the current results we obtain:

$$\begin{aligned} \mathsf{blowup}^{\mathsf{NE}}_2 \circ \mathsf{M}_{V\to O} &= \mathsf{M}_O \circ \iota_{V\to O} && \text{by Lemma 5.3.5} \\ &= \mathsf{G}_O \circ \iota_{V\to O} && \text{by Theorem 5.3.1.} \end{aligned}$$

It thus remains to show: $\mathsf{G}_V = \mathsf{blocksum}_2 \circ \mathsf{G}_O \circ \iota_{V\to O}$. Let V be a fixed vacillating tableau of weight zero and length n. Let $\mathsf{O} = \iota_{V\to O}(\mathsf{V})$. Let $M = (m_{i,j})_{1\leqslant i,j\leqslant 2n} = \mathsf{G}_O(\mathsf{O})$ and let $B^{(2)}_{i,j}$ be its block matrix decomposition. Let $\alpha_{i,j}$ for $0 \leqslant j \leqslant i \leqslant 2n$ be the partition in the i-th row and j-th column in the growth diagram of O. Above calculation shows that the nonzero entries in the matrices

$$[B^{(2)}_{i,i+1}, B^{(2)}_{i,i+2}, \ldots, B^{(2)}_{i,i+n-1}] \qquad \text{and}$$
$$[B^{(2)}_{i+1,i}, B^{(2)}_{i+2,i}, \ldots, B^{(2)}_{i+n-1,i}]$$

form north-east chains.

Thus the squares

$$\begin{array}{cc} \alpha_{2i,2j} & \alpha_{2i,2(j+1)} \\ \alpha_{2(i+1),2j} & \alpha_{2(i+1),2(j+1)} \end{array}$$

with entry $m_{2i,2j} + m_{2i+1,2j} + m_{2i,2j+1} + m_{2i+1,2j+1}$ satisfy the rules RSK F0-F2 and RSK B0-B2. As in proof of Lemma 5.3.4, the entries of the first subdiagonal of M are zero. Hence M is uniquely determined by the labels $\alpha 2i, 2i$ and $\alpha_{2i,2i+1}$. Again by proof of Lemma 5.3.4 we have $\alpha_{2i,2i} = 2\lambda^i$ and $\alpha_{2i,2i+1} = (2\lambda^i) \cup (2\lambda^{i+1})$. As these partitions agree with the labels in Construction 5.2.4, we get $\mathsf{G}_V(\mathsf{V}) = \mathsf{blocksum}_2(\mathsf{G}_O(\mathsf{O}))$. $\square$

Problem 5.3.1. *Find a characterization of the image of the injective maps* M_F*,* $\mathsf{M}_{V\to O}$ *and* $\mathsf{M}_{V\to F}$*.*

Remark 5.3.3. *For* M_O *the solution to the above problem is known (see [**75**]). The set of* r*-symplectic oscillating tableaux of weight zero are in bijection with the set of* $(r+1)$*-noncrossing perfect matchings of* $\{1, 2, \ldots, n\}$*.*

5.3.4. Cyclic sieving. The cyclic sieving phenomenon was introduced by Reiner, Stanton and White [**77**] as a generalization of Stembridge's $q = -1$ phenomenon.

Definition 5.3.3. *Let* X *be a finite set and* C *be a cyclic group generated by* c *acting on* X*. Let* $\zeta \in \mathbb{C}$ *be a* $|C|^{th}$ *primitive root of unity and* $f(q) \in \mathbb{Z}[q]$ *be a polynomial in* q*. Then the triple* (X, C, f) *exhibits the cyclic sieving phenomenon if for all* $d \geqslant 0$ *we have that the size of the fixed point set of* c^d *(denoted* X^{c^d}*) satisfies* $|X^{c^d}| = f(\zeta^d)$*.*

In this section, we will state cyclic sieving phenomena for the promotion action on oscillating tableaux, fans of Dyck paths, and vacillating tableaux. In Section 5.3.4.1 we review an approach using the energy function. In Sections 5.3.4.2 and 5.3.4.3 we give new cyclic sieving phenomena for fans of Dyck paths and vacillating tableaux, respectively.

5.3.4.1. *Cyclic sieving using the energy function.* We first introduce the energy function on tensor products of crystals. The energy function is defined on affine crystals, meaning that the crystal $\mathcal{C}_\square$ needs to be upgraded to a crystal of affine Kac–Moody type $C_r^{(1)}$ and the crystals $\mathcal{B}_\square$ and $\mathcal{B}_{\mathsf{spin}}$ need to be upgraded to crystals of affine Kac–Moody type $B_r^{(1)}$. In particular, these affine crystals have additional crystals operators f_0 and e_0. For further details, see for example [**33**,**67**,**68**].

For an affine crystal $\mathcal{B}$, the *local energy function*

$$H\colon \mathcal{B}\otimes\mathcal{B}\to\mathbb{Z}$$

is defined recursively (up to an overall constant) by

$$H(e_i(b_1\otimes b_2)) = H(b_1\otimes b_2) + \begin{cases} +1 & \text{if } i=0 \text{ and } \varepsilon_0(b_1) > \varphi_0(b_2),\\ -1 & \text{if } i=0 \text{ and } \varepsilon_0(b_1) \leqslant \varphi_0(b_2),\\ 0 & \text{otherwise.}\end{cases}$$

The crystals we consider here are simple, meaning that there exists a dominant weight λ such that $\mathcal{B}$ contains a unique element, denoted $u(\mathcal{B})$, of weight λ such that every extremal vector of $\mathcal{B}$ is contained in the Weyl group orbit of λ. We normalize H such that

$$H(u(\mathcal{B})\otimes u(\mathcal{B})) = 0.$$

Example 5.3.1. *The affine crystal $\mathcal{C}_\square^{\mathsf{af}}$ of type $C_r^{(1)}$ is, for example, constructed in [**33**, Theorem 5.7]. The case of type $C_2^{(1)}$ is depicted in Figure 5.11. Using the ordering $1<2<\cdots<r<\overline{r}<\cdots<\overline{2}<\overline{1}$, we have that $H(a\otimes b)=0$ if $a\leqslant b$ and $H(a\otimes b)=1$ if $a>b$.*

Example 5.3.2. *The affine crystal $\mathcal{B}_\square^{\mathsf{af}}$ of type $B_r^{(1)}$ is, for example, constructed in [**33**, Theorem 5.1]. The case $B_2^{(1)}$ is depicted in Figure 5.11. Using the ordering $1<2<\cdots<r<0<\overline{r}<\cdots<\overline{2}<\overline{1}$, we have that $H(a\otimes b)=0$ if $a\leqslant b$ and $a\otimes b\neq 0\otimes 0$, $H(\overline{1}\otimes 1)=2$, and $H(a\otimes b)=1$ otherwise.*

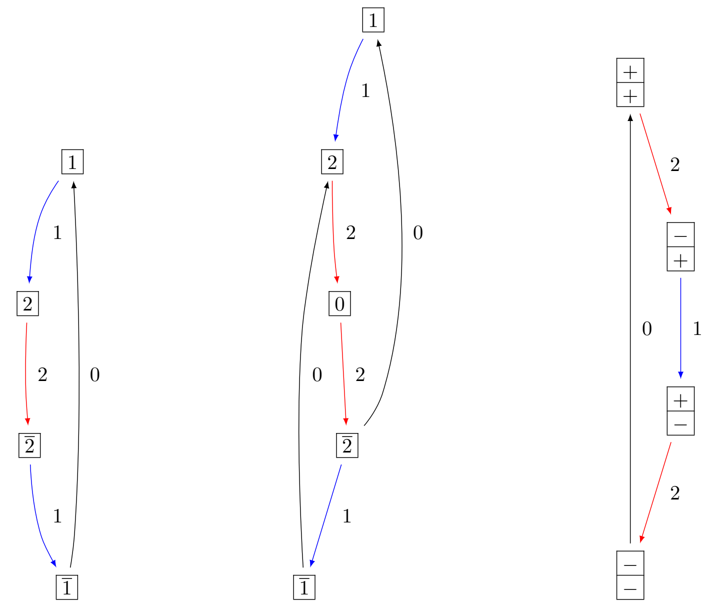

FIGURE 5.11. Left: Affine crystal $\mathcal{C}^{\mathsf{af}}_{\square}$ of type $C_2^{(1)}$. Middle: Affine crystal $\mathcal{B}^{\mathsf{af}}_{\square}$ of type $B_2^{(1)}$. Right: Affine crystal $\mathcal{B}^{\mathsf{af}}_{\mathsf{spin}}$ of type $B_2^{(1)}$.

EXAMPLE 5.3.3. *The affine crystal $\mathcal{B}^{\mathsf{af}}_{\mathsf{spin}}$ of type $B_r^{(1)}$ is constructed in [**33**, Theorem 5.3]. The case $B_2^{(1)}$ is depicted in Figure 5.11. The classical highest weight elements in $\mathcal{B}^{\mathsf{af}}_{\mathsf{spin}} \otimes \mathcal{B}^{\mathsf{af}}_{\mathsf{spin}}$ are $(\epsilon_1, \ldots, \epsilon_r) \otimes (+, +, \ldots, +)$ with $\epsilon_i = +$ for $1 \leqslant i \leqslant k$ and $\epsilon_i = -$ for $k < i \leqslant r$ for some $0 \leqslant k \leqslant r$. Denoting by $m(\epsilon_1, \ldots, \epsilon_r)$ the number of $-$ in the ϵ_i, we have*

$$H((\epsilon_1, \ldots, \epsilon_r) \otimes (+, \ldots, +)) = \left\lfloor \frac{m(\epsilon_1, \ldots, \epsilon_r) + 1}{2} \right\rfloor.$$

By definition, the local energy is constant on classical components.

The *energy function*

$$E \colon \mathcal{B}^{\otimes n} \to \mathbb{Z}$$

is defined as follows for $b_1 \otimes \cdots \otimes b_n \in \mathcal{B}^{\otimes n}$

$$E(b_1 \otimes \cdots \otimes b_n) = \sum_{i=1}^{n-1} i H(b_i \otimes b_{i+1}).$$

Let us now define a polynomial in q using the energy function for highest weight elements in $\mathcal{B}^{\otimes n}$ of weight zero

$$f_{n,r}(q) = q^{c_{n,r}} \sum_{\substack{b \in \mathcal{B}^{\otimes n} \\ \mathsf{wt}(b)=0 \\ e_i(b)=0 \text{ for } 1 \leqslant i \leqslant r}} q^{E(b)},$$

where r is the rank of the type of the underlying root system and $c_{n,r}$ is a constant depending on the type. Namely,

$$c_{n,r} = \begin{cases} 0 & \text{for } \mathcal{B}_\square \text{ all } r \text{ and } \mathcal{B}_{\mathsf{spin}} \text{ for } r \equiv 0,3 \pmod 4, \\ q^{\frac{n}{2}} & \text{for } \mathcal{C}_\square \text{ all } r \text{ and } \mathcal{B}_{\mathsf{spin}} \text{ for } r \equiv 1,2 \pmod 4. \end{cases}$$

The following theorem clarifies statements in [**97**].

Theorem 5.3.4. *Let X be the set of highest weight elements in $\mathcal{B}^{\otimes n}$ of weight zero, where $\mathcal{B}$ is minuscule. Then $(X, C_n, f_{n,r}(q))$ exhibits the cyclic sieving phenomenon, where C_n is the cyclic group of order n given by the action of promotion* pr *on $\mathcal{B}^{\otimes n}$.*

Proof. Fontaine and Kamnitzer [**31**] proved that $(X, C_n, \widetilde{f}_{n,r}(q))$ exhibits the cyclic sieving phenomenon, where $\widetilde{f}_{n,r}(q)$ is a polynomial defined in terms of current algebra actions on Weyl modules of Fourier and Littelmann [**32**]. By [**34**], this is equal to the energy function polynomial up to an overall constant, proving the claim. □

For the vector representation of type A, highest weight elements in the tensor product of weight zero under RSK are in correspondence with standard tableaux of rectangular shape. The energy function relates to the major index under correspondence. Hence in this case, Theorem 5.3.4 relates to results in [**78**].

Note that $\mathcal{C}_\square$ and $\mathcal{B}_{\mathsf{spin}}$ are minuscule, and hence Theorem 5.3.4 gives a cyclic sieving phenomenon for oscillating tableaux and fans of Dyck paths. We conjecture that the results of Theorem 5.3.4 also hold for $\mathcal{B}_\square$ even though this crystal is not minuscule. This has been verified for all $2 \leqslant r \leqslant 10$ and $1 \leqslant n \leqslant 10$.

5.3.4.2. *Cyclic sieving for fans of Dyck paths.* Recall from Section 5.1.3.2 that highest weight elements of weight zero in $\mathcal{B}_{\mathsf{spin}}^{\otimes 2n}$ of type B_r are in bijection with r-fans of Dyck paths of length $2n$. Denote by $D_n^{(r)}$ the set of all r-fans of Dyck paths of length $2n$. The cardinality of this set is given by $\prod_{1\leqslant i\leqslant j\leqslant n-1}\frac{i+j+2r}{i+j}$, see [**22, 53**]. Define the q-analogue of this formula as

$$g_{n,r}(q) = \prod_{1\leqslant i\leqslant j\leqslant n-1} \frac{[i+j+2r]_q}{[i+j]_q}, \tag{5.3.3}$$

where $[m]_q = 1+q+q^2+\cdots+q^{m-1}$.

CONJECTURE 5.3.1. *The triple $(D_n^{(r)}, C_{2n}, g_{n,r}(q))$ exhibits the cyclic sieving phenomenon, where C_{2n} is the cyclic group of order $2n$ that acts on $D_n^{(r)}$ by applying promotion.*

EXAMPLE 5.3.4. *We have*

$$q^{-4}f_{4,2}(q) = g_{2,2}(q) = q^4+q^2+1$$

and

$$g_{3,2}(q) = q^{12}+q^{10}+q^9+2q^8+q^7+2q^6+q^5+2q^4+q^3+q^2+1,$$

$$q^{-6}f_{6,2}(q) = q^{10}+q^9+2q^8+q^7+3q^6+q^5+2q^4+q^3+q^2+1.$$

Note that $g_{3,2}(q) = f_{6,2}(q) \pmod{q^6-1}$.

In general, we conjecture that $g_{n,r}(q) = f_{2n,r}(q) \pmod{q^{2n}-1}$ which has been verified for all $n+r\leqslant 10$.

Note that by [**53**, Theorem 10]

$$g_{n,r}(q) = \prod_{1\leqslant i\leqslant j\leqslant n-1} \frac{[i+j+2r]_q}{[i+j]_q} = \sum_{\substack{\lambda \\ \lambda_1\leqslant r}} s_{2\lambda}(q,q^2,\ldots,q^{n-1}).$$

REMARK 5.3.4. *Conjecture 5.3.1 is equivalent to [**43**, Conjecture 5.2], [**45**, Conjecture 4.28], and [**44**, Conjecture 5.9] on plane partitions and root posets.*

REMARK 5.3.5. *There is a bijection between r-fans of Dyck paths of length $2(n-2r)$ and r-triangulations of n-gons. A cyclic sieving phenomenon in this setting was conjectured by Serrano and Stump [**85**]. Even though the polynomial in this conjectured cyclic sieving phenomenon is $g_{n-2r,r}$, the cyclic group acting is C_{2n}, which is different from our setting.*

5.3.4.3. *Cyclic sieving for vacillating tableaux.* Before giving our cyclic sieving phenomenon result for vacillating tableaux, we review Jagenteufel's major statistic for vacillating tableaux [**48**]. As vacillating tableaux are in bijection with highest weight elements of $\mathcal{B}_{\square}^{\otimes n}$, it suffices to define the major statistic on highest weight elements of $\mathcal{B}_{\square}^{\otimes n}$.

Let $u = u_n \otimes \cdots \otimes u_2 \otimes u_1$ be a highest weight element in $\mathcal{B}_{\square}^{\otimes n}$ of type B_r. As before let $<$ denote the ordering $1 < 2 < \cdots < r < 0 < \bar{r} < \cdots < \bar{2} < \bar{1}$ on the elements of $\mathcal{B}_{\square}$. We say that position i is a *descent* for u if

(1) $u_{i+1} > u_i$, and
(2) if the suffix $u_{i-1} \otimes \cdots \otimes u_2 \otimes u_1$ has an equal number of j's and $\bar{j}$'s, then $u_{i+1} \otimes u_i \neq \bar{j} \otimes j$.

Denote the set of descents of u by $\mathsf{Des}(u)$. Define the *major index* of u, denoted by $\mathrm{maj}(u)$, as the sum of its descents $\sum_{i \in \mathsf{Des}(u)} i$. Let $h_{n,r}(q)$ denote the polynomial in q given by

$$h_{n,r}(q) = \sum_{u \in V_n^{(r)}} q^{\mathrm{maj}(u)}$$

where $V_n^{(r)}$ denotes the set of all highest weight elements of weight zero in $\mathcal{B}_{\square}^{\otimes n}$ of type B_r.

From [**48**, Theorem 2.1] and [**97**, Theorem 6.8], we obtain the following result.

THEOREM 5.3.5. *The triple $(V_n^{(r)}, C_n, h_{n,r}(q))$ exhibits the cyclic sieving phenomenon, where the cyclic group on n elements, C_n, acts on $V_n^{(r)}$ by applying promotion.*

Using the descent-preserving bijection in [**48**], we obtain another interpretation of $h_{n,r}(q)$ in terms of standard Young tableaux. Adopting the notation and terminology of [**87**] for standard Young tableaux, we say that i is a descent for the standard Young tableau T if $i+1$ sits in a lower row than i in T in English notation. Given this, we analogously define $\mathrm{maj}(T)$ to be the sum of the descents of T. Letting $\mathrm{SYT}(\lambda)$ denote the set of all standard Young tableaux of shape λ, the polynomial $h_{n,r}(q)$ can be reinterpreted as follows.

THEOREM 5.3.6. *[**48**] Let $n, r \geqslant 1$. Then*

$$h_{n,r}(q) = \sum_{T \in \mathrm{SYT}(\lambda)} q^{\mathrm{maj}(T)},$$

where λ ranges over all partitions of n with only even parts and length at most $2r+1$ when n is even and λ ranges over all partitions of n with only odd parts and length exactly $2r+1$ when n is odd.

EXAMPLE 5.3.5. *We have*

$$f_{7,2}(q) = q^{22} + q^{21} + q^{20} + q^{19} + 2q^{18} + 2q^{17} + 2q^{16} + q^{15} + 2q^{14} + q^{13} + q^{12}$$
$$h_{7,2}(q) = q^{18} + q^{17} + 2q^{16} + 2q^{15} + 3q^{14} + 2q^{13} + 2q^{12} + q^{11} + q^{10}$$

Note that $f_{7,2}(q) = h_{7,2}(q) \pmod{q^7 - 1}$.

Bibliography

[1] R. M. Adin and Y. Roichman, *On maximal chains in the non-crossing partition lattice*, J. Combin. Theory Ser. A, 125 (2014), pp. 18–46.

[2] G. E. Andrews, C. Krattenthaler, L. Orsina, and P. Papi, *ad-nilpotent $\mathfrak{b}$-ideals in* $\mathrm{sl}(n)$ *having a fixed class of nilpotence: combinatorics and enumeration*, Trans. Amer. Math. Soc., 354 (2002), pp. 3835–3853.

[3] F. Ardila, *The Catalan matroid*, J. Combin. Theory Ser. A, 104 (2003), pp. 49–62.

[4] D. Armstrong, N. A. Loehr, and G. S. Warrington, *Sweep maps: a continuous family of sorting algorithms*, Adv. Math., 284 (2015), pp. 159–185.

[5] C. A. Athanasiadis, *Gamma-positivity in combinatorics and geometry*, Sém. Lothar. Combin., 77 ([2016–2018]), pp. Art. B77i, 64 pp.

[6] A. Ayyer, S. Klee, and A. Schilling, *Combinatorial Markov chains on linear extensions*, J. Algebraic Combin., 39 (2014), pp. 853–881.

[7] A. Bacher and G. Schaeffer, *Multivariate Lagrange inversion formula and the cycle lemma*, in The Seventh European Conference on Combinatorics, Graph Theory and Applications, vol. 16 of CRM Series, Ed. Norm., Pisa, 2013, pp. 551–556.

[8] J. Bandlow, A. Schilling, and N. M. Thiéry, *On the uniqueness of promotion operators on tensor products of type A crystals*, J. Algebraic Combin., 31 (2010), pp. 217–251.

[9] S. Benchekroun and P. Moszkowski, *A new bijection between ordered trees and legal bracketings*, European J. Combin., 17 (1996), pp. 605–611.

[10] S. A. Blanco and T. K. Petersen, *Counting Dyck paths by area and rank*, Ann. Comb., 18 (2014), pp. 171–197.

[11] M. Bóna, S. Dimitrov, G. Labelle, Y. Li, J. Pappe, A. R. Vindas-Meléndez, and Y. Zhuang, *A combinatorial proof of a tantalizing symmetry on Catalan objects*. Preprint, `https://arxiv.org/abs/2212.10586`, 2022.

[12] P. Brändén, *Sign-graded posets, unimodality of W-polynomials and the Charney-Davis conjecture*, Electron. J. Combin., 11 (2004/06), pp. Research Paper 9, 15 pp.

[13] ———, *Actions on permutations and unimodality of descent polynomials*, European J. Combin., 29 (2008), pp. 514–531.

[14] ———, *Unimodality, log-concavity, real-rootedness and beyond*, in Handbook of enumerative combinatorics, Discrete Math. Appl. (Boca Raton), CRC Press, Boca Raton, FL, 2015, pp. 437–483.

[15] T. Britz and S. Fomin, *Finite posets and Ferrers shapes*, Adv. Math., 158 (2001), pp. 86–127.

[16] D. Bump and A. Schilling, *Crystal bases*, World Scientific Publishing Co. Pte. Ltd., Hackensack, NJ, 2017. Representations and combinatorics.

[17] W. H. Burge, *Four correspondences between graphs and generalized Young tableaux*, J. Combinatorial Theory Ser. A, 17 (1974), pp. 12–30.

[18] D. Callan, *Generalized Narayana numbers*. `https://oeis.org/A281260/a281260.pdf`, 2017.

[19] C. Ceballos, T. Denton, and C. R. H. Hanusa, *Combinatorics of the zeta map on rational Dyck paths*, J. Combin. Theory Ser. A, 141 (2016), pp. 33–77.

[20] C. Ceballos, W. Fang, and H. Mühle, *The steep-bounce zeta map in parabolic Cataland*, J. Combin. Theory Ser. A, 172 (2020), pp. 105210, 59.

[21] X. Chen, A. L. B. Yang, and J. J. Y. Zhao, *Recurrences for Callan's Generalization of Narayana Polynomials*, J. Syst. Sci. Complex., 35 (2022), pp. 1573–1585.

[22] M. de Sainte-Catherine and G. Viennot, *Enumeration of certain Young tableaux with bounded height*, in Combinatoire énumérative (Montreal, Que., 1985/Quebec, Que., 1985), vol. 1234 of Lecture Notes in Math., Springer, Berlin, 1986, pp. 58–67.

[23] N. Dershowitz and S. Zaks, *The cycle lemma and some applications*, European J. Combin., 11 (1990), pp. 35–40.

[24] E. Deutsch, *Dyck path enumeration*, Discrete Math., 204 (1999), pp. 167–202.

[25] ———, *An involution on Dyck paths and its consequences*, Discrete Math., 204 (1999), pp. 163–166.

[26] R. Domagalski, S. Elizalde, J. Liang, Q. Minnich, B. E. Sagan, J. Schmidt, and A. Sietsema, *Cyclic pattern containment and avoidance*, Adv. in Appl. Math., 135 (2022), pp. Paper No. 102320, 28 pp.

[27] R. Domagalski, J. Liang, Q. Minnich, B. E. Sagan, J. Schmidt, and A. Sietsema, *Cyclic shuffle compatibility*, Sém. Lothar. Combin., 85 ([2020–2021]), pp. Art. B85d, 11 pp.

[28] A. Dvoretzky and T. Motzkin, *A problem of arrangements*, Duke Math. J., 14 (1947), pp. 305–313.

[29] P. Flajolet and R. Sedgewick, *Analytic combinatorics*, Cambridge University Press, Cambridge, 2009.

[30] S. V. Fomin, *The generalized Robinson-Schensted-Knuth correspondence*, Zap. Nauchn. Sem. Leningrad. Otdel. Mat. Inst. Steklov. (LOMI), 155 (1986), pp. 156–175, 195.

[31] B. Fontaine and J. Kamnitzer, *Cyclic sieving, rotation, and geometric representation theory*, Selecta Math. (N.S.), 20 (2014), pp. 609–625.

[32] G. Fourier and P. Littelmann, *Weyl modules, Demazure modules, KR-modules, crystals, fusion products and limit constructions*, Adv. Math., 211 (2007), pp. 566–593.

[33] G. Fourier, M. Okado, and A. Schilling, *Kirillov-Reshetikhin crystals for nonexceptional types*, Adv. Math., 222 (2009), pp. 1080–1116.

[34] G. Fourier, A. Schilling, and M. Shimozono, *Demazure structure inside Kirillov-Reshetikhin crystals*, J. Algebra, 309 (2007), pp. 386–404.

[35] A. M. Garsia and J. Haglund, *A proof of the q,t-Catalan positivity conjecture*, vol. 256, 2002, pp. 677–717. LaCIM 2000 Conference on Combinatorics, Computer Science and Applications (Montreal, QC).

[36] A. M. Garsia and M. Haiman, *A remarkable q,t-Catalan sequence and q-Lagrange inversion*, J. Algebraic Combin., 5 (1996), pp. 191–244.

[37] C. Greene, *An extension of Schensted's theorem*, Advances in Math., 14 (1974), pp. 254–265.

[38] J. Haglund, *Conjectured statistics for the q,t-Catalan numbers*, Adv. Math., 175 (2003), pp. 319–334.

[39] J. Haglund, *The q,t-Catalan numbers and the space of diagonal harmonics*, vol. 41 of University Lecture Series, American Mathematical Society, Providence, RI, 2008. With an appendix on the combinatorics of Macdonald polynomials.

[40] J. Haglund and N. Loehr, *A conjectured combinatorial formula for the Hilbert series for diagonal harmonics*, Discrete Math., 298 (2005), pp. 189–204.

[41] A. Henriques and J. Kamnitzer, *Crystals and coboundary categories*, Duke Math. J., 132 (2006), pp. 191–216.

[42] J. Hong and S.-J. Kang, *Introduction to quantum groups and crystal bases*, vol. 42 of Graduate Studies in Mathematics, American Mathematical Society, Providence, RI, 2002.

[43] S. Hopkins, *Cyclic sieving for plane partitions and symmetry*, SIGMA Symmetry Integrability Geom. Methods Appl., 16 (2020), pp. Paper No. 130, 40.

[44] ———, *Order polynomial product formulas and poset dynamics*. Preprint, `https://arxiv.org/abs/2006.01568`, 2020.

[45] ———, *Minuscule doppelgängers, the coincidental down-degree expectations property, and rowmotion*, Exp. Math., 31 (2022), pp. 946–974.

[46] O. F. Inc., *The On-Line Encyclopedia of Integer Sequences, A116395*. `https://oeis.org/A116395`, 2021.

[47] J. Irving and A. Rattan, *Trees, parking functions and factorizations of full cycles*, European J. Combin., 93 (2021), pp. Paper No. 103257, 22.

[48] J. Jagenteufel, *A Sundaram type bijection for* $\mathrm{SO}(2k+1)$*: vacillating tableaux and pairs consisting of a standard Young tableau and an orthogonal Littlewood-Richardson tableau*, Sém. Lothar. Combin., 82B (2020), pp. Art. 33, 12.

[49] M. Kashiwara, *Crystalizing the q-analogue of universal enveloping algebras*, Comm. Math. Phys., 133 (1990), pp. 249–260.

[50] ———, *Crystal bases of modified quantized enveloping algebra*, Duke Math. J., 73 (1994), pp. 383–413.

[51] ———, *Similarity of crystal bases*, in Lie algebras and their representations (Seoul, 1995), vol. 194 of Contemp. Math., Amer. Math. Soc., Providence, RI, 1996, pp. 177–186.

[52] D. E. Knuth, *Permutations, matrices, and generalized Young tableaux*, Pacific J. Math., 34 (1970), pp. 709–727.

[53] C. Krattenthaler, *The major counting of nonintersecting lattice paths and generating functions for tableaux*, Mem. Amer. Math. Soc., 115 (1995), pp. vi+109.

[54] ———, *Growth diagrams, and increasing and decreasing chains in fillings of Ferrers shapes*, Adv. in Appl. Math., 37 (2006), pp. 404–431.

[55] G. Kreweras, *Sur les éventails de segments*, Cahiers du Bureau universitaire de recherche opérationnelle Série Recherche, 15 (1970), pp. 3–41.

[56] ———, *Sur les partitions non croisées d'un cycle*, Discrete Math., 1 (1972), pp. 333–350.

[57] G. Kuperberg, *Spiders for rank 2 Lie algebras*, Comm. Math. Phys., 180 (1996), pp. 109–151.

[58] J.-C. Lalanne, *Une involution sur les chemins de Dyck*, European J. Combin., 13 (1992), pp. 477–487.

[59] C. Lemus-Vidales, *Lattice Path Enumeration and Factorization*, ProQuest LLC, Ann Arbor, MI, 2017. Thesis (Ph.D.)–Brandeis University.

[60] C. Lenart, *On the combinatorics of crystal graphs. II. The crystal commutor*, Proc. Amer. Math. Soc., 136 (2008), pp. 825–837.

[61] J. Liang, *Enriched toric $[\vec{D}]$-partitions*. Preprint, `https://arxiv.org/abs/2209.00051`, 2022.

[62] J. Liang, B. E. Sagan, and Y. Zhuang, *Cyclic shuffle-compatibility via cyclic shuffle algebras*. Preprint, `https://arxiv.org/abs/2212.14522`, 2022.

[63] I. G. Macdonald, *Symmetric functions and Hall polynomials*, Oxford Classic Texts in the Physical Sciences, The Clarendon Press, Oxford University Press, New York, second ed., 2015. With contribution by A. V. Zelevinsky and a foreword by Richard Stanley, Reprint of the 2008 paperback edition [MR1354144].

[64] N. V. R. Mahadev and U. N. Peled, *Threshold graphs and related topics*, vol. 56 of Annals of Discrete Mathematics, North-Holland Publishing Co., Amsterdam, 1995.

[65] E. Malo, *Note sur équations algébriques dont toutes les racines sont réelles*, Journal de Mathematiques speciales, (ser. 4), 4 (1895), pp. 7–10.

[66] S.-j. Oh and T. Scrimshaw, *Identities from representation theory*, Discrete Math., 342 (2019), pp. 2493–2541.

[67] M. Okado and A. Schilling, *Existence of Kirillov-Reshetikhin crystals for nonexceptional types*, Represent. Theory, 12 (2008), pp. 186–207.

[68] M. Okado, A. Schilling, and M. Shimozono, *Virtual crystals and fermionic formulas of type $D_{n+1}^{(2)}, A_{2n}^{(2)}$, and $C_n^{(1)}$*, Represent. Theory, 7 (2003), pp. 101–163.

[69] J. Pappe, D. Paul, and A. Schilling, *An area-depth symmetric q,t-Catalan polynomial*, Electron. J. Comb., 29 (2022).

[70] J. Pappe, D. Paul, and A. Schilling, *The Burge correspondence and crystal graphs*, European J. Combin., 108 (2023), pp. Paper No. 103640, 19.

[71] J. Pappe, S. Pfannerer, M. C. Simone, and A. Schilling, *Promotion and growth diagrams for fans of dyck paths and vacillating tableaux*. Preprint, `https://arxiv.org/abs/2212.13588`, 2022.

[72] R. Patrias, *Promotion on generalized oscillating tableaux and web rotation*, J. Combin. Theory Ser. A, 161 (2019), pp. 1–28.

[73] T. K. Petersen, P. Pylyavskyy, and B. Rhoades, *Promotion and cyclic sieving via webs*, J. Algebraic Combin., 30 (2009), pp. 19–41.

[74] S. Pfannerer, *Promotion and evacuation diagrams*. 2022.

[75] S. Pfannerer, M. Rubey, and B. Westbury, *Promotion on oscillating and alternating tableaux and rotation of matchings and permutations*, Algebr. Comb., 3 (2020), pp. 107–141.

[76] G. N. Raney, *Functional composition patterns and power series reversion*, Trans. Amer. Math. Soc., 94 (1960), pp. 441–451.

[77] V. Reiner, D. Stanton, and D. White, *The cyclic sieving phenomenon*, Journal of Combinatorial Theory, Series A, 108 (2004), pp. 17–50.

[78] B. Rhoades, *Cyclic sieving, promotion, and representation theory*, J. Combin. Theory Ser. A, 117 (2010), pp. 38–76.

[79] G. d. B. Robinson, *On the Representations of the Symmetric Group*, Amer. J. Math., 60 (1938), pp. 745–760.

[80] T. W. Roby, V., *Applications and extensions of Fomin's generalization of the Robinson-Schensted correspondence to differential posets*, ProQuest LLC, Ann Arbor, MI, 1991. Thesis (Ph.D.)–Massachusetts Institute of Technology.

[81] M. Rubey, C. Stump, et al., *FindStat - The combinatorial statistics database*. `http://www.FindStat.org`. Accessed: May 17, 2023.

[82] G. Rumer, E. Teller, and H. Weyl, *Eine für die Valenztheorie geeignete Basis der binären Vektorinvarianten*, Nachrichten von der Gesellschaft der Wissenschaften zu Göttingen, Mathematisch-Physikalische Klasse, 1932 (1932), pp. 499–504.

[83] A. Sapounakis, I. Tasoulas, and P. Tsikouras, *Counting strings in Dyck paths*, Discrete Math., 307 (2007), pp. 2909–2924.

[84] C. Schensted, *Longest increasing and decreasing subsequences*, Canadian J. Math., 13 (1961), pp. 179–191.

[85] L. Serrano and C. Stump, *Maximal fillings of moon polyominoes, simplicial complexes, and Schubert polynomials*, Electron. J. Combin., 19 (2012), pp. Paper 16, 18.

[86] D. Speyer, *A double grading of Catalan numbers*. `http://www.mathoverflow.net/questions/131809`, 2013.

[87] R. P. Stanley, *Enumerative combinatorics. Vol. 2*, vol. 62 of Cambridge Studies in Advanced Mathematics, Cambridge University Press, Cambridge, 1999. With a foreword by Gian-Carlo Rota and appendix 1 by Sergey Fomin.

[88] ———, *Promotion and evacuation*, Electron. J. Combin., 16 (2009), pp. Research Paper 9, 24.

[89] ———, *Catalan numbers*, Cambridge University Press, New York, 2015.

[90] J. R. Stembridge, *A local characterization of simply-laced crystals*, Trans. Amer. Math. Soc., 355 (2003), pp. 4807–4823.

[91] C. Stump, *On a new collection of words in the Catalan family*, J. Integer Seq., 17 (2014), pp. Article 14.7.1, 8.

[92] S. Sundaram, *Orthogonal tableaux and an insertion algorithm for* $\mathrm{SO}(2n+1)$, J. Combin. Theory Ser. A, 53 (1990), pp. 239–256.

[93] H. Thomas and N. Williams, *Sweeping up zeta*, Selecta Math. (N.S.), 24 (2018), pp. 2003–2034.

[94] M. A. A. van Leeuwen, *An analogue of jeu de taquin for Littelmann's crystal paths*, Sém. Lothar. Combin., 41 (1998), pp. Art. B41b, 23 pp.

[95] ———, *Spin-preserving Knuth correspondences for ribbon tableaux*, Electron. J. Combin., 12 (2005), pp. Research Paper 10, 65.

[96] C.-J. Wang, *Applications of the Goulden-Jackson cluster method to counting Dyck paths by occurrences of subwords*, ProQuest LLC, Ann Arbor, MI, 2011. Thesis (Ph.D.)–Brandeis University.

[97] B. W. Westbury, *Invariant tensors and the cyclic sieving phenomenon*, Electron. J. Combin., 23 (2016), pp. Paper 4.25, 40.

[98] ———, *Coboundary categories and local rules*, Electron. J. Combin., 25 (2018), pp. Paper No. 4.9, 22.

[99] Y. Zhuang, *A generalized Goulden-Jackson cluster method and lattice path enumeration*, Discrete Math., 341 (2018), pp. 358–379.